The effect of muscle type and ageing on Near Infrared (NIR) Spectroscopy classification of game meat species using a portable instrument

by

Pholisa Dumalisile

Dissertation presented for the degree of

Doctor of Philosophy

(Food Science)

at

Stellenbosch University

Department of Food Science, Faculty of AgriSciences

The financial assistance of the National Research Foundation (NRF) towards this research is hereby acknowledged. Opinions expressed, and conclusions arrived at are those of the author and are not necessarily to be attributed to the NRF

Supervisor: Dr Paul J. Williams

Co-supervisor: Prof Marena Manley

Co-supervisor: Prof Louwrens C. Hoffman

March 2021

Declaration

By submitting this thesis electronically, I declare that the entirety of the work contained therein is my own, original work, that I am the sole author thereof (save to the extent explicitly otherwise stated), that reproduction and publication thereof by Stellenbosch University will not infringe any third party rights and that I have not previously in its entirety or in part submitted it for obtaining any qualification.

Pholisa Dumalisile
March 2021

Abstract

Meat and meat products represent a large proportion of the human diet as it is known to provide valuable proteins, and is a good source of minerals, particularly iron, and zinc. Because of its nutritional characteristics it tends to be a commodity of demand to consumers. Game meat offers even higher nutritional attributes than any other red meat category because of its low fat and high protein levels making game meat a highly priced product thereby causing it to be an appealing target for species substitution. Also, fraudsters prefer to use products that are easy to adulterate and difficult to detect. To mitigate the fraudulent substitution of meat products, food authentication and labelling is promoted. The conventional methods of authentication such as DNA based techniques are expensive and slow for the rapidly expanding meat trade. Near infrared (NIR) spectroscopy, a rapid non-destructive, environmentally friendly instrument is thought to be an alternative and cheap solution for on-site meat authentication purposes, although this technology has not yet been evaluated for its suitability to distinguish different South African game species and/or muscles.

To evaluate the ability of NIR spectroscopy to distinguish between selected game species' (impala *(Aepyceros melampus),* blesbok *(Damaliscus pygargus phillipsi),* springbok *(Antidorcas marsupialis)*, eland *(Taurotragus oryx),* black wildebeest *(Connochaetes gnou)* and zebra *(Equus quagga)) Longissimus thoracis et lumborum* (LTL) muscle steaks, a handheld MicroNIR™ OnSite spectrophotometer was used in a spectral range of 908–1700 nm. After the spectral data was pre-treated with smoothing, SNV-Detrend, the PCA scores plot revealed two clear clusters separating the medium-sized antelopes and large-sized species. The waveband responsible for the separation as indicated by the loadings line plot situated at 1372 nm, was associated with fat. The developed classification models revealed that the steaks could be distinguished with linear discriminant analysis (LDA), soft independent modelling by class analogy (SIMCA) and partial least squares discriminant analysis (PLS-DA) at classification accuracies ranging from 68 - 100%, 67 - 100% and 70 - 96%, respectively.

Also, NIR spectroscopy in combination with multivariate data analysis techniques was used to discriminate between different muscle steaks from *longissimus thoracis et lumborum* (LTL), *infraspinatus* (IS) and *supraspinatus* (SS), *biceps femoris* (BF), *semitendinosus* (ST) and *semimembranosus* (SM) of impala and eland species; and samples from fan fillet (FF), big drum (BD), triangle steak (TS), moon steak (MS) and rump steak (RS) of ostriches. Classification accuracies developed with PLS-DA models ranged from 85 to 100% throughout. It is interesting that good classifications accuracies were achieved when the muscles were grouped according to their anatomical locations, irrespective of the muscle used, PLS-DA models yielded accuracies of 97%, 81% and 92% for eland, impala and ostrich, respectively.

Even though NIR spectroscopy in combination with multivariate data analysis techniques could successfully distinguish the different muscle types within animals, and muscles across different species, the instrument did fall short in discriminating the ageing periods of blesbok, eland, and ostrich muscles. However, it is postulated that there is still room for improvement when the device is coupled with machine learning.

In summary, the handheld MicroNIR™ OnSite spectrophotometer demonstrated its capability in discriminating between different species of game meat indicating that the instrument could potentially be used in the authentication of game meat.

Opsomming

Vleis en vleisprodukte verteenwoordig ‘n groot deel van die menslike dieet aangesien dit waardevolle proteïene verskaf, en dit is ‘n goeie bron van minerale, veral yster en sink. As gevolg van die voedingseienskappe is dit geneig om ‘n kommoditeit van aanvraag vir verbruikers te wees. Wildsvleis bied selfs hoër voedingseienskappe as enige ander rooivleis kategorie vanweë die lae vet en hoë proteïen vlakke, wat wildsvleis ‘n duur produk maak, wat veroorsaak dat dit ‘n aantreklike teiken is vir spesie-substitusie. Bedrieërs verkies ook om produkte te gebruik wat maklik is om te vervals en wat moeilik opgespoor kan word. Om die bedrieglike substitusie van vleisprodukte te verminder, word voedselverifikasie en etikettering aangemoedig. Die konvensionele verifikasiemetodes soos DNA-gebaseerde tegnieke is duur en stadig vir die vinnig-groeiende vleishandel. Naby infrarooi (NIR) spektroskopie, ‘n vinnige, nie-vernietigende, omgewingsvriendelike instrument, word beskou as ‘n alternatiewe en goedkoop oplossing vir ‘op-perseel’ vleisverifikasie doeleindes, alhoewel hierdie tegnologie nog nie geëvalueer is vir die geskiktheid om tussen verskillende Suid-Afrikaanse wildspesies en/of spiere te onderskei nie.

Die vermoë van NIR spektroskopie om te onderskei tussen *Longissimus thoracis et lumborum* (LTL) spierskywe van spesifieke wildspesies (rooibok *(Aepyceros melampus),* blesbok *(Damaliscus pygargus phillipsi),* springbok *(Antidorcas marsupialis)*, eland *(Taurotragus oryx),* swart wildebees *(Connochaetes gnou)* en zebra *(Equus quagga))* is geëvalueer deur ‘n draagbare MicroNIR™ OnSite spektrofotometer te gebruik in ‘n spektrale reeks van 908-1700 nm. Nadat die spektrale data vooraf behandel is met SNV-Detrend gladmaaking, het die PCA tellingsplot twee duidelike groeperings getoon wat die mediumgrootte wildsbokke en die groter spesies van mekaar skei. Die golfband wat verantwoordelik is vir die skeiding wat aangedui is deur die beladingslynplot by 1372nm, is geassosieer met vet. Die ontwikkelde klassifikasiemodelle het aan die lig gebring dat daar tussen die steaks onderskeid getref kon word met lineêre diskriminante analise (LDA), sagte onafhanklike modellering volgens klasanalogie (SIMCA) en gedeeltelike kleinste kwadrate diskriminante analise (PLS-DA) met klassifikasieakkuraatheid tussen 68-100%, 67-100%, en 70-96%, onderskeidelik.

NIR spektroskopie is ook in kombinasie met meerveranderlike dataontledingstegnieke gebruik om te onderskei tussen verskillende spiersnitte van *longissimus thoracis et lumborum* (LTL), *infraspinatus* (IS) en *supraspinatus* (SS), *biceps femoris* (BF), *semitendinosus* (ST) en *semimembranosus* (SM) van rooibok en eland spesies; en monsters van waaierfilet (FF), groot drom (BD), driehoek steak (TS), maan steak (MS) en kruis steak (RS) van volstruise. Klassifikasie-akkuraatheid wat met PLS-DA modelle ontwikkel is, het deurgaans gewissel van 85% tot 100%. Dit is interessant dat goeie klassifikasie akkuraatheid behaal is wanneer die spiere volgens hul

anatomiese ligging gegroepeer is; ongeag die spiere wat gebruik is, het PLS-DA modelle akkuraathede van 97%, 81% en 92% behaal vir, onderskeidelik, eland, rooibok en volstruis.

Alhoewel NIR spektroskopie in kombinasie met meervoudige data-analise tegnieke suksesvol kon onderskei tussen die verskillende spiertipes binne diere, en spiere oor verskillende spesies, het die instrument te kort geskiet wanneer dit gekom het by onderskeiding van verouderingstydperke van blesbok, eland en volstruis spiere. Daar word egter gepostuleer dat daar steeds ruimte is vir verbetering wanneer die instrument met masjienleer gekombineer word.

Ten slotte, die draagbare MicroNIR™ OnSite spektrofotometer het die vermoë gedemonstreer om tussen verskillende wildsvleis spesies te onderskei, wat aandui dat die instrument moontlik gebruik kan word vir die verifikasie van wildsvleis.

“Blessed are those who find wisdom, those who gain understanding, for she is more profitable than silver and yields better returns than gold” (Proverbs 3: 13-14).

Acknowledgements

Firstly, I would like to thank my heavenly Father, for bestowing me the ability, strength, health, and motivation to succeed. If it had not been for the Lord on my side, I would not have reached this phase. To God be the glory!

Additionally, I would like to express my most sincere gratitude to the following people and institutions for their contribution towards the successful completion of this study:

My supervisor, Dr Paul Williams, for his professional supervision, guidance, advice, motivation, patience and confidence in my abilities. His attention to detail, passion for Chemometrics and NIR data interpretation, and insight were invaluable to the completion of this study. There are not enough words to express my gratitude;

My co-supervisor, Professor Marena Manley, for her expert advice, guidance, motivation and her enthusiasm for NIR technology and data interpretation; and above all for connecting me with the company that funded my studies, Pioneer Foods;

My co-supervisor, Professor Louwrens Hoffman, for his expert advice on game meat, and continuous support and encouragement. His willingness to go the extra mile whenever help/advice was needed, even when he relocated to Australia;

Professor Trevor Britz, my M.Sc (Food Science) supervisor, for connecting me with Dr Paul Williams when I wanted to come back and study for PhD (Food Science);

The Pioneer Foods Education Community Trust (PFECT) for funding me the years of my PhD studies;

The Stellenbosch University for awarding me a merit bursary in 2019;

The Pioneer Foods Education Community Trust (PFECT) for awarding me the student travel grant to attend the 18th International Conference on Near Infrared Spectroscopy (ICNIRS 2017), 11 – 15 June 2017, Copenhagen – Denmark;

The Council for Near Infrared Spectroscopy (CNIRS) for the student travel award to attend the 19th International Diffuse Reflectance Conference (IDRC 2018), 29 July – 2 August, Wilson College, Chambersburg, Pennsylvania – USA;

This research is supported by the South African Research Chairs Initiative (SARChI) and funded by the South African Department of Science and Technology (UID: 84633), as administered by the National Research Foundation (NRF) of South Africa;

The Postgraduate office, Stellenbosch University for their very informative workshops;

All the staff and postgraduate students of the Food Science Department, thank you for your motivation and support; especially Richard and Kiah Edwards for assisting me with the Solo PLS Toolbox;

Petro du Buisson, for translating the Abstract into the Afrikaans version;

The following Animal Science students, Johann Laubser, Mzuvukile Mcayiya, Angelique Henn, Karla Pretorius, and Retha Engels for the laboratory assistance at the meat science lab;

My parents, siblings, and friends whose unconditional love, encouragement, and never-ending support have meant more to me than words can express. I am truly grateful for your prayers and continuous interest;

Thank you Singata Stofile and Philiswa Sikhilongo for being there to offload when work got rough, your prayers and daily words of encouragement are very much appreciated; and

To my dear sister, Sisonke Dumalisile, thank you for opening your home for me while I was studying.

Preface

This dissertation is presented as a compilation of 6 chapters. Each chapter is introduced separately and is written according to the style of the International Journal of Food Science and Technology.

Chapter 1	**General Introduction and project aims**
Chapter 2	**Literature review** **Near infrared (NIR) spectroscopy: The current approach of species identification in meat and meat products**
Chapter 3	**Near infrared (NIR) spectroscopy to differentiate *Longissimus thoracis et lumborum* (LTL) muscles of game species**
Chapter 4	**Discriminating muscle type of selected game species using near infrared (NIR) spectroscopy**
Chapter 5	**Effect of ageing on the near infrared (NIR) spectra of selected game species' muscles**
Chapter 6	**General discussion and conclusions**

Two Chapters from this dissertation have been published

Chapter 3:

Dumalisile, P., Manley, M., Hoffman, L. & Williams, P.J. (2020). Near-Infrared (NIR) Spectroscopy to Differentiate *Longissimus thoracis et lumborum* (LTL) Muscles of Game Species. *Food Analytical Methods,* **13**, 1220-1233. https://link.springer.com/article/10.1007%2Fs12161-020-01739-x

Chapter 4:

Dumalisile, P., Manley, M., Hoffman, L. & Williams, P.J. (2020). Discriminating muscle type of selected game species using near infrared (NIR) spectroscopy. *Food Control*, **110**, 106981. https://doi:10.1016/j.foodcont.2019.106981

Table of Contents

List of Figures

List of Tables

List of Abbreviations

Abbreviation	Expansion
3-D	Three-dimensional
°C	degree Celsius
-	negative
%	percentage
+	positive
A	absorbance
ANN	artificial neural network
AGID	agar gel immune diffusion
BD	big drum muscle
BF	*biceps femoris* muscle
Cal	calibration
CDA	canonical discriminant analysis
cm	centimetre
D	day
dd	droplet digital
DAFF	Department of Agriculture, Forestry and Fisheries
DoH	Department of Health
ELISA	enzyme-linked immunosorbent assay
e.g.	*exempli gratia* (for example)
EIA	enzyme immunoassays
ELISA	enzyme-linked immunosorbent assay
EU	European Union
et al.	*et alibi* (and elsewhere)
FF	fan fillet muscle
Fig.	figure
FN	false negative
FP	false positive

FT	Fourier Transform
GC	gas chromatography
GC-MS	gas chromatography mass spectrometer
GDP	Gross Domestic Profit
h	hour
HPLC	high-performance liquid chromatography
InGaAs	Indium Gallium Arsenide
IS	*infraspinatus* muscle
kg	kilogram
KS	Kennard-Stone
LED	Light Emitting Diode
LC	liquid chromatography
LC-MS	liquid chromatography-mass spectroscopy
LC-QQQ	liquid chromatography-triple quadrupole mass spectrometry
LD	longissimus dorsi
LDA	linear discriminant analysis
LTL	*longissimus thoracis et lumborum* muscle
LS-SVM	least square support vector machine
LV	latent variable
LOD	limit of detection
min	minutes
ML	machine learning
MLR	multiple linear regression
MS	moon steak muscle
N	Newton
n	number
NIR	near infrared
NIRS	near infrared spectroscopy
NIT	near infrared transmittance
nm	nanometre

PC	principal component
PCA	principal component analysis
PCR	polymerase chain reaction
PLS	partial least squares
PLS-DA	partial least squares discriminant analysis
PLSR	partial least squares regression
R	reflectance
R^2	coefficient of determination
RMSECV	root mean square error of cross validation
RFLP	Restriction Fragment Length Polymorphism
RS	rump steak muscle
SIMCA	Soft independent modelling by class analogy
SM	*semimembranosus* muscle
SNV	Standard normal variate
SS	*supraspinatus* muscle
ST	*semitendinosus* muscle
TN	true negative
TP	true positive
TS	triangle steak muscle
Val	validation
Vis-NIR	visible and near infrared
vs.	versus (against)
WBSF	Warner Bratzler shear force
WHO	World Health Organization

Chapter 1

General Introduction and project aim

Meat and meat products represent an important component of the human diet, and also play an integral role in global eating (Grunert, 2006; Ballin and Lametsch, 2008). In addition to proteins, red meat is also recognized as a source of vitamin B12, Vitamin D, and essential omega-3 fatty acids, as well as bio-available minerals, particularly iron, zinc and selenium (Schönfeldt and Gibson, 2008). Thus, the nutritional attributes of red meat deliver a major proportion of consumer requirements. In particular game meat, also high in proteins (20.0–23.8%), offers a healthy alternative to other red meat as it is known to be much lower in fat (0.8–2.45%) compared to beef (14.2% fat; 19.2% protein) (Hoffman, 2007). Its low fat content is mainly composed of structural lipid components (phospholipid and cholesterol) that have high proportions of polyunsaturated fatty acids (Hoffman and Wiklund, 2006). Various game species in other parts of the world are semi-domesticated, while South African (SA) game animals are wild and free-roaming, thus giving SA game meat an advantage of being considered an organic food product (Hoffman & Wiklund, 2006; Mostert & Hoffman, 2007). For this reason, SA game meat is a highly priced commodity making it an attractive target for species substitution (Ballin, 2010; Kamruzzaman *et al.*, 2013).

In general, meat and meat products are often targets of food fraud, and are currently leading the top 5 list of EU food categories of illegal import fraud examples (Soon and Manning, 2018). Food fraud is defined by Spink and Moyer (2011) as a collective term used to encompass the deliberate and intentional substitution, addition, tampering, or misrepresentation of food, food ingredients, or food packaging – or false or misleading statements made about a product, for economic gain. Numerous studies (Cawthorn *et al.*, 2013; O'Mahony, 2013; Walker *et al.*, 2013) have shown that at least some consumers are undoubtedly encountering undeclared animal species in meat products. After horse meat was found in beef burgers produced in Ireland in 2013 (O'Mahony, 2013; Walker *et al.*, 2013), the scandal received media attention which subsequently raised consumers' concerns regarding meat fraud. A similar case happened in South Africa, as species (such as chicken, goat, water buffalo and donkey) that were not declared on the product labelling were found in beef sausages (Cawthorn *et al.*, 2013). Thus, meat species substitution is a current problem involving economic and safety issues since one cannot easily detect the source of origin or differentiate between species when evaluating meat visually (Kamruzzaman *et al.*, 2013).

On the other hand, the South African game meat industry does not have standardized meat cuts or quality standards in place (Hoffman *et al.*, 2004). Consequently, this allows the legal selling of game meat of inferior quality. Consumers are very aware of the different muscle cuts and their retail value, mainly due to quality differences. It is known that within an animal, different muscles have diverse textural and chemical properties (Ba *et al.*, 2014). Moreover, different muscle cuts differ in their retail price as their quality is not the same, for example fillet is more expensive than sirloin

steak. Thus, the absence of game meat regulations creates a gap in the intentional meat substitution of muscle cuts.

Another common bad practice of meat substitution is selling the low-priced meat as high value aged meat. Meat ageing is a popular method used for decades with the purpose of increasing and enhancing tenderness (Dransfield, 1994). This is done by storage of the meat under controlled refrigeration for extended periods of time (Dransfield, 1994; Starkey *et al.*, 2015; Bhat *et al.*, 2018). From a consumer's perspective, aged meat is characterized by tenderness and juiciness. These two properties are also used in the eating quality evaluation of meat (Cheng *et al.,* 2017). A number of studies indicate that consumers can differentiate between tough and tender meat, and that they are willing to pay a premium price for a guaranteed tender steak (Rhee *et al.*, 2004; Koohmaraie and Geesink, 2006; Hildrum *et al.*, 2009; ElMasry and Sun, 2010; Konda Naganathan *et al.*, 2015). It is then unacceptable and fraudulent to offer such a product for sale what is thought to be a tender expensive muscle, only to discover it is tough and likely a low-priced muscle because of undeclared labelling. Thus, the reported and unreported incidents of undeclared labelling of meat products have subsequently raised the consumers' awareness of quality, traceability, and origin of the food they eat (Verbeke & Ward, 2006).

Proper labelling of meat products is important to help fair trade and to enable consumers to make informed choices (Department of Health, 2010; Department of Agriculture, 2015). In South Africa, there are regulatory bodies governing food legislation. The Foodstuff, Cosmetics and Disinfectant Act, under the Department of Health (DoH), controls the labelling and advertising guidelines of meat and meat products to ensure consumers are not misled and given false information (Department of Health, 2010). As much as there are regulations in place to protect consumers, the food products need to be authenticated. Food authentication is a procedure that verifies that food complies with its label description (Danezis *et al.*, 2016).

Conventional analytical methods (chromatography, electrophoretic separation of proteins, enzyme-linked immunosorbent assay (ELISA) procedures and DNA based techniques) have been successfully used for authenticity issues associated with substitution of meat and meat products (Jonker *et al.*, 2008; Fajardo *et al.*, 2010; Nakyinsige *et al.*, 2012; Cawthorn *et al.*, 2013; Amaral *et al.*, 2014; Doosti *et al.*, 2014; Von Bargen *et al.*, 2014). Analytical authentication of food products often requires sample preparation such as extraction of proteins, DNA and organic compounds (Ballin, 2010). These methods have an advantage of being able to detect low levels of adulteration with high reliability. However, due to the cost of these conventional methods, raw meat products are not tested on a regular basis. In addition to their high cost, all these methods are tedious, require complicated laboratory procedures, and have a destructive step that damages the quality of the product being tested (Kamruzzaman *et al.*, 2013; Manley, 2014). To address this inadequacy, near infrared (NIR) spectroscopy can be used as a rapid screening method (Manley, 2014) for detection of potential substitution of meat species (Ding & Xu, 1999; Cozzolino and Murray, 2004).

Near infrared spectroscopy is a rapid, non-invasive, chemical free, non-destructive, and environmentally friendly method of analysis. The absorption of radiation is the main recordable phenomena in the NIR region (780 to 2500 nm) of the electromagnetic spectrum (Davies, 1998; Osborne, 2000; Cen and He, 2007; Alamprese *et al.*, 2013). Absorption bands observed are produced when NIR radiation of a specific frequency vibrates at the same frequency as a specific molecular bond present in the sample in the form of X-H bonds, where X is a carbon, nitrogen, oxygen or sulphur (Shenk *et al.,* 1992; Roggo *et al.*, 2007; Shenk *et al.,* 2008; Manley, 2014; Peng and Wang, 2015). Thus, NIR technology does not only assess chemical structures through the analysis of the molecular bonds in the NIR spectrum, but also builds a characteristic spectrum that represents the 'finger print' of the sample (Cozzolino and Murray, 2004). A typical NIR spectrum consists of several bands formed by absorption peaks and valleys due to overtones of fundamental bond stretching resulting from overlapping signals (Davies, 1998). Because of the complexity of the analytical information present in the NIR spectra, this technology is mostly coupled with multivariate data analysis (Reid and Downey, 2006; Pasquini, 2018).

In the past years, the suitability of spectroscopy techniques coupled with multivariate data analysis for the detection of adulterants in foods has been demonstrated (Ding and Xu, 1999, 2000; Leroy *et al.*, 2004; Cozzolino and Murray, 2004; Prieto *et al.*, 2008, 2009; Andrés *et al.*, 2008; Mamani-Linares *et al.*, 2012; Rahim and Ghazali, 2012; Alamprese *et al.*, 2013, 2016; Morsy and Sun, 2013; Barbin *et al.*, 2013a,b, 2015; Mamani-Linares and Gallo, 2014; Moran *et al.*, 2018; Nolasco Perez *et al.*, 2018; Grassi *et al.*, 2018; Silva *et al.*, 2020). Several multivariate analysis methods can be classified according to their purpose and the algorithms or computational procedures that they use. For example, the multivariate techniques commonly used, allow samples with similar characteristics to be grouped to establish classification methods for unknown samples (qualitative analysis). Again, they can also perform methods predicting some characteristic of the unknown samples (quantitative analysis) (Blanco and Villarroya, 2002). Qualitative multivariate analytical techniques are known collectively as 'pattern-recognition methods', which are labelled 'supervised' or 'unsupervised', depending on whether or not the class to which the samples belong is known.

Ding and Xu (1999), Cozzolino and Murray (2004) and Mamani-Linares *et al.* (2012) coupled NIR spectroscopy with chemometrics to achieve good classification models of meat species. Visible-near infrared (vis-NIR) spectroscopy was used in initial studies on meat species classification. Discrimination of cattle, llama and horse meat species was possible with accuracies of 100, 95 and 89%, respectively (Mamani-Linares *et al.,* 2012). Prieto *et al.* (2008) used only the NIR region (1100–2500 nm) to discriminate ground meat samples of adult steers (oxen) from that of young cattle. Using partial least squares discriminant analysis (PLS-DA), an overall classification accuracy of 100% was obtained. Kamruzzaman *et al.* (2011) used NIR hyperspectral imaging to discriminate lamb muscles (*Semitendinosus* (ST), i.e. *Longissimus dorsi* (LD) and *Psoas major* (PM)) in a wavelength range of 900–1700 nm. They used principal component analysis (PCA) for data reduction and linear

discriminant analysis (LDA) (Fisher, 1936) to build classification models. The results showed that it was possible to discriminate between the three lamb muscles with an overall accuracy of 100%. Furthermore, Alomar *et al.* (2003) segregated different types of bovine meat and predicted several chemical fractions from two breeds and three muscles (LD, ST and *Supraspinatus* (SS)) using NIR spectroscopy in the wavelength range of 400–2500 nm. The results showed the two breeds were correctly classified with 78.8% accuracy and the three muscle types yielded 97.8 (LD), 97.7 (SS) and 89.5% (ST) classification accuracy.

In a preliminary study, Moran *et al.* (2018) predicted the ageing time of beef steaks to assess vis-NIR (400-2400 nm) as an authentication tool. The steaks were aged for 3, 7, 14, and 21 days post-mortem. They applied partial least squares discriminant analysis (PLS-DA) to classify steaks based on the number of days aged. They achieved overall correct classifications ranging from 94.2 to 100%, which indicated the ability of the vis-NIR instrument to discriminate the steaks based on different ageing periods. Furthermore, Prieto *et al.* (2015) studied the rapid discrimination of enhanced quality pork with vis-NIR spectroscopy in the wavelength range of 350–2500 nm and used PLS-DA to predict the ageing days. They correctly classified 94 and 97% of aged samples for the 2nd and 14th ageing days, respectively.

The structure of the muscle cut, and the chemical composition of meat have been identified amongst other characteristics that contribute to the NIR differentiation of muscles. For example, the fibre type distribution of each muscle affects the way the light moves within the muscle, which subsequently influences the measurements of the diffuse reflectance (Dixit *et al.,* 2021). In addition to the above characteristics, textural features of the muscles including rigor process, ageing, and colour are also contributors to the NIR distinction of muscles (Reis *et al.,* 2018). Therefore, the scattering of light in the meat/muscle related NIR studies differs from sample to sample because of these characteristics.

These studies have displayed that there are definite physicochemical differences between the meat of different species and between different muscles. It is observed that spectroscopy, when coupled with multivariate mathematical techniques can be a suitable alternative to traditional methods for species identification. Despite the comprehensive literature available on NIR spectroscopy applications to determine meat quality, no studies were found on impala *(Aepyceros melampus),* blesbok *(Damaliscus pygargus phillipsi)*, springbok *(Antidorcas marsupialis)*, eland *(Taurotragus oryx),* black wildebeest *(Connochaetes gnou)* and zebra *(Equus quagga)* discrimination, thus further study was required. Game meat is characterized by darker muscles compared to the meat of domestic animals that have been investigated the most. Hence the aim of this study is focused on game meat.

The aim of this dissertation was to investigate the effect of muscle type and ageing on NIR spectroscopy classification of South African game meat species using a portable instrument. Specific objectives were to:

- use portable NIR spectroscopy coupled with various discriminant and classification methods to differentiate between *longissimus thoracis et lumborum* (LTL) muscle steaks of selected game species;
- investigate the ability of portable NIR spectroscopy in discriminating selected game muscle types and, to discriminate different species irrespective of the muscle used; and
- determine whether portable NIR spectroscopy can be used to distinguish between different ageing periods of blesbok, eland, and ostrich muscles.

References

Alamprese, C., Amigo, J.M., Casiraghi, E. & Engelsen, S.B. (2016). Identification and quantification of turkey meat adulteration in fresh, frozen-thawed and cooked minced beef by FT-NIR spectroscopy and chemometrics. *Meat Science*, **121,** 175-181.

Alamprese, C., Casale, M., Sinelli, N., Lanteri, S. & Casiraghi, E. (2013). Detection of minced beef adulteration with turkey meat by UV-vis, NIR and MIR spectroscopy. *LWT - Food Science and Technology*, **53**.

Alomar, D., Gallo, C., Castañeda, M. & Fuchslocher, R. (2003). Chemical and discriminant analysis of bovine meat by near infrared reflectance spectroscopy (NIRS). *Meat Science*, **63**, 441–450.

Amaral, J.S., Santos, C.G., Melo, V.S., Oliveira, M.B.P.P. & Mafra, I. (2014). Authentication of a traditional game meat sausage (Alheira) by species-specific PCR assays to detect hare, rabbit, red deer, pork and cow meats. *Food Research International*, **60**, 140–145.

Andrés, S., Silva, A., Soares-Pereira, A.L., Martins, C., Bruno-Soares, A.M. & Murray, I. (2008). The use of visible and near infrared reflectance spectroscopy to predict beef M. longissimus thoracis et lumborum quality attributes. *Meat Science*, **78**, 217–224.

Ba, H. Van, Park, K., Dashmaa, D. & Hwang, I. (2014). Effect of muscle type and vacuum chiller ageing period on the chemical compositions, meat quality, sensory attributes and volatile compounds of Korean native cattle beef. *Animal Science Journal*, **85**, 164–173.

Ballin, N.Z. (2010). Authentication of meat and meat products. *Meat Science*, **86**, 577–587.

Ballin, N.Z. & Lametsch, R. (2008). Analytical methods for authentication of fresh vs. thawed meat - A review. *Meat Science*, **80**, 151–158.

Barbin, D.F., ElMasry, G., Sun, D.-W. & Allen, P. (2013a). Non-destructive determination of chemical composition in intact and minced pork using near-infrared hyperspectral imaging. *Food Chemistry*, **138**, 1162–1171.

Barbin, D.F., Kaminishikawahara, C.M., Soares, A.L., Mizubuti, I.Y., Grespan, M., Shimokomaki, M. & Hirooka, E.Y. (2015). Prediction of chicken quality attributes by near infrared spectroscopy. *Food Chemistry*, **168**, 554–560.

Barbin, D.F., Valous, N.A. & Sun, D.W. (2013b). Tenderness prediction in porcine longissimus dorsi muscles using instrumental measurements along with NIR hyperspectral and computer vision

imagery. *Innovative Food Science and Emerging Technologies*, **20**, 335–342.

Bargen, C. Von, Brockmeyer, J. & Humpf, H.U. (2014). Meat authentication: A new HPLC-MS/MS based method for the fast and sensitive detection of horse and pork in highly processed food. *Journal of Agricultural and Food Chemistry*, **62**, 9428–9435.

Bhat, Z.F., Morton, J.D., Mason, S.L. & Bekhit, A.E.A. (2018). Food Science and Human Wellness Role of calpain system in meat tenderness: A review. *Food Science and Human Wellness*, **7**, 196–204.

Blanco, M. & Villarroya, I. (2002). NIR spectroscopy: A rapid-response analytical tool. *TrAC - Trends in Analytical Chemistry*, **21**, 240–250.

Cawthorn, D.M., Steinman, H.A. & Hoffman, L.C. (2013). A high incidence of species substitution and mislabelling detected in meat products sold in South Africa. *Food Control*, **32**, 440–449.

Cen, H. & He, Y. (2007). Theory and application of near infrared reflectance spectroscopy in determination of food quality. *Trends in Food Science and Technology*, **18**, 72–83.

Cheng, J.H., Nicolai, B. & Sun, D.W. (2017). Hyperspectral imaging with multivariate analysis for technological parameters prediction and classification of muscle foods: A review. *Meat Science*, **123**, 182–191.

Cozzolino, D. & Murray, I. (2004). Identification of animal meat muscles by visible and near infrared reflectance spectroscopy. *LWT - Food Science and Technology*, **37**, 447–452.

Danezis, G.P., Tsagkaris, A.S., Camin, F., Brusic, V. & Georgiou, C.A. (2016). Food authentication: Techniques, trends & emerging approaches. *TrAC - Trends in Analytical Chemistry*, **85**, 123–132.

Davies, T. (1998). The history of near infrared spectroscopic analysis: Past, present and future “From sleeping technique to the morning star of spectroscopy.” *Analusis*, **26**, 17–19.

Ding, H.B. & Xu, R.J. (1999). Differentiation of beef and kangaroo meat by visible/near-infrared reflectance spectroscopy. *Journal of Food Science*, **64**, 814–817.

Ding, H.B. & Xu, R.J. (2000). Near-infrared spectroscopic technique for detection of beef hamburger adulteration. *Journal of Agricultural and Food Chemistry*, **48**, 2193–2198.

Dixit, Y., Al-Sarayreh, M., Craigie, C.R. & Reis, M.M. (2021). A global calibration model for prediction of intramuscular fat and pH in red meat using hyperspectral imaging. *Meat Science*, 108405.

Department of Agriculture (DoA). 2015. Agricultural Product Standards Act, 1990 (Act 119 of 1990): Regulations regarding the classification and marking of meat intended for sale in the Republic of South Africa (R. 55/2015). Government Printing Offices, South Africa.

Department of Health (DoH). 2010. Foodstuffs, Cosmetics and Disinfectants Act, 1972 (Act 54 of 1972): Regulations relating to the labelling and advertising of foods: (R. 146/2010, As amended up to and including R.45 of 19 January 2012). Government Printing Offices, South Africa.

Doosti, A., Ghasemi Dehkordi, P. & Rahimi, E. (2014). Molecular assay to fraud identification of meat products. *Journal of Food Science and Technology*, **51**, 148–152.

Dransfield, E. (1994). Optimisation of tenderisation, ageing and tenderness, *Meat Science,* **36**, 105–

121.

ElMasry, G. & Sun, D.-W. (2010). *{Chapter} 6 - Meat Quality Assessment Using a Hyperspectral Imaging System*. *Hyperspectral Imaging for Food Quality Analysis and Control*.

Fajardo, V., González Isabel, I., Rojas, M., García, T. & Martín, R. (2010). A review of current PCR-based methodologies for the authentication of meats from game animal species. *Trends in Food Science and Technology*, **21**, 408–421.

Grassi, S., Casiraghi, E. & Alamprese, C. (2018). Handheld NIR device: A non-targeted approach to assess authenticity of fish fillets and patties. *Food Chemistry*, **243**, 382–388.

Grunert, K.G. (2006). Future trends and consumer lifestyles with regard to meat consumption. *Meat Science*, **74**, 149–160.

Hildrum, K.I., Rødbotten, R., Høy, M., Berg, J., Narum, B. & Wold, J.P. (2009). Classification of different bovine muscles according to sensory characteristics and Warner Bratzler shear force. *Meat Science*, **83**, 302–307.

Hoffman, L. C. (2007). The meat we eat: are you game? *Inaugural Addess.* Stellenbosch University, Western Cape, South Africa.

Hoffman, L.C., Muller, M., Schutte, W. De & Crafford, K. (2004). The retail of South African game meat: Current trade and marketing trends. *African Journal of Wildlife Research*, **34**, 123–134.

Hoffman, L.C., Schalkwyk, S. van & Muller, M. (2011). Quality Characteristics of Blue Wildebeest (Connochaetes taurinus) Meat. *South African Journal of Wildlife Research*, **41**, 210–213.

Hoffman, L.C. & Wiklund, E. (2006). Game and venison - meat for the modern consumer. *Meat Science*, **74**, 197–208.

Jonker, K.M., Tilburg, J.J.H.C., Hagele, G.H. & Boer, E. de. (2008). Species identification in meat products using real-time PCR. *Food additives & contaminants. Part A, Chemistry, analysis, control, exposure & risk assessment*, **25**, 527–533.

Kamruzzaman, M., Elmasry, G., Sun, D.W. & Allen, P. (2011). Application of NIR hyperspectral imaging for discrimination of lamb muscles. *Journal of Food Engineering*, **104**, 332–340.

Kamruzzaman, M., Sun, D.W., ElMasry, G. & Allen, P. (2013). Fast detection and visualization of minced lamb meat adulteration using NIR hyperspectral imaging and multivariate image analysis. *Talanta*, **103**, 130–136.

Konda Naganathan, G., Cluff, K., Samal, A., Calkins, C.R., Jones, D.D., Lorenzen, C.L. & Subbiah, J. (2015). Hyperspectral imaging of ribeye muscle on hanging beef carcasses for tenderness assessment. *Computers and Electronics in Agriculture*, **116**, 55–64.

Koohmaraie, M. & Geesink, G.H. (2006). Contribution of postmortem muscle biochemistry to the delivery of consistent meat quality with particular focus on the calpain system. *Meat Science*, **74**, 34–43.

Leroy, B., Lambotte, S., Dotreppe, O., Lecocq, H., Istasse, L. & Clinquart, A. (2004). Prediction of technological and organoleptic properties of beef Longissimus thoracis from near-infrared reflectance and transmission spectra. *Meat Science*, **66**, 45–54.

Mamani-Linares, L.W., Gallo, C. & Alomar, D. (2012). Identification of cattle, llama and horse meat by near infrared reflectance or transflectance spectroscopy. *Meat Science*.

Mamani-Linares, L.W. & Gallo, C.B. (2014). Meat quality, proximate composition and muscle fatty acid profile of young llamas (Lama glama) supplemented with hay or concentrate during the dry season. *Meat Science*, **96**, 394–399.

Manley, M. (2014). Near-infrared spectroscopy and hyperspectral imaging: non-destructive analysis of biological materials. *Chem. Soc. Rev.*, **43**, 8200–8214.

Moran, L., Andres, S., Allen, P. & Moloney, A.P. (2018). Visible and near infrared spectroscopy as an authentication tool: Preliminary investigation of the prediction of the ageing time of beef steaks. *Meat Science*, **142**, 52–58.

Morsy, N. & Sun, D.W. (2013). Robust linear and non-linear models of NIR spectroscopy for detection and quantification of adulterants in fresh and frozen-thawed minced beef. *Meat Science*, **93**, 292–302.

Mostert, R. & Hoffman, L.C. (2007). Effect of gender on the meat quality characteristics and chemical composition of kudu (Tragelaphus strepsiceros), an African antelope species. *Food Chemistry*, **104**, 565–570.

Nakyinsige, K., Man, Y.B.C. & Sazili, A.Q. (2012). Halal authenticity issues in meat and meat products. *Meat Science*, **91**, 207–214.

Nolasco Perez, I.M., Badaró, A.T., Barbon, S., Barbon, A.P.A.C., Pollonio, M.A.R. & Barbin, D.F. (2018). Classification of Chicken Parts Using a Portable Near-Infrared (NIR) Spectrophotometer and Machine Learning. *Applied Spectroscopy*, **72**, 1774–1780.

O'Mahony, P.J. (2013). Finding horse meat in beef products-a global problem. *Qjm*, **106**, 595–597.

Osborne, B.G. (2000). Near-Infrared Spectroscopy in Food Analysis. *Encyclopedia of Analytical Chemistry*, 1–14.

Pasquini, C. (2018). Near infrared spectroscopy: A mature analytical technique with new perspectives – A review. *Analytica Chimica Acta*, **1026**, 8–36.

Peng, Y. & Wang, W. (2015). Application of Near-infrared Spectroscopy for Assessing Meat Quality and Safety. *Infrared Spectroscopy - Anharmonicity of Biomolecules, Crosslinking of Biopolymers, Food Quality and Medical Applications*, 137–163.

Prieto, N., Andrés, S., Giráldez, F.J., Mantecón, A.R. & Lavín, P. (2008). Discrimination of adult steers (oxen) and young cattle ground meat samples by near infrared reflectance spectroscopy (NIRS). *Meat Science*, **79**, 198–201.

Prieto, N., Juárez, M., Larsen, I.L., López-Campos, Zijlstra, R.T. & Aalhus, J.L. (2015). Rapid discrimination of enhanced quality pork by visible and near infrared spectroscopy. *Meat Science*, **110**, 76–84.

Prieto, N., Roehe, R., Lavin, P., Batten, G. & Andres, S. (2009). Application of near infrared reflectance spectroscopy to predict meat and meat products quality: A review. *Meat Science*, **83**, 175–186.

Rahim, H.A. & Ghazali, R. (2012). The application of Near-Infrared Spectroscopy for poultry meat grading. In: *Proceedings - 2012 IEEE 8th International Colloquium on Signal Processing and Its Applications, CSPA 2012*. Pp. 58–62.

Reid, L.M. & Downey, G. (2006). Recent technological advances for the determination of food authenticity, **17**, 344–353.

Reis, M.M., Beers, R. Van, Al-Sarayreh, M., Shorten, P., Yan, W.Q., Saeys, W., Klette, R. & Craigie, C. (2018). Chemometrics and hyperspectral imaging applied to assessment of chemical, textural and structural characteristics of meat. *Meat Science*, **144**, 100–109.

Rhee, M.S., Wheeler, T.L., Shackelford, S.D. & Koohmaraie, M. (2004). The online version of this article , along with updated information and services , is located on the World Wide Web at : Variation in palatability and biochemical traits within and among eleven beef muscles 1 , 2 , 3 , 4, 534–550.

Roggo, Y., Chalus, P., Maurer, L., Lema-martinez, C. & Jent, N. (2007). A review of near infrared spectroscopy and chemometrics in pharmaceutical technologies, **44**, 683–700.

Schönfeldt, H.C. & Gibson, N. (2008). Changes in the nutrient quality of meat in an obesity context. *Meat Science*, **80**, 20–27.

Silva, L.C.R., Folli, G.S., Santos, L.P., Barros, I.H.A.S., Oliveira, B.G., Borghi, F.T., Santos, F.D. do., Filgueiras, P.R. & Romão, W. (2020). Quantification of beef, pork, and chicken in ground meat using a portable NIR spectrometer. *Vibrational Spectroscopy*, **111**.

Soon, J.M. & Manning, L. (2018). Food smuggling and trafficking: The key factors of influence. *Trends in Food Science and Technology*, **81**, 132–138.

Spink, J. & Moyer, D.C. (2011). Defining the Public Health Threat of Food Fraud. *Journal of Food Science*, **76**.

Starkey, C.P., Geesink, G.H., Oddy, V.H. & Hopkins, D.L. (2015). Explaining the variation in lamb longissimus shear force across and within ageing periods using protein degradation, sarcomere length and collagen characteristics. *MESC*, **105**, 32–37.

Verbeke, J., & Ward, R. W. (2006). Consumer interest in information cues denoting quality, traceability and origin: An application of ordered probit models to beef labels. *Food Quality and Preference, 17,* 453-467.

Walker, M.J., Burns, M. & Burns, D.T. (2013). Horse Meat in Beef Products- Species Substitution 2013. *Journal of the Association of Public Analysts (Online)*, **41**, 67–106.

Chapter 2

Literature review

Near infrared (NIR) spectroscopy: The current approach of species identification in meat and meat products

Introduction

The increasing human population puts more pressure on the food industries to supply more food. In the 1950's the world's population was estimated to be 2.53 billion, compared to 7.67 billion that was reported in 2019 (Statista, 2019). The drastic population increase that almost tripled within 67 years is associated with the challenge that all these people need to be nourished (Govindan, 2018). Thus, the high food demand is a challenge to food producers. Among other food commodities that are in high demand is meat and meat products.

Meat and meat products epitomize a large section of human food as it provides valuable proteins. Subsequently, that makes the consumers, retailers, and governmental control authorities concerned about its quality (Ballin and Lametsch, 2008). In addition to domestic meat, game meat consumption is becoming more prevalent in many countries around the world (Moreno-ortega *et al.*, 2018). Game meat is known to have high protein (20.0–23.8%) and low fat (0.8–2.45%) content, compared to beef (19.2% protein, 14.2% fat). Hence, it is a well-known offering of a healthy choice to red meat eaters (Hoffman, 2007). Since South African (SA) game animals are wild and free-roaming, in contrast to numerous game species in other parts of the world that are semi-domesticated, it has an advantage of being regarded as an organic food product (Hoffman & Wiklund, 2006; Mostert & Hoffman, 2007). For this motive, SA game meat is a highly priced product causing it to be an appealing target for species substitution (Ballin, 2010; Kamruzzaman *et al.*, 2013). Since meat is in demand, adulteration is the main concern to the consumers and meat industry. Fraudsters prefer to use products that are easy to adulterate and difficult to be discovered.

That brings us to the purpose of this literature review which explains the subject of food fraud, food adulteration, the importance of food labelling, and food authentication. Some of the utmost commonly used conventional analytical methods for meat products authentication are discussed. Subsequently, near infrared (NIR) spectroscopy, which is a rapid, environmentally friendly, non-destructive technique is discussed based on its historical overview, principles, instrumentation, and its application in meat and meat products.

Food fraud

The food fraud subject has been noted as a global public health and economical issue for quite some time in the food industry (Moore *et al.*, 2012; Valdés *et al.*, 2018). Spink and Moyer (2011) define food fraud as a collective term used to incorporate the considered and intentional substitution, addition, tampering, or misrepresentation of food, food ingredients, or food packaging; or false or misleading declarations made about a product, for economic gain.

Adulteration, counterfeiting, substitution, and deliberate mislabelling of food products are different types of food fraud which can occur for a variety of reasons. However, most of the time these food fraud types are associated to financial gain attained by adulteration intended to improve the perceived quality of products, lower manufacturing prices or allow shelf life extension (Abbas *et al.*, 2018). According to Ballin (2010), meat fraud is utmost expected to occur under the following types: meat substitution, meat origin, addition of non-meat ingredients, and meat processing. He continues to describe the major fraudulent practices encountered in the meat industry sector being caused by meat substitutions with other animal species, breeds, muscle types, proteins; falsifying of meat origin and animal feeding system (especially when it comes to free range and organic products); alterations of processing methods, and the addition of non-meat components such as soya. The most common fraud observed for meat products are substitution of species with a lower quality counterpart and mislabelling (Böhme *et al.*, 2019). As tempting as it might be to suppliers or retailers, the consequences of food fraud are devastating and might include damaging the reputation of the company practising it (van Ruth *et al.*, 2018).

In Figure 2.1 it is shown that out of all the food fraud cases reported by the European Commission in 2016, approximately 68% of them were animal and vegetable food products with high fat content (27% meat, 13% fish, 11% fats and oils, 10% milk and milk products, 4% nuts, nut products and seeds and finally, 3% animal by-products). In other countries a similar trend has been reported as well. On the other hand, in 2015 the UK Food Standards Agency (FSA) reported a cautionary recall of profitable palm oil adulterated by possibly carcinogenic red dye known as Sudan IV. Though a majority of food frauds are not possibly harmful, a selected number of them could be a public health risk for consumers (Valdés *et al.*, 2018).

Food adulteration

Food adulteration is a type of food fraud where a different food ingredient is deliberately and intentionally added for economic gain. This is an ancient problem, especially when there is a challenge between the product availability, and the market demand for a food product (Manning and Soon, 2014). A good example of food adulteration is the addition of melamine, a nitrogen-rich organic base usually used in plastic manufacturing industries. Melamine was once added to food products including milk in China, for the purpose of increasing nitrogen-based tests for protein content (Manning and Soon, 2014). The World Health Organisation (WHO) entitled China's international milk disaster as one of the largest food safety events the UN health agency has ever had to deal with in

recent years (Ellis *et al.*, 2012). Another example of adulterated food is the addition of non-meat components to meat processed products, such as additives or water (Sentandreu and Sentandreu, 2014). Whenever there are new methods to identify a certain adulterant, potential fraudsters can become aware of new techniques and then add or remove the targeted component from the adulterated foodstuff (Ellis *et al.*, 2012).

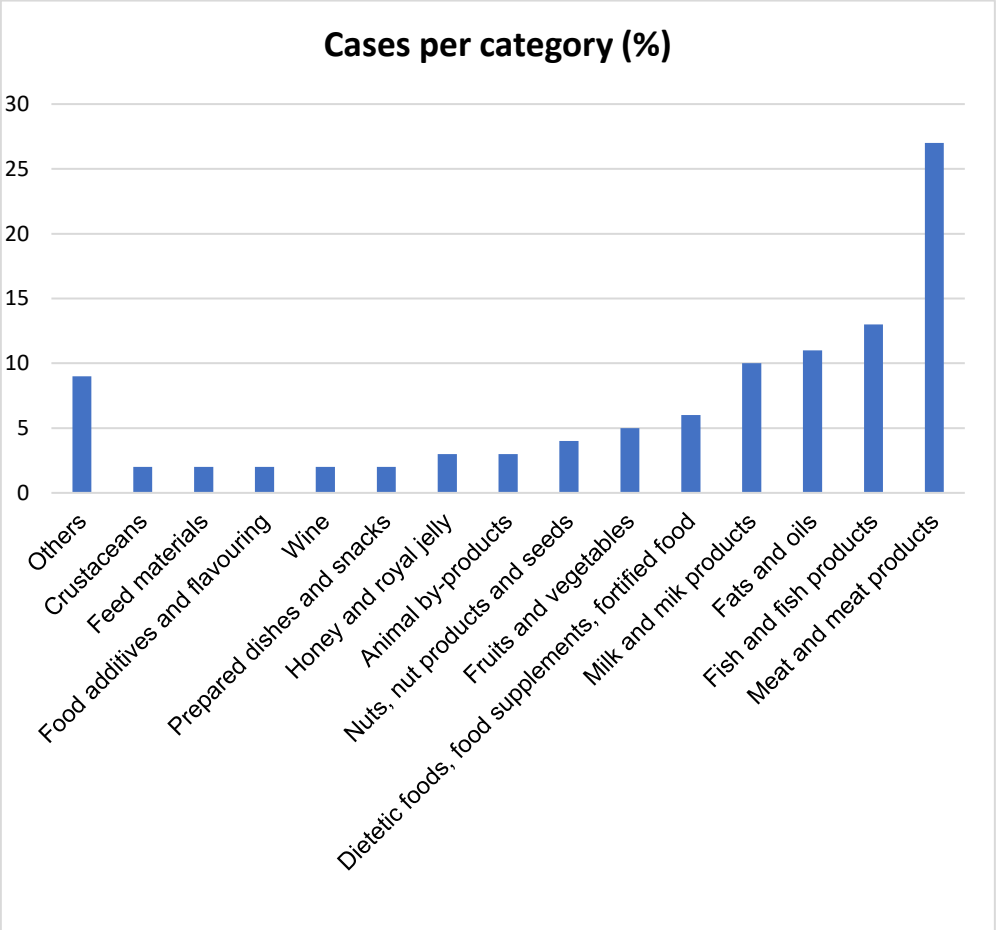

Figure 2.1 Cases of food fraud (%) per product category reported by EU-Member States in 2016, adapted from Valdés *et al.* (2018).

There is a rising concern that in some ways food fraud might be more unsafe than traditional hazards to the food supply (Spink and Moyer, 2011; Layton 2010). In some instances the adulterants used in these activities often are unconventional (Spink and Moyer, 2011; Moore *et al.*, 2012). As already mentioned above, adulteration is still a key problem for both the consumers and the food industry for many reasons. Adulteration has been practiced in the food industry for a while, and yet it is still difficult to detect, since the adulterant components are normally very similar to the original product. Thus, adulteration of meat is a modern problem involving quality, economic, and safety concerns since one cannot easily identify the species, source of origin, or certain muscle types when

evaluating meat visually (Kamruzzaman *et al.*, 2013). The horse meat scandal that transpired in Ireland in 2013 revealed that consumers are certainly encountering undeclared animal species in meat products (O'Mahony, 2013; Walker *et al.*, 2013). A similar incident occurred in South Africa, as Cawthorn, Steinman, & Hoffman (2013) discovered species that were not declared on the product labelling in sausages. Thus, the incidents of undeclared labelling in meat products whether reported or unreported have subsequently elevated the consumer's curiosity regarding traceability, quality, and origin of the food they eat (Verbeke and Ward, 2006).

Food labelling

It is required that the consumers must be informed with well-defined and trustworthy information about meat and meat products. The detailed information ought to be labelled in the packaging according to the appropriate laws and regulations. This is an obligation that has a great impact in the food industry since the declared food composition guides the consumer's selection of preferred food products (Valdés *et al.*, 2018). In South Africa, Regulation 146 of 2010, under the Department of Health (DoH) is specifically relating to the labelling and advertising of foodstuffs and must be applied in all food industries (DoH, 2010). Subsequently, everything declared on the food label must be authenticated.

Food authentication

Authentication is the process of determining whether an object is, in fact what is really declared to be on the label. The process involves techniques qualified to verify that the product matches the label statements and that it follows the requirements of applicable laws and regulations of the country of origin and where the product will be sold (Abbas *et al.*, 2018). The procedures of verification involve the testing of ingredient composition, the establishing of geographical origin, the nutritional properties, and the production technology (Abbas *et al.*, 2018; Nunes *et al.*, 2020). The authentication of food products is of extreme importance in the food industry, not only for economic reasons, but also for safety and health reasons (Abbas *et al.*, 2018; Valdés *et al.*, 2018). Since food adulteration can have serious consequences on human health, consumer confidence can be destroyed and eventually affect the market growth. Therefore, authentication of food is not only important for food retailers, processors, and consumers, but also for regulatory authorities (Abbas *et al.*, 2018).

Among other food products, the authenticity of meat is currently one of the major considerations in the multi-step food chain from production of animals on the farm to fork (consumer consumption of the final meat product) (Monahan *et al.*, 2018). In general, the challenges associated with meat authentication include many topics. Amongst the topics are the geographic origin, breed/variety identification, production method, the verification of the dietary background, technical processing, undeclared ingredients, discovery of genetically modified organisms (Woods and Fearon, 2009).

To minimize fraudulent occurrences, some sensitive and accurate detection methods are used as the methods of authentication. Thus, the introduction of conventional analytical methods for animal species identification in meat and meat products.

Conventional analytical methods used for meat and meat products authentication

Conventional analytical techniques have been widely used for the detection and classification of meat and meat products at species level (Amaral *et al.*, 2014; Bargen *et al.*, 2014; Doosti *et al.*, 2014; Von Surowiec *et al.,* 2011; Fæste and Plassen, 2008; Jonker *et al.*, 2008). These methods can be grouped into protein-based and DNA-based techniques. Within the protein-based techniques are the immunoassays, electrophoretic and chromatographic methods (Rahmati *et al.*, 2016; Chen *et al.*, 2010). On the other side, the DNA based molecular techniques can be categorized into DNA hybridization and polymerase chain reaction (PCR) techniques. These techniques have been used in the past decades and their ability has proven to detect species listed in Table 2.1 (Macedo-Silva *et al.*, 2000; Giovannacci *et al.*, 2004; Fæste & Plassen, 2008; Jonker *et al.*, 2008; Surowiec *et al.,* 2011; Amaral *et al.*, 2014; Doosti *et al.*, 2014; Von Bargen *et al.*, 2014; Druml *et al.*, 2015; Floren *et al.*, 2015). Out of all these techniques, only the most popular and commonly used methods will be discussed. That will include the immunological procedures, chromatography techniques, and the DNA based methods.

Immunological procedures

Immunological procedures are techniques that are based on the antigen and antibody interaction, which is protein specific (Ovesna *et al.*, 2008). Of the different immunological procedures (hemagglutination inhibition tests, agar gel immune diffusion (AGID), enzyme immunoassays (EIA), radioimmunoassay (RIA), non-enzymatic chromatographic immunoassays, enzyme-linked immunosorbent assay (ELISA)), ELISA is probably the most ideal for the species identification and authentication of meat products (Sentandreu and Sentandreu, 2014; Rahmati *et al.*, 2016). ELISA test kits are known of attaining high specificity and good sensitivity results compared to other methods. Due to their specific nature, they offer an advantage of being able to analyse many samples per kit within a short time (Hahnau & Julicher, 1996; Toldra & Reig, 2006). Another added advantage is that the technique has the qualitative and quantitative ability to detect the proteins in general (Reid *et al.*, 2006). Some reports on species detection of meat products achieved by ELISA methods include the study by Giovannacci *et al.* (2004) who could detect low contents of animal species whilst Martin *et al.* (1998) successfully managed to quantify pork adulteration in raw ground beef using ELISA methods.

It has been reported that for ELISA procedures the authentication capabilities are limited to unprocessed foods rather than to highly processed foods, as the protein structure denatures at high temperatures (Ovesna *et al.*, 2008). However, Giovannacci *et al.* (2004) considers that the limit of detection in processed meat products depends on several factors, including the severity of heat

processing, the fat content, the origin of muscle and the maturation state of the meat. In addition, as this is a screening technique it should be considered that some false positives may arise. For example, in the case where there is a structural resemblance of the assayed substance with other substances, interference may cause cross-reactions which may result to false positives. In cases of uncertainty, samples are usually subjected to confirmatory analysis for further confirmation (Reig & Toldra, 2008). Moving on, the chromatographic techniques will be considered.

Chromatography techniques

Chromatographic procedures are used to determine specific ingredients and are efficient in distinguishing a large amount of compounds in different food products (Abbas *et al.*, 2018). These techniques were earliest applied in organic chemistry (Zhang *et al.*, 2011). They make their separation based on the difference of distribution coefficient and adsorption ability of the material in two phases (Ellis *et al.*, 2012). They can be classified into gas chromatography (GC), liquid chromatography (LC), and high-performance liquid chromatography (HPLC). The difference between these chromatographic techniques is that gas chromatography uses gas a mobile phase, while liquid chromatography uses liquid as mobile phase. That makes the GC to have an advantage of a higher separation velocity and sensitivity compared to LC. The advantage of LC over GC is its wider application domain which could test 20% of organics with low boiling point (Ellis *et al.*, 2012). Not only it could test organics with low boiling point, nonetheless, macromolecules with high boiling point as well as thermal stability could be analysed as well (Zhang *et al.*, 2011).

Sjoberg *et al.* (1992), in their study to evaluate gas chromatographic method for detection of irradiation of chicken and chicken products, demonstrated that it was possible to analytically evaluate the irradiated chicken. They also found that it could be also possible to distinguish samples irradiated with doses below 5 kGy. In another case of adulterant identification in mutton by electronic nose and gas chromatography mass spectrometer (GC-MS), Wang *et al.* (2019) discovered that the GC-MS can be used to identify duck adulteration in mutton. Those results were confirmed by the electronic nose. In another case, species-specific peptide-based liquid chromatography-mass spectroscopy (LC-MS) was used to monitor three poultry species in processed meat products (Fornal and Montowska, 2019). They developed a qualitative liquid chromatography-triple quadrupole mass spectrometry (LC-QQQ) multiple reaction monitoring (MRM) method which allowed high confidence monitoring of duck, goose, and chicken meat (ten specific peptides). It was concluded that the developed LC-MS methods could be used for food authentication. And, it is acknowledged that the selection of analytical technique to apply has an impact on the nature of the target chemical; for example, both HPLC and GC may be suitable instruments to detect organic compounds added to meat products (Ballin, 2010). That leads the discussion to the next commonly used technique, the DNA based procedures.

DNA based techniques

DNA-based techniques have been employed and trusted for species authentication of meat products (Murugaiah *et al.*, 2009). These techniques have a unique attribute, also an advantage compared to protein-based methods, which is their stability in high temperature conditions (Lockley and Bardsley, 2000; Ballin *et al.*, 2009). Of the DNA-based molecular techniques, PCR techniques are most frequently used compared to DNA-hybridization methods. That could be because of the low sensitivity of the DNA microarrays (reported as the currently used principle for DNA-hybridization), compared to the PCR techniques (Ballin *et al.*, 2009). For the DNA-hybridization, the limit of detection (LOD) is reported to range from 0.1 to 0.01%, depending on the meat species (Rahmati *et al.,* 2016); while PCR techniques are described to have the lowest LOD that can be as low as 0.00004% (Ballin *et al.*, 2009).

In a PCR procedure, a single or several copies of the specific target DNA are amplified, and a thousand to million-folds of that particular DNA are produced within few hours (Reid *et al.*, 2006; Kumar *et al.,* 2013; Rahmati *et al.*, 2016). The approach of targeting a specific DNA (usually originating from mitochondrial or genomic DNA) gives the PCR method an advantage of high discriminating power. Thus, clear results are obtained, resulting in PCR being an efficient and reliable technique (Sentandreu and Sentandreu, 2014). A variety of PCR methods are available. Rahmati *et al.* (2016) categorized these methods as follows: species-specific PCR, PCR sequencing, restriction fragment length polymorphism (PCR-RFLP), single-strand conformation polymorphism (PCR-SSCP), multiplex PCR, quantitative competitive PCR (QC-PCR) and the real-time PCR. Therefore, the analytical technique of choice and the DNA targeted has a great influence on the limit of species detection (Ballin *et al.*, 2009). And also, when choosing the target DNA to be amplified it is important to know whether the analysis is for qualitative or quantitative species determination, because each target DNA type responds differently. For example, the mitochondrial target DNA is best appropriate for qualitative species determination because of its low LOD, high mutation rate and most cells have multiple copies of the mitochondrial DNA. In contrast, for quantitative species determination the same mitochondrial DNA has its shortcomings, which include its inability to perform a meaningful quantification based on neither DNA nor meat contents. In addition, the large variation of mitochondria in different tissues might be a setback. That makes the single copy genomic DNA a better preference for quantitative analysis because based on its DNA equivalents, a constant number of copies enables quantification (Ballin *et al.*, 2009).

Jonker *et al.* (2008) identified the species of beef, pork, horse, mutton, chicken, and turkey from processed meat products using real-time PCR. In their study they managed to detect levels as low as 0.01%, demonstrating how low it can detect species. Then again, species-specific PCR has been successfully utilized in the detection of undeclared meat species in South African meat products (Cawthorn *et al.*, 2013), and also, in a study of halal authentication of raw meats, PCR-RFLP identification assay yielded excellent results for the detection of pig species (Aida *et al.*, 2005).

Targeted approaches like the DNA-based and chromatography methods happen to be frequently used for the detection of specific ingredients or substitution thereof. In addition, their advantages such as high accuracy, sensitivity and selectivity make them to be the most preferred techniques in the official food control laboratories.

All these conventional methods, as good as they are, have some common shortcomings which include their expensive price, extended duration of analysis, whilst the laboratory throughput is limited (Jonker *et al.*, 2008; Fajardo *et al.*, 2010; Cawthorn *et al.*, 2013). Due to the cost of these conventional methods, meat products are not regularly tested. Therefore, there is a need for a rapid screening method for potential substitution of meat products; and near infrared spectroscopy offers that (Ding and Xu, 2000; Cozzolino and Murray, 2004).

NIR spectroscopy

NIR historical overview

Near infrared (NIR) spectroscopy is a rapid, non-invasive, chemical free, non-destructive, and environmentally friendly method of analysis. It measures the reflection or transmission of radiation from the NIR region of the electromagnetic spectrum (Davies, 1998; Osborne, 2000; Cen and He, 2007). The NIR region is located in the wavelength range of 780 to 2500 nm (12 800–4 000 cm^{-1}) (Davies, 1998; Osborne, 2000; Cen and He, 2007). In addition to the NIR, there are two other regions of infrared: the mid (2500–15000 nm) and the far (15000–50000 nm) infrared regions. Thus, near infrared is exactly located between the visible (380–780 nm) and the mid infrared (MIR) (2500–15000 nm) regions in the electromagnetic spectrum (Manley, 2014).

The NIR region was discovered and recorded by Frederick William Herschel in 1800 on his experiments while investigating the illuminating power of coloured rays (Herschel, 1800). For some time, Herschel's NIR findings were not applied until in the 1950s, when Karl Norris first realized that computers could be used to analyse the mass of absorbers. Karl Norris together with his co-workers established the spectroscopy development by demonstrating the possibility of using the NIR information to determine moisture content of soybeans. Later, NIR spectroscopy was first demonstrated for commercial application in 1972, and the system was fully online in 1976. One of the first experiments where NIR spectroscopy was first used was the analysis of wheat protein and moisture content (Williams, 2006). The technology that was first used in the cereal industry has now been widely used in all agricultural sectors, pharmaceutical, and mining industries. In recent years the near infrared technique has shown to be a modern system for quality and safety assessment of food commodities, including meat products (Cen and He, 2007).

Principles/ how does it work?

Near infrared (NIR) spectroscopy measures the reflecting/transmitting light of the electromagnetic radiation in the wavelength of 780–2500 nm (Davies, 1998; Osborne, 2000; Blanco and Villarroya, 2002; Cen and He, 2007). The principle of NIR spectroscopy depends on the absorption**,** reflection,

transmission, and/or scattering of light in or through the sample material (Kademi *et al.*, 2019). A typical NIR spectrum consists of several bands formed by absorption peaks and valleys due to overtones of fundamental bond stretching resulting from overlapping signals (Davies, 1998). Absorption bands observed in the near infrared region are formed when NIR radiation of specific frequencies vibrate at the similar frequency. Thus, producing the specific molecular bond in the sample in the form of X-H bonds, where X is a carbon, nitrogen, oxygen, sulphur (Shenk *et al.,* 1992; Roggo *et al.*, 2007; Shenk *et al.,* 2008; Manley, 2014; Peng and Wang, 2015). In these bonds the meaningful information of the sample is contained. Thus, a unique spectrum which acts as a 'fingerprint' is produced when the electromagnetic radiation absorbed from those molecular bonds in the NIR wavelengths is recorded (Prieto *et al.*, 2017; Peng and Wang, 2015). In general, every molecule containing hydrogen will have a measurable NIR spectrum. The obtained spectral signature is interpreted statistically using chemometric analysis. NIR spectra include broad bands that arise from absorptions in overlapping wavelengths. The absorption measured by NIR spectroscopy generally match the overtones and combinations of vibrational modes involving C–H, O–H, and N–H chemical bonds. These absorption bands are the results of the overtones and combinations of molecular vibrations. The major bands of the NIR region are usually at the second and third overtone regions. Bands that are commonly found in the near infrared region are summarized and displayed in Figure 2.2. It is noted in Figure 2.2 that the combination bands are closer to the mid infrared region.

Table 2.1 Application of conventional techniques in authentication of meat and meat products

Animal origin	Purpose of analysis	Analytical Technique	Reference
Turkey, beef, sheep, pork	Species identification of meat products	ELISA	Giovannacci *et al.*, 2004
Bovine, chicken, swine, horse	Hamburger meat identification	dot-ELISA	Macedo-Silva *et al.*, 2000
Different fish species	Determination of fish in foods	sandwich ELISA	Fæste and Plassen, 2008
Chicken and pork	Detection of mechanically recovered meat	GC-MS	Surowiec *et al.*, 2011
Horse, pork and beef	Detection of horse and pork in highly processed food	HPLC	Von Bargen *et al.*, 2014
Beef, sheep, pork, chicken, donkey and horse	Detection of beef, sheep, pork, chicken, donkey, and horse meats in food products	PCR-RFLP	Doosti *et al.*, 2014
Beef, pork, horse, sheep, chicken, turkey	Species identification in meat products	real-time PCR	Jonker *et al.*, 2008
Beef, pork and horse meat	Species identification and quantification in meat and meat products	dd-PCR	Floren *et al.*, 2015
Pork, cow, hare, red deer, and wild rabbit	Authentication of traditional game meat sausage	species-specific PCR	Amaral *et al.*, 2014
Fallow deer, red deer, and sika deer	Detection and quantifying adulteration	Real-time PCR	Druml *et al.*, 2015

ELISA (Enzyme-Linked Immunosorbent Assay), HPLC (High Performance Liquid Chromatography), GC-MS (Gas Chromatography-Mass Spectrometry), PCR (Polymerase Chain Reaction), RFLP (Restriction Fragment Length Polymorphism), dd (droplet digital)

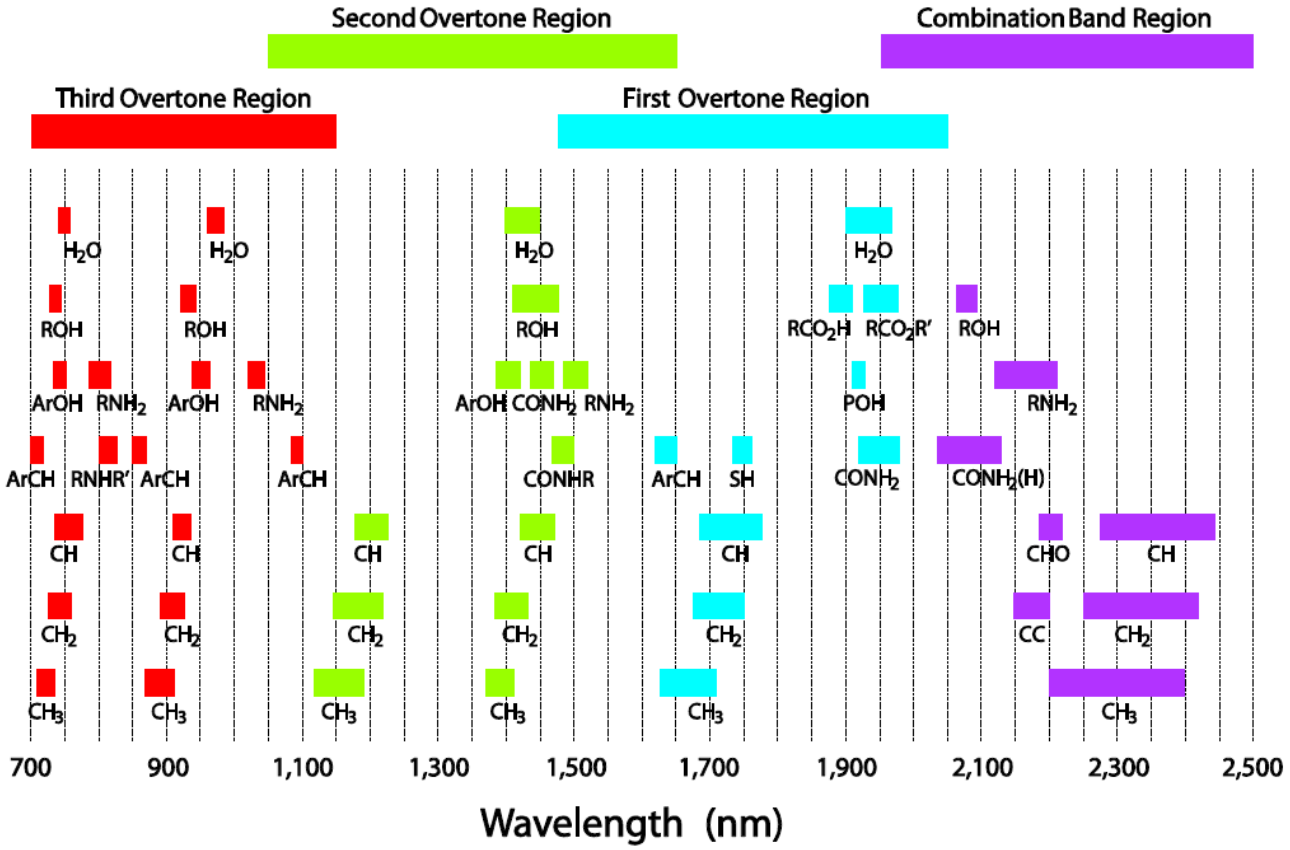

Figure 2.2 Major analytical bands and relative peak positions for prominent near infrared absorptions. Most chemical and biological products exhibit unique absorptions that can be used for qualitative and quantitative analysis; adapted from Metrohm blog, https://metrohm.blog/2020/02/24/nir-spectroscopy-benefits-part-2/.

Getting the best out of light

There are different pathways that light energy can travel through or from a sample. Figure 2.3 below illustrates the different pathways of light (reflection, absorption, and transmittance) in or through a sample. When the light energy is reflected from the surface, reflectance is revealed in 3 setups; i.e. regular (specular), external diffuse reflectance, and scattering. Regular reflectance occurs when the light incident angle with the object surface equals with the angle at which it is reflected. In this case, usually little or no interaction with the sample. Thus, no information is carried. While the external diffuse reflectance carries the information concerning the characteristics and the composition of the object. In this case, both the light source and the detectors should always be at the same side, and the detectors are usually positioned at an angle of 45 degrees to the sample plane to avoid specular (regular) reflection. The remaining part of light is scattered through the meat sample (Reis *et al.,* 2018; Mollazade *et al.,* 2012; Alander *et al.*, 2013). On the other hand, some of the energy passes right through the sample in transmission mode (Williams *et al.,* 2019). In transmission mode the incident light is measured as it exits the sample at a point directly opposite to the light source. The detector is usually placed at an angle of 180 degrees, especially when solid samples are being analysed (Alander *et al.*, 2013). On the other side, some energy gets scattered and absorbed within the sample. From Figure 2.3 it is observed that only the light energy that can reach the detectors are able to carry the meaningful information (Williams *et al.,* 2019).

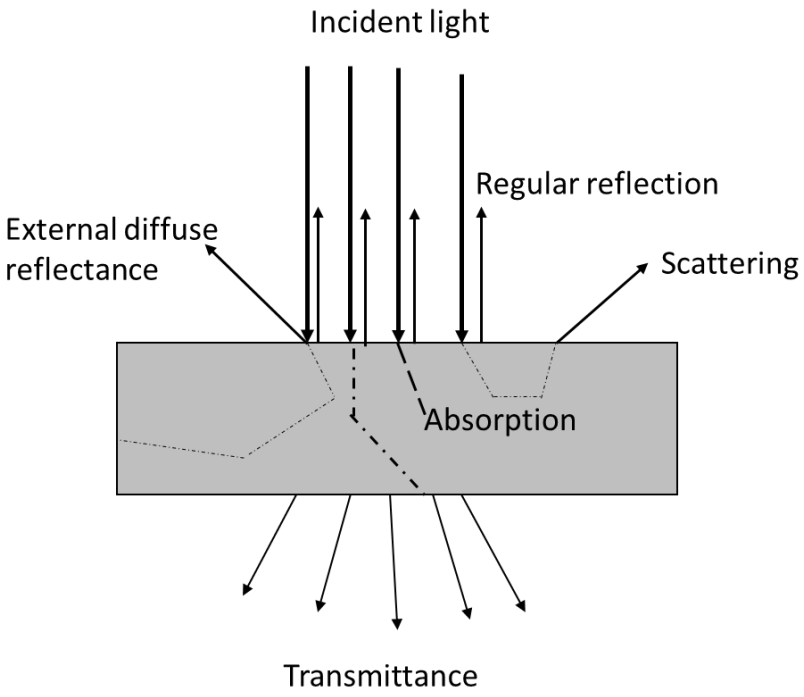

Figure 2.3 The pathways of light in a sample, adapted from Mollazade *et al.* (2012)

And then, there is the Transflection mode which occurs when both the reflection and transmission modes combine. In this case the sample is usually located as if reflection is measured, and a reflector is positioned on the other side of the sample opposite to the light source, resulting in reflecting the light transmitted through the sample back to the detector. This mode is usually applied for NIR devices that have no transmission capabilities (Alander *et al.,* 2013).

NIR instrumentation

A typical NIR instrument mainly consists of a light source, a detector, a wavelength selection system, and a signal processor (Blanco and Villarroya, 2002). Generally, light source instruments can be thermal (tungsten coil or a halogen lamp) and non-thermal (Light Emitting Diode (LED) sources) (Blanco and Villarroya, 2002; Manley and Baeten, 2018); and the sample can be illuminated from either above or below. Then, the commonly used detectors for the NIR spectral region are based on silicon, PbS (lead sulphide), and InGaAs (Indium Gallium Arsenide) photoconductive materials. Amongst them, the cooled InGaAS semiconductors are the most recognized, and employed by modern instruments because of their best quality, possessing a high response speed, and a very high detectivity in the 1100–1750 nm region (Pasquini, 2003, 2018). Even though Mercury cadmium telluride (MCT) detectors were employed in the beginning of NIR instrumentation, they are still used regardless of their low performance over the NIR range. Currently, there is a promising new detector functioning as a solid-state photomultiplier. It is known to have an outstanding performance in the 1000–1700 nm region compared to the present detectors. Nonetheless, no marketable instruments have implemented it up to now (Pasquini, 2003).

In addition to detectors, the NIR instruments are also classified according to the wavelength selection expertise. The available wavelength selection categories are, the filter-based instruments, LED sources, dispersive optics-based instruments, and Interferometric (Fourier Transform) (Blanco and Villarroya, 2002; Pasquini, 2003). Within the wavelength selection classes, NIR spectrophotometers can be of two types, namely discrete wavelength and whole spectrum, and most miniatures have a discrete wavelength spectrum (Blanco and Villarroya, 2002). Whereas the whole spectrum instruments which maybe of Fourier Transform (FT) NIR type. The whole spectrum instruments have an advantage of being much more flexible than the discrete wavelength and can be used in a wide variety of situations. On the other hand, the discrete wavelength spectrophotometers can also be called the LED (light-emitting diodes) based, because of their mode of wavelength selection (Blanco and Villarroya, 2002).

Generally, instrument selection should be based on end purpose. For example, Fourier-based instruments must be of preference when calibration transference and wide spectral range are of concern. And, for low cost instruments to be applied for routine purposes in the field, filters and LEDs are the best choice (Pasquini, 2003).

The first commercial NIR spectroscopy instrument that employed a digital computer and allowed the operator to optimize the wavelength range was the ADA, and it was designed and built

by Neoec (now Foss Analytical Inc, Denmark) in 1974. Again in 1978, Neotec introduced the first computerized NIR spectroscopy scanning spectrophotometer, the Model 6350. This model was the first one to display the spectrum across the entire wavelength range from 1100 to 2500 nm. And, since then all other companies followed the trend of developing computerized scanning spectrophotometers (Williams *et al.,* 2019). Then, the miniaturized spectrophotometers across the vibrational spectroscopy (Raman, mid-infrared, and NIR) instruments were launched with the aim of taking the instrument to the sample, rather than taking the sample to the instrument. The miniaturized portable NIR spectroscopy devices offer a great potential for on-site quality control not only in the meat sector but also all other food industries (Kademi *et al.*, 2019).

Desktop and miniaturized instrumentation

Desktop visible near infrared (vis-NIR) spectrophotometers have been applied since the early studies on meat species classification and prediction (Cozzolino and Murray, 2004; Monroy *et al.*, 2010; Alamprese *et al.*, 2013; Balage *et al.*, 2015; Prieto *et al.*, 2015). Amongst the desktop spectrophotometers are the Fourier Transform NIR spectroscopy (FT-NIR) which used to limit their applicability to liquids. However, in recent developments, an opportunity has opened to the field of solid samples application which resulted in the introduction of a turntable/rotating cell technique (Williams *et al.,* 2019). Amongst other things, the advantage of the FT technology is the ability to provide highest spectral resolutions and wide spectral range that extends throughout the entire NIR spectral range. Even though the desktop NIR instruments might deliver more accurate results because of their wide wavelength range, the fast-paced industrial meat sector has a challenge of depending on large and expensive desktop devices for meat analysis. Hence, the introduction of miniaturization of Raman, mid infrared, and NIR instruments is the new era. Miniaturization of NIR instrumentation involves acquiring the key features such as compactness, speed capability, stability, and portability in any field of purpose (Yan and Siesler, 2018).

One of the first studies done using NIR handheld devices was the authentication of fish fillets (O'Brien *et al.*, 2013). In 2016, Wei *et al.* self-developed a LED based handheld NIR instrument for the estimation of freshness in pork meat. Therefore, the creative developments in NIR instrumentation have unlocked new opportunities for NIR applications. The development of portable micro-electromechanical supported miniaturized spectrometers is appropriate (Borin *et al.*, 2006; O'Brien *et al.*, 2013; Wei *et al.*, 2016; Karunathilaka *et al.*, 2017; Grassi *et al.*, 2018; Wiedemair *et al.*, 2018). Thus, miniaturization of NIR spectrometers has attained a remarkable level of technology compared to Raman and MIR spectrometers. The mobility of these devices permit the portable NIR spectrometers the opportunity of being used for onsite and in-field testing (Yan and Siesler, 2018). Thus, creating an opportunity for the instruments to be frequently used. The only factor that will sustain the miniaturization in the marketplace is their performance compared to other devices. Figure 2.4, 2.5, and 2.6 below are a demonstration of the desktops and portable NIR instruments, respectively. Table 2.2 outlines the success of the handheld instruments.

Figure 2.4 Desktop UV-Vis near infrared spectrophotometer, adapted from https://www.lpdlabservices.co.uk/analytical_techniques/chemical_analysis/uv_vis_nir.php. Accessed 20/09/2020

Figure 2.5 FT-NIR Spectrophotometer: adapted from https://www.informmagazine-digital.org/informmagazine/november_december_2015/MobilePagedArticle.action?articleId=686069#articleId686069. Accessed 20/09/2020.

Figure 2.6 Illustration of a portable NIR spectrophotometer scanning meat samples using a 2 mm thick glass Steriplan petri dish to prevent the meat surface moisture coming into direct contact with the instrument.

Table 2.2 An outline of the successful use of Handheld devices

Spectrophotometer	Food type	Research purpose	Wavelength (nm)	Pre-processing	Classification algorithm	Reference
Micro Phazir NIR	Extra virgin olive oil	Authentication	1600–2400	SNV	SIMCA	Karunathilaka *et al.*, 2017
Cary 5G UV/VIS/ NIR	Powdered milk	Alternative calibration method for milk adulterants	1026–2400	MSC	PLSR, SVM	Borin *et al.*, 2006
MicroNIR Onsite	Game muscle types	Discrimination	908–1700	SNV-Detrend, 1st derivative	PLS-DA	Dumalisile *et al.*, 2020
Micro Phazir NIR	Chicken, pork, turkey, beef, mutton, and horse meat	Detection of meat fraud	1600–2439	SNV, Savitzky Golay 2nd derivative	SVM, PLSR	Wiedemair *et al.*, 2018
JDSU MicroNIR	Fish fillets	Authentication	887–1667	MSC	PCA, SIMCA	O'Brien *et al.*, 2013
MicroNIR Onsite	Fish fillets	Authentication	950–1650	SNV, MSC, Smoothing Savitzky Golay, 1st, 2nd derivative Savitzky Golay	SIMCA, LDA	Grassi *et al.*, 2018
Self-developed LED based	Pork	Freshness estimation	400–1100	Unprocessed	MLR, PLSR	Wei *et al.*, 2016

PLSR: partial least squares regression; MLR: Multiple linear regression; SIMCA: soft independent modelling of class analogy; MSC: multiplicative scatter correction; PLS-DA: partial least squares discriminant analysis; SVM: support vector machine; SNV: standard normal variate

Applications

Several investigations on authentication of meat and meat products have been effectively done using near infrared technologies. Table 2.3 summarizes the successful work already done. In addition to those listed in Table 2.3, the most recent studies are discussed.

Moran *et al.* (2018), López-Maestresalas *et al.* (2019), and Savoia *et al.* (2020) combined NIR with chemometrics to attain satisfactory classification models of meat species. In a preliminary investigation, Moran *et al.* (2018) predicted the ageing time of beef steaks to assess visible and NIR spectroscopy (Vis-NIR; 400–2400 nm) as an authentication tool. They applied partial least squares discriminant analysis (PLS-DA) to classify steaks based on the number of days aged. The overall correct classification rate achieved ranged from 94.2 to 100%, which indicated the ability of the Vis-NIR instrument to discriminate the steaks based on different ageing periods. Furthermore, López-Maestresalas *et al.* (2019), investigated the ability of NIR spectroscopy to detect adulteration in minced lamb and beef mixed with other types of meat using the 1100–2300 nm region of the spectra. Using PLS-DA, overall classification results between 78.9 and 100% were achieved. Moreover, in a study of predicting meat quality traits in the abattoir, Savoia *et al.* (2020) used the portable Vis-NIR (350–1830 nm) and handheld Micro-NIR Pro (905–1649 nm) to analyse the quality of traits of Piemontese young bulls. They discovered that it was possible for both spectrometers to obtain the major sources of variation in most of the meat quality attributes.

In recent studies NIR spectroscopy is being coupled with machine learning (ML), and is delivering excellent and promising results (Nolasco Perez *et al.*, 2018; Parastar *et al.*, 2020). Nolasco Perez *et al.*, 2018, classified chicken portions (breasts, thighs, and drumstick) using NIR (900–1700 nm) coupled with machine learning procedures. They compared support vector machine (SVM) as well as random forest algorithms for chicken meat classification. The results confirmed the ability of NIR to differentiate the chicken parts with 98% accuracy. Parastar *et al.* (2020) studied the integration of handheld NIR and machine learning to measure and monitor chicken. They discriminated fresh from thawed meat, and classified chicken fillets in a wavelength range of 908–1676 nm according to their growth conditions with good accuracy. They applied both random subspace discriminant ensemble (RSDE) and other common methods (PLS-DA, SVM, and artificial neural network (ANN). However, the RSDE outshone the other methods with a classification accuracy of greater than 95 %.

Table 2.3 Examples of NIR spectroscopy and NIR hyperspectral imaging applications concerning the evaluation of meat and meat products

Technique	Meat type	Research purpose	Wavelength (nm)	Classification	Reference
NIR spectroscopy	Seafood	Authentication of seafood	900–1700 nm	PCA, SIMCA	O'Brien *et al.*, 2013
	Oxen	Estimation of chemical composition of oxen meat samples	1100–2500 nm	PLSR	Prieto *et al.*, 2006
	Beef and kangaroo	Differentiation of beef and kangaroo meat	400–2500 nm	MLR, CDA	Ding and Xu, 1999
	Beef hamburger	Detection of beef hamburger adulteration	400–2500 nm	PCA, CDA, KNN	Ding and Xu, 2000b
	Minced beef	Detection and quantification of adulterants in fresh and frozen-thawed minced beef	400–2500 nm	PLSR, PLS-DA, LDA	Morsy and Sun, 2013
	Adult steers (oxen) and young cattle	Discrimination of adult steers (oxen) and young cattle ground meat samples	1100–2500 nm	PLSR	Prieto *et al.*, 2008
	Cattle, llama and horse meat	Identification of cattle, llama and horse meat	400–2500 nm	PLSR	Mamani-Linares *et al.*, 2012
	Beef LTL muscles	Prediction of quality attributes	400–2500 nm	PCA, PLSR	Andrés *et al.*, 2008
	Beef LTL	Prediction of organoleptic properties of beef	800–2500 nm	PLSR	Leroy *et al.*, 2004

	Cattle meat	Chemical and discriminant analysis of bovine meat	400–2500 nm	PLSR	Alomar *et al.*, 2003
	Lamb meat	Prediction of sensory characteristics of lamb	400–1900 nm	PCA	Andrés *et al.*, 2007
	Beef, lamb, chicken and pork	Identification of animal meat muscles	400–2500 nm	PCA, PLSR	Cozzolino and Murray, 2004
NIR hyperspectral imaging	Lamb muscles	Discrimination of lamb muscles	900–1700 nm	PCA, LDA	Kamruzzaman *et al.*, 2011
	Fresh beef	Predicting colour, pH and tenderness of fresh beef	900–1700 nm	PLSR	Elmasry *et al.*, 2012
	Porcine LD muscles	Tenderness prediction	900–1700 nm	PLSR	Barbin *et al.*, 2013b
	Minced lamb	Meat adulteration	900–1700 nm	MLR, PLSR	Kamruzzaman *et al.*, 2013
	Spanish cooked ham	Prediction of water and protein contents and quality classification	900–1700 nm	PLSR	Talens *et al.*, 2013
	Raw salmon fillets	Assessing and visualising tenderness distribution	400–1720 nm	PLSR, LS-SVM	He *et al.*, 2014
	Minced beef	A tool for detection of horse meat adulteration	400–1000 nm	PLSR	Kamruzzaman *et al.*, 2015b
	Pork	Grading and classification of pork	900–1700 nm	PCA	Barbin *et al.*, 2012

PCA: principal component analysis; PLSR: partial least squares regression; PLS-DA: partial least squares discriminant analysis; SIMCA: soft independent modelling of class analogy; LDA: linear discriminant analysis; MLR: multiple linear regression; CDA: canonical discriminant analysis; KNN: K-nearest neighbour and LS-SVM: least square support vector machine

Prediction processes

NIR spectroscopy is regularly used for both qualitative and quantitative analysis of agricultural and food commodities (Peng and Wang, 2015). Figure 2.7 below is an illustration of the process of model prediction. The first step in building models is the spectral acquisition using the NIR technique of choice, depending on the purpose of the research. Once the spectra are collected, the next step is the spectral pre-treatment, and subsequently the calibration and building of desired models. This can be accomplished by the application of chemometrics.

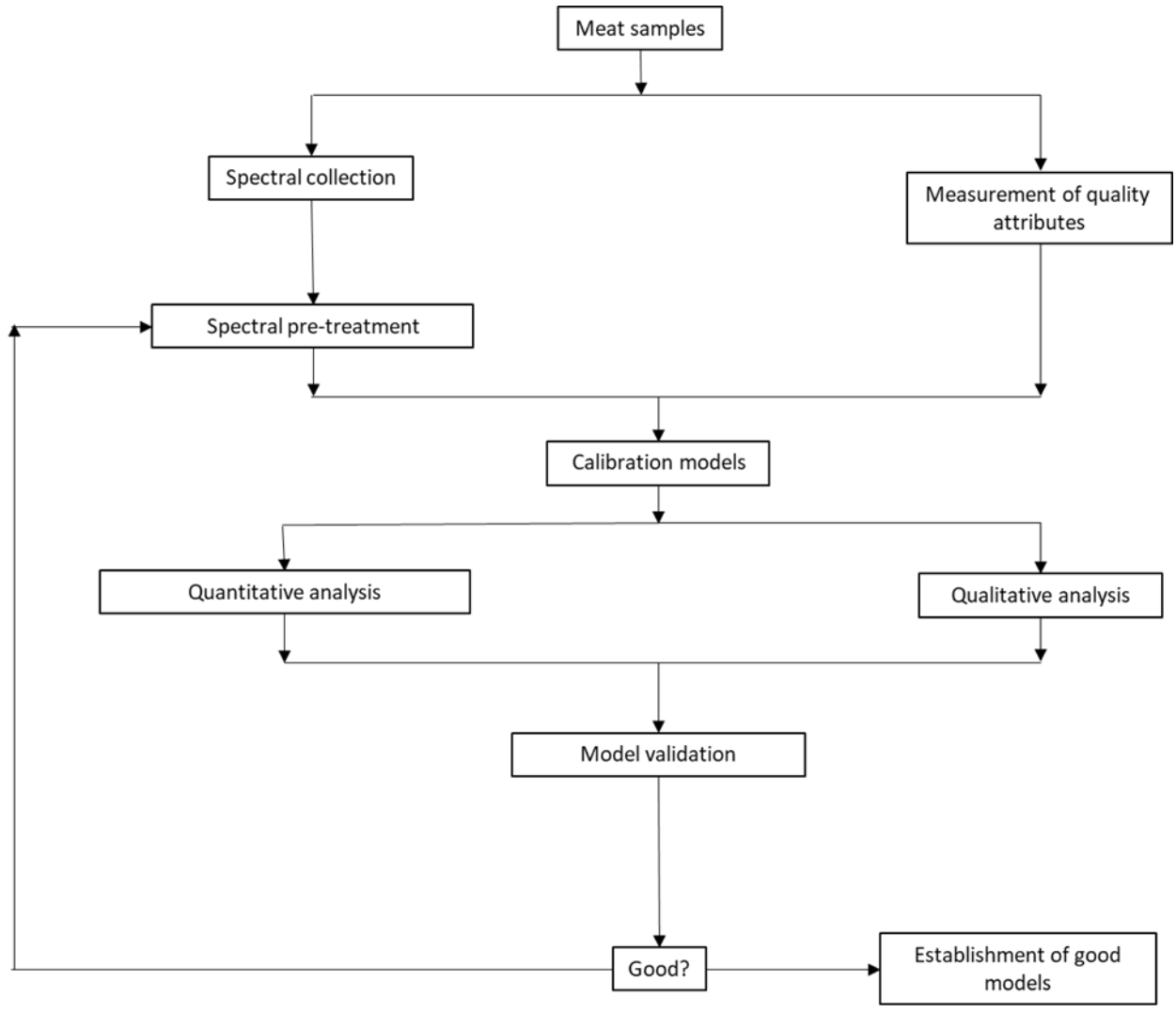

Figure 2.7 The process of model prediction, adapted from Peng and Wang, (2015)

Chemometrics

Spectroscopic methods are generally used for the identification or classification of samples by recognizing particular or complex chemical or physical properties of the sample. However, spectral data consists of several hundreds to thousands of wavelengths, which can be difficult to interpret without the help of chemometrics (Lohumi *et al.*, 2015). Thus, chemometrics explains the statistical and mathematical methodologies used to improve the understanding of chemical information and to obtain useful information from large and complex data sets (Varmuza and Filzmoser, 2009)**.** Chemometrics was introduced in the late 1960s by several research groups in the analytical and physical organic chemistry sphere with the purpose of introducing instrumentation giving multivariate responses, and the availability of computers (Geladi, 2003). It originated from the requirement to analyse data having many variables (Geladi *et al.*, 1985). Thus, in simple terms, Williams *et al.* (2019) describes chemometrics as the "marriage" between spectroscopy and applied statistics. Data collection, which is the first step of chemometrics includes the sample selection, measurements, and chemical analysis (Alander *et al.*, 2013).

Pre-processing

Generally, the spectral data acquired from the NIR spectrometer usually include the background information and noise in addition to the sample information. Therefore, it is necessary to pre-process spectral data to obtain reliable, accurate and stable calibration models (Cen and He, 2007). Pre-processing (mathematical transformation) of spectral data is the most essential step after spectral data collection, before classification can be applied (Rinnan *et al.*, 2009). The purpose of pre-processing data is to reduce and remove non-chemical features from the spectral information and prepare the data for further processing. To reduce the scattering effects, baseline shifts and background information (noise) in the data, different pre-processing methods (Baseline offset correction, Linear baseline correction, Derivatives, Savitzky-Golay derivatives, Detrending, Normalization, Standard Normal Variate (SNV), multiplicative scatter correction (MSC), Smoothing method, and Savitzky Golay Smoothing) are applied (Helland *et al.*, 1995; Luypaert *et al.*, 2004; Cen and He, 2007; Manley and Baeten, 2018). Amongst these methods, a few will be discussed.

Multiplicative Scatter Correction (MSC) (Geladi *et al.*, 1985) pre-processing is one of the commonly used pre-processing methods. It is a very useful and powerful correction method for removing additive and multiplicative differences such as changes mainly caused by samples with inconsistent particle sizes (Manley and Baeten, 2018). Detrend correction is applied to remove nonlinear trends and baseline shifts in a spectroscopic data. The log (1/R) values in NIR spectra, with R being the reflectance, often shown increasing trend between 1100 and 2500 nm (Luypaert *et al.*, 2004).

Standard Normal Variate (SNV) correction is usually applied to remove the scatter effects by centering and scaling each individual spectrum. To perform this correction, the mean of each spectrum is subtracted from the whole spectrum and these centred values are divided by the

standard deviation of each spectrum. Sometimes this is applied in combination with detrending (DT) (Barnes *et al.*, 1989), baseline shift and curvature in spectroscopic data. It must be noted that the use of a combination of pre-processing methods is common in the literature (Rinnan *et al.*, 2009), however in this principle there is a sequence that is followed e.g. SNV can be followed by Detrend (SNV+Detrend), not the other way round. Savitzky Golay smoothing moving average (Savitzky and Golay, 1964) is a moving window averaging method. Each value in a row can be replaced by the average of its nearest neighbours to reduce the effect of noise on a spectrum by removing small variations.

Derivatives (Savitzky and Golay, 1964) are one of the most popular pre-processing algorithms used for spectroscopic applications. They are used to improve slight spectral differences between samples; and resulting in resolving overlapped bands to correct the baseline shifts. In such cases, the 'hidden' information in a spectrum may be more easily revealed when working on a first or second derivative. Therefore, Savitzky-Golay 2nd derivative is usually applied to smooth the noise fluctuations without introducing distortions to the data, and to expose the peaks that were not clearly visible in the original spectra. The use of first and second derivatives of the log 1/R spectral data was developed and introduced by Karl Norris during the 1974-1978 period (Williams *et al.,* 2019).

Principal component analysis (PCA)

Principal component analysis (PCA) (Cowe & McNicol, 1985) is the most widely used unsupervised chemometric technique applied as a screening method of multivariate statistical data (Wold, 1987). Its main objectives include to reduce a multivariate dataset into few principal components (PCs), to identify important variables, and to detect outliers. Thus, the statistical procedure uses an orthogonal transformation to transform a set of observations of possibly correlated variables into a set of values of linearly uncorrelated variables called principal components. This results in providing an arrangement of PCs in decreasing rates of variance with corresponding scores and loadings. These new PCs define a new component for explaining the structure of the data (Ghosh *et al.*, 2016). It is usually performed to illustrate the distribution and potential clustering of samples according to the spectral features of each species.

In simple terms, PCA decomposes the raw data matrix (**X**) into scores and loadings, according to the following equation (Wold, 1987):

$$\mathbf{X} = \mathbf{t_1 p_1^t + t_2 p_2^t + \ldots\ldots\ldots\ldots + t_k p_k^t + E}$$

where:

X = raw data matrix

t = scores vector

p = loadings vector

E = residuals

k = must be less than or equal to the smaller dimension of **X**

In this equation, **E** is that part of the original matrix **X** that cannot be accounted for by available PCs. It cannot be explained by the model as it represents the error (background noise). Thus, the explainable part is $t.p^t$, which forms the actual structure of the PC model.

Qualitative analysis (Classification methods)

Classification methods are supervised techniques that group samples together according to their class, for identification purposes. Among the commonly used techniques are: linear discrimination analysis (LDA) (Fisher, 1936), partial least squares discriminant analysis (PLS-DA) (Barker & Rayens, 2003), and soft independent modelling of class analogy (SIMCA) (Wold, 1976; Brereton, 2011).

LDA is a supervised classification technique that provides a linear transformation, so that samples belonging to the same class are close together but those from different classes are far apart from each other (Fisher, 1936). It is known to be the simplest of all possible classification methods. The objective of LDA is to determine the best fit parameters of a class with similar features to develop a model. It discovers the linear combination of features which best separate two or more classes which may be used as linear classifiers (Balabin *et al.*, 2010). The discrimination model is calculated using all samples, which implies the model cannot be easily validated using external samples (Granato *et al.*, 2018).

PLS-DA consists of a classical Partial Least Square (PLS) regression where the response variable expresses the class membership of the statistical units. PLS-DA considers only those variables for analysis that already define the groups of individuals and do not allow for other response variables. Consequently, all measured variables play the same role with respect to the class assignment. PLS components are built by trying to find a proper compromise between describing the set of explanatory variables and predicting the responses. Generally, PLS-DA is performed in order to sharpen the separation between groups of observations, such that a maximum separation among classes is obtained, and to understand which variables carry the class separating information (Ghosh *et al.*, 2016).

SIMCA consists of separate PCA models of investigated classes in the data set (Wold, 1976). It is known as a distance-based method, which can also be used as a method of discrimination. Single PCA models are capable of estimating any continuous variation within a single class (Wold, 1976), hence Brereton (2011) describes SIMCA in the category of one class classifiers.

NIR Hyperspectral imaging

In recent years, hyperspectral imaging has been regarded as a smart and promising analytical tool for investigation studies conducted in research, control, and industries (ElMasry and Sun, 2010). Hyperspectral imaging is a non-contact, cutting edge analytical technology that has been around for some time. It combines conventional spectroscopy and digital imaging to attain both spatial and spectral information from an object. Although it was originally developed for remote sensing, it has

recently emerged as a powerful process analytical tool for non-destructive food analysis (Gowen *et al.*, 2007).

Principles

A typical hyperspectral imaging system consists of a light source that illuminates the material of interest, a lens to ensure adequate focus and outline the field of view (Gowen *et al.*, 2007). It also has a wavelength dispersion unit to split the light into various spectral bands, a camera (detector) to capture the resultant spatial–spectral images, and a computer supported with software to control the image acquisition process. The system provides images in a three-dimensional (3-D) form called "hypercubes" (Kamruzzaman *et al.*, 2011). The 3-D block comprises of two spatial dimensions (x rows and y columns) and one spectral dimension (of wavelengths).

The 3 modes for hyperspectral imaging, namely reflectance, transmittance, and interactance, differ in lighting and detector configurations, resulting in different effects on data acquisition for the same substance. The appropriate acquisition mode depends on the type of sample and the constituent and/or property being analysed (Kamruzzaman *et al.*, 2015a)**.**

Applications

A lot of work has been successfully done in the discrimination of meat and meat products using NIR hyperspectral imaging. To name a few, NIR hyperspectral imaging has been applied in the following investigations: discrimination of lamb muscles (Kamruzzaman *et al.*, 2011), prediction of colour, pH, and tenderness of fresh beef (Elmasry *et al.*, 2012), assessing and visualising tenderness distribution in raw farmed salmon fillets (He *et al.*, 2014), recognition of fresh and frozen-thawed porcine longissimus dorsi muscles (Talens *et al.*, 2013; Barbin *et al.*, 2013b), determination of chemical composition in intact and minced pork (Barbin *et al.*, 2013a), and for grading and classification of pork (Barbin *et al.*, 2012), and many more.

Concerns of the NIR technology

As much as NIR technology has gained a lot of popularity, there are concerns. According to Osborne et al. (1993) and Manley, (2014), one of the main disadvantages of NIR spectroscopy is model development using chemometrics and its reliance on reference methods. However, NIR predictions and measurements are considered more reproducible. Also, its quantitative analysis when constructing models requires prior knowledge of the value for the target parameters, which must be previously determined using a reference method (Blanco and Villarroya, 2002). Another concern is that accurate, robust calibration models are difficult to obtain as their construction entails using a large enough number of samples to encompass all variation in physical and/or chemical properties (Blanco and Villarroya, 2002).

Conclusions

Non-destructive techniques for food quality analysis provide an interesting platform for screening meat and are the solution in an environmentally friendly society. The growing interest in the NIR techniques is due to its advantages over alternative instruments. With technological advancements and the increasing quality, safety, and environmental concern, it has become notable to a lot of research institutions and industries. The technology that started in the Agricultural food sector has now expanded its applications to the other sectors like Petrochemical, Pharmaceutical, Chemical and Biochemical, Environmental, and Process control sectors. A lot of meat studies using NIR spectroscopy have been successfully done around the world, however there is still a gap on work done on game meat. To date, this is the second study after Edwards *et al.* (2020) investigated the performance of handheld NIR instrument to identify different species, and different muscles of South African game meat. However, in their study fresh, frozen, and thawed meat was investigated, while in this study only fresh meat was explored in addition to meat ageing. Thus, the objective of this study was to investigate the ability of a handheld NIR spectroscopy in differentiating the selected game meat species, their muscle types, species regardless of the muscles used, and meat aged in different days.

References

Abbas, O., Zadravec, M., Baeten, V., Mikuš, T., Lešić, T., Vulić, A., Prpić, J., Jemeršić, L. & Pleadin, J. (2018). Analytical methods used for the authentication of food of animal origin. *Food Chemistry*, **246**, 6–17.

Aida, A.A., Man, Y.B.C., Wong, C.M.V.L., Raha, A.R. & Son, R. (2005). Analysis of raw meats and fats of pigs using polymerase chain reaction for Halal authentication. *Meat Science*, **69**, 47–52.

Alamprese, C., Casale, M., Sinelli, N., Lanteri, S. & Casiraghi, E. (2013). Detection of minced beef adulteration with turkey meat by UV-vis, NIR and MIR spectroscopy. *LWT - Food Science and Technology*, **53**.

Alander, J.T., Bochko, V., Martinkauppi, B., Saranwong, S. & Mantere, T. (2013). A Review of Optical Nondestructive Visual and Near-Infrared Methods for Food Quality and Safety. *International Journal of Spectroscopy*, **2013**, 1–36.

Alomar, D., Gallo, C., Castañeda, M. & Fuchslocher, R. (2003). Chemical and discriminant analysis of bovine meat by near infrared reflectance spectroscopy (NIRS). *Meat Science*, **63**, 441–450.

Amaral, J.S., Santos, C.G., Melo, V.S., Oliveira, M.B.P.P. & Mafra, I. (2014). Authentication of a traditional game meat sausage (Alheira) by species-specific PCR assays to detect hare, rabbit, red deer, pork and cow meats. *Food Research International*, **60**, 140–145.

Andrés, S., Murray, I., Navajas, E.A., Fisher, A. V., Lambe, N.R. & Bünger, L. (2007). Prediction of sensory characteristics of lamb meat samples by near infrared reflectance spectroscopy. *Meat Science*, **76**, 509–516.

Andrés, S., Silva, A., Soares-Pereira, A.L., Martins, C., Bruno-Soares, A.M. & Murray, I. (2008). The

use of visible and near infrared reflectance spectroscopy to predict beef M. longissimus thoracis et lumborum quality attributes. *Meat Science*, **78**, 217–224.

Anonymous (2015). FT-NIR Spectroscopy: A valuable tool for the edible oil industry: Inform Magazine. [www document]. https://www.informmagazine-digital.org/informmagazine/november_december_2015/MobilePagedArticle.action?articleId=686069#articleId686069. Accessed 20/09/2020

Anonymous (2020). Ultraviolet visible and near infrared analysis: Analytical Techniques: LPD Lab Services. [www document]. https://www.lpdlabservices.co.uk/analytical_techniques/chemical_analysis/uv_vis_nir.php. Accessed 20/09/2020

Balabin, R.M., Safieva, R.Z. & Lomakina, E.I. (2010). Gasoline classification using near infrared (NIR) spectroscopy data: Comparison of multivariate techniques. *Analytica Chimica Acta*, **671**, 27–35.

Balage, J.M., Luz e Silva, S. da, Gomide, C.A., Bonin, M. de N. & Figueira, A.C. (2015). Predicting pork quality using Vis/NIR spectroscopy. *Meat Science*, **108**, 37–43.

Ballin, N.Z. (2010). Authentication of meat and meat products. Meat Science, 86, 577-587.

Ballin, N.Z. & Lametsch, R. (2008). Analytical methods for authentication of fresh vs. thawed meat - A review. *Meat Science*, **80**, 151–158.

Ballin, N.Z., Vogensen, F.K. & Karlsson, A.H. (2009). Species determination - Can we detect and quantify meat adulteration? *Meat Science*, **83**, 165–174.

Barbin, D., Elmasry, G., Sun, D.W. & Allen, P. (2012). Near-infrared hyperspectral imaging for grading and classification of pork. *Meat Science*, **90**, 259–268.

Barbin, D.F., Elmasry, G., Sun, D.W. & Allen, P. (2013a). Non-destructive determination of chemical composition in intact and minced pork using near-infrared hyperspectral imaging. *Food Chemistry*, **138**, 1162–1171.

Barbin, D.F., Valous, N.A. & Sun, D.W. (2013b). Tenderness prediction in porcine longissimus dorsi muscles using instrumental measurements along with NIR hyperspectral and computer vision imagery. *Innovative Food Science and Emerging Technologies*, **20**.

Bargen, C. Von, Brockmeyer, J. & Humpf, H.U. (2014). Meat authentication: A new HPLC-MS/MS based method for the fast and sensitive detection of horse and pork in highly processed food. *Journal of Agricultural and Food Chemistry*, **62**, 9428–9435.

Barker, M. & Rayens, W. (2003). Partial least squares for discrimination. *Journal of Chemometrics*, **17**, 166–173.

Barnes, R.J., Dhanoa, M.S. & Lister, S.J. (1989). Standard normal variate transformation and de-trending of near-infrared diffuse reflectance spectra. *Applied Spectroscopy*, **43**, 772–777.

Blanco, M. & Villarroya, I. (2002). NIR spectroscopy: A rapid-response analytical tool. *TrAC - Trends in Analytical Chemistry*, **21**, 240–250.

Böhme, K., Calo-Mata, P., Barros-Velázquez, J. & Ortea, I. (2019). Recent applications of omics-

based technologies to main topics in food authentication. *TrAC - Trends in Analytical Chemistry*, **110**, 221–232.

Borin, A., Ferrão, M.F., Mello, C., Maretto, D.A. & Poppi, R.J. (2006). Least-squares support vector machines and near infrared spectroscopy for quantification of common adulterants in powdered milk. *Analytica Chimica Acta*, **579**, 25–32.

Brereton, R.G. (2011). One-class classifiers. *Journal of Chemometrics*, **25**, 225–246.

Cawthorn, D.M., Steinman, H.A. & Hoffman, L.C. (2013). A high incidence of species substitution and mislabelling detected in meat products sold in South Africa. *Food Control*, **32**, 440–449.

Cen, H. & He, Y. (2007). Theory and application of near infrared reflectance spectroscopy in determination of food quality. *Trends in Food Science and Technology*, **18**, 72–83.

Chen, S.Y., Liu, Y.P. & Yao, Y.G. (2010). Species authentication of commercial beef jerky based on PCR-RFLP analysis of the mitochondrial 12S rRNA gene. *Journal of Genetics and Genomics*, **37**, 763–769.

Cowe, I.A. & McNicol, J.W. (1985). The use of principal components in the analysis of near-infrared spectra. Applied spectroscopy, **39,** 257-266.

Cozzolino, D. & Murray, I. (2004). Identification of animal meat muscles by visible and near infrared reflectance spectroscopy. *LWT - Food Science and Technology*, **37**, 447–452.

Davies, T. (1998). The history of near infrared spectroscopic analysis: Past, present and future “From sleeping technique to the morning star of spectroscopy.” *Analusis*, **26**, 17–19.

Ding, H.B. & Xu, R.J. (1999). Differentiation of beef and kangaroo meat by visible/near-infrared reflectance spectroscopy. *Journal of Food Science*, **64**, 814–817.

Ding, H.B. & Xu, R.J. (2000). Near-infrared spectroscopic technique for detection of beef hamburger adulteration. *Journal of Agricultural and Food Chemistry*, **48**, 2193–2198.

DoH (Department of Health). 2010. Foodstuffs, Cosmetics and Disinfectants Act, 1972 (Act 54 of 1972): Regulations relating to the labelling and advertising of foods: Amendment (R. 146/2010). Government Printing Offices, South Africa.

Doosti, A., Ghasemi Dehkordi, P. & Rahimi, E. (2014). Molecular assay to fraud identification of meat products. *Journal of Food Science and Technology*, **51**, 148–152.

Druml, B., Mayer, W., Cichna-markl, M. & Hochegger, R. (2015). Development and validation of a TaqMan real-time PCR assay for the identification and quantification of roe deer (Capreolus capreolus) in food to detect food adulteration. *Food Chemistry*, **178**, 319–326.

Du, C.J. & Sun, D.W. (2006). Learning techniques used in computer vision for food quality evaluation: A review. *Journal of Food Engineering*, **72**, 39–55.

Dumalisile, P., Manley, M., Hoffman, L. & Williams, P.J. (2020a). Discriminating muscle type of selected game species using near infrared (NIR) spectroscopy. *Food Control*, **110**.

Edwards, K., Manley, M., Hoffman, L.C., Beganovic, A., Kirchler, C.G., Huck, C.W. & Williams, P.J. (2020). Differentiation of South African game meat using near-infrared (NIR) spectroscopy and hierarchical modelling. Molecules, 25.

Ellis, D.I., Brewster, V.L., Dunn, W.B., Allwood, J.W., Golovanov, A.P. & Goodacre, R. (2012). Fingerprinting food: Current technologies for the detection of food adulteration and contamination. *Chemical Society Reviews*, **41**, 5706–5727.

ElMasry, G. & Sun, D. (2010). Principles of Hyperspectral Imaging Technology. *Hyperspectral Imaging for Food Quality Analysis and Control*, 3–43.

Elmasry, G., Sun, D.W. & Allen, P. (2012). Near-infrared hyperspectral imaging for predicting colour, pH and tenderness of fresh beef. *Journal of Food Engineering*, **110**, 127–140.

Fæste, C.K. & Plassen, C. (2008). Quantitative sandwich ELISA for the determination of fish in foods. *Journal of Immunological Methods*, **329**, 45–55.

Fajardo, V., González Isabel, I., Rojas, M., García, T. & Martín, R. (2010). A review of current PCR-based methodologies for the authentication of meats from game animal species. *Trends in Food Science and Technology*, **21**, 408–421.

Fisher, R.A. (1936). The use of multiple measurements in taxonomic problems. Annals of Eugenics, 7, 179- 188.

Floren, C., Wiedemann, I., Brenig, B., Schütz, E. & Beck, J. (2015). Species identification and quantification in meat and meat products using droplet digital PCR (ddPCR). *Food Chemistry*, **173**, 1054–1058.

Fornal, E. & Montowska, M. (2019). Species-specific peptide-based liquid chromatography–mass spectrometry monitoring of three poultry species in processed meat products. *Food Chemistry*, **283**, 489–498.

Geladi, P. (2003). Chemometrics in spectroscopy. Part 1. Classical chemometrics. *Spectrochimica Acta Part B: Atomic Spectroscopy*, **58**, 767–782.

Geladi, P., MacDougall, D. & Martens, H. (1985). Linearization and scatter-correction for near-infrared reflectance spectra of meat. *Applied Spectroscopy*, **39**, 491–500.

Ghosh, S., Mishra, P., Mohamad, S.N.H., Santos, R.M. de, Iglesias, B.D. & Elorza, P.B. (2016). Discrimination of peanuts from bulk cereals and nuts by near infrared reflectance spectroscopy. *Biosystems Engineering*, **151**, 178–186.

Giovannacci, I., Guizard, C., Carlier, M., Duval, V., Martin, J.L. & Demeulemester, C. (2004). Species identification of meat products by ELISA. *International Journal of Food Science and Technology*, **39**, 863–867.

Govindan, K. (2018). Sustainable consumption and production in the food supply chain: A conceptual framework. *International Journal of Production Economics*, **195**, 419–431.

Gowen, A.A., O'Donnell, C.P., Cullen, P.J., Downey, G. & Frias, J.M. (2007). Hyperspectral imaging - an emerging process analytical tool for food quality and safety control. *Trends in Food Science and Technology*, **18**, 590–598.

Granato, D., Putnik, P., Kovačević, D.B., Santos, J.S., Calado, V., Rocha, R.S., Cruz, A.G. Da, Jarvis, B., Rodionova, O.Y. & Pomerantsev, A. (2018). Trends in Chemometrics: Food Authentication, Microbiology, and Effects of Processing. *Comprehensive Reviews in Food*

Science and Food Safety, **17**, 663–677.

Grassi, S., Casiraghi, E. & Alamprese, C. (2018). *Handheld NIR device: A non-targeted approach to assess authenticity of fish fillets and patties*. *Food Chemistry*.

He, H.J., Wu, D. & Sun, D.W. (2014). Potential of hyperspectral imaging combined with chemometric analysis for assessing and visualising tenderness distribution in raw farmed salmon fillets. *Journal of Food Engineering*, **126**.

Helland, I.S., Næs, T. & Isaksson, T. (1995). Related versions of the multiplicative scatter correction method for preprocessing spectroscopic data. *Chemometrics and Intelligent Laboratory Systems*, **29**, 233–241.

Herschel, W. (1800). Investigation of the powers of the prismatic colours to heat and illuminate objects; with remarks, that prove the different refrangibility of radiant heat. To which is added, an inquiry into the method of viewing the sun advantageously, with telescopes of large apertures and high magnifying powers. Philosophical Transactions of the Royal Society of London, 90, 255-283.

Hoffman, L. (2007). The Meat We Eat: are you game? *Inaugeral Addess*.

Hoffman, L.C., Schalkwyk, S. van & Muller, M. (2011). Quality Characteristics of Blue Wildebeest (Connochaetes taurinus) Meat. *South African Journal of Wildlife Research*, **41**, 210–213.

Hoffman, L.C. & Wiklund, E. (2006). Game and venison - meat for the modern consumer. *Meat Science*, **74**, 197–208.

Jonker, K.M., Tilburg, J.J.H.C., Hagele, G.H. & Boer, E. de. (2008). Species identification in meat products using real-time PCR. *Food additives & contaminants. Part A, Chemistry, analysis, control, exposure & risk assessment*, **25**, 527–533.

Kademi, H.I., Ulusoy, B.H. & Hecer, C. (2019). Applications of miniaturized and portable near infrared spectroscopy (NIRS) for inspection and control of meat and meat products. *Food Reviews International*, **35**, 201–220.

Kamruzzaman, M., Elmasry, G., Sun, D.W. & Allen, P. (2011). Application of NIR hyperspectral imaging for discrimination of lamb muscles. *Journal of Food Engineering*, **104**, 332–340.

Kamruzzaman, M., Makino, Y. & Oshita, S. (2015a). Non-invasive analytical technology for the detection of contamination, adulteration, and authenticity of meat, poultry, and fish: A review. *Analytica Chimica Acta*, **853**, 19–29.

Kamruzzaman, M., Makino, Y., Oshita, S. & Liu, S. (2015b). Assessment of Visible Near-Infrared Hyperspectral Imaging as a Tool for Detection of Horsemeat Adulteration in Minced Beef. *Food and Bioprocess Technology*, **8**, 1054–1062.

Kamruzzaman, M., Sun, D.W., ElMasry, G. & Allen, P. (2013). Fast detection and visualization of minced lamb meat adulteration using NIR hyperspectral imaging and multivariate image analysis. *Talanta*, **103**, 130–136.

Karunathilaka, S.R., Fardin-Kia, A.R., Srigley, C., Chung, J.K. & Mossoba, M.M. (2017). Rapid screening of commercial extra virgin olive oil products for authenticity: Performance of a

handheld NIR device. *NIR news*, **28**, 9–14.

Layton L. 2010. At U.S. dinner tables, the food may be a fraud; Deception, mislabeling increase, but FDA lacks enforcement re-sources. The Washington Post, Mar 30, p. 1.

Leroy, B., Lambotte, S., Dotreppe, O., Lecocq, H., Istasse, L. & Clinquart, A. (2004). Prediction of technological and organoleptic properties of beef Longissimus thoracis from near-infrared reflectance and transmission spectra. *Meat Science*, **66**, 45–54.

Lockley, A.K. & Bardsley, R.G. (2000). DNA-based methods for food authentication. *Trends in Food Science and Technology*, **11**, 67–77.

Lohumi, S., Lee, S., Lee, H. & Cho, B. (2015). Trends in Food Science & Technology A review of vibrational spectroscopic techniques for the detection of food authenticity and adulteration. *Trends in Food Science & Technology*, **46**, 85–98.

López-Maestresalas, A., Insausti, K., Jarén, C., Pérez-Roncal, C., Urrutia, O., Beriain, M.J. & Arazuri, S. (2019). Detection of minced lamb and beef fraud using NIR spectroscopy. *Food Control*.

Luypaert, J., Heuerding, S., Heyden, Y. Vander & Massart, D.L. (2004). The effect of preprocessing methods in reducing interfering variability from near-infrared measurements of creams. *Journal of Pharmaceutical and Biomedical Analysis*, **36**, 495–503.

Macedo-Silva, A., Barbosa, S.F.C., Alkmin, M.G.A., Vaz, A.J., Shimokomaki, M. & Tenuta-Filho, A. (2000). Hamburger meat identification by dot-ELISA. *Meat Science*, **56**, 189–192.

Mamani-Linares, L.W., Gallo, C. & Alomar, D. (2012). Identification of cattle, llama and horse meat by near infrared reflectance or transflectance spectroscopy. *Meat Science*.

Manley, M. (2014). Near-infrared spectroscopy and hyperspectral imaging: Non-destructive analysis of biological materials. *Chemical Society Reviews*, **43**, 8200–8214.

Manley, M. & Baeten, V. (2018). *Spectroscopic Technique: Near Infrared (NIR) Spectroscopy*. *Modern Techniques for Food Authentication*. 2nd edn. Elsevier Inc.

Manning, L. & Soon, J.M. (2014). Developing systems to control food adulteration. *Food Policy*, **49**, 23–32.

Metrohm blog, https://metrohm.blog/2020/02/24/nir-spectroscopy-benefits-part-2/.

Mollazade, K., Omid, M., Tab, F.A. & Mohtasebi, S.S. (2012). Principles and Applications of Light Backscattering Imaging in Quality Evaluation of Agro-food Products: A Review. *Food and Bioprocess Technology*, **5**, 1465–1485.

Monahan, F.J., Schmidt, O. & Moloney, A.P. (2018). Meat provenance: Authentication of geographical origin and dietary background of meat. *Meat Science*, 0–1.

Monroy, M., Prasher, S., Ngadi, M.O., Wang, N. & Karimi, Y. (2010). Pork meat quality classification using Visible/Near-Infrared spectroscopic data. *Biosystems Engineering*, **107**, 271–276.

Moore, J.C., Spink, J. & Lipp, M. (2012). Development and Application of a Database of Food Ingredient Fraud and Economically Motivated Adulteration from 1980 to 2010. *Journal of Food Science*, **77**.

Moran, L., Andres, S., Allen, P. & Moloney, A.P. (2018). Visible and near infrared spectroscopy as an authentication tool: Preliminary investigation of the prediction of the ageing time of beef steaks. *Meat Science*, **142**, 52–58.

Moreno-ortega, A., Morales, J.S., Moreno-ortega, A., Angel, M., Lopez, A., Casas, A.A., Cámara-martos, F., Moreno-rojas, R., Sevillano, J., Moreno-ortega, A. & Amaro, M.A. (2018). Game meat consumption by hunters and their relatives : A probabilistic Game meat consumption by hunters and their relatives : a probabilistic approach. *Food Additives & Contaminants: Part A*, **00**, 1–10.

Morsy, N. & Sun, D.W. (2013). Robust linear and non-linear models of NIR spectroscopy for detection and quantification of adulterants in fresh and frozen-thawed minced beef. *Meat Science*, **93**, 292–302.

Mostert, R. & Hoffman, L.C. (2007). Effect of gender on the meat quality characteristics and chemical composition of kudu (Tragelaphus strepsiceros), an African antelope species. *Food Chemistry*, **104**, 565–570.

Murugaiah, C., Noor, Z.M., Mastakim, M., Bilung, L.M., Selamat, J. & Radu, S. (2009). Meat species identification and Halal authentication analysis using mitochondrial DNA. *Meat Science*, **83**, 57–61.

Nolasco Perez, I.M., Badaró, A.T., Barbon, S., Barbon, A.P.A.C., Pollonio, M.A.R. & Barbin, D.F. (2018). Classification of Chicken Parts Using a Portable Near-Infrared (NIR) Spectrophotometer and Machine Learning. *Applied Spectroscopy*, **72**, 1774–1780.

Nunes, K.M., Andrade, M.V.O., Almeida, M.R. & Sena, M.M. (2020). A soft discriminant model based on mid-infrared spectra of bovine meat purges to detect economic motivated adulteration by the addition of non-meat ingredients. *Food Analytical Methods*.

O'Brien, N., Hulse, C.A., Pfeifer, F. & Siesler, H.W. (2013). Near infrared spectroscopic authentication of seafood. *Journal of Near Infrared Spectroscopy*, **21**, 299–305.

O'Mahony, P.J. (2013). Finding horse meat in beef products-a global problem. *Qjm*, **106**, 595–597.

Osborne, B.G. (2000). Near-Infrared Spectroscopy in Food Analysis. *Encyclopedia of Analytical Chemistry*, 1–14.

Osborne, B.G., Fearn, T., Hindle, P.H., 1993. Spectroscopy With Application in Food and Beverage Analysis. Longman Scientific & Technical, Singapore, pp. 1–77. 120–141.

Parastar, H., Kollenburg, G. van, Weesepoel, Y., Doel, A. van den, Buydens, L. & Jansen, J. (2020). Integration of handheld NIR and machine learning to "Measure & Monitor" chicken meat authenticity. *Food Control*, **112**, 107149.

Park, B., Chen, Y.R., Hruschka, W.R., Shackelford, S.D. & Koohmaraie, M. (1998). ABSTRACT :, 2115–2120.

Pasquini, C. (2003). Near infrared spectroscopy: Fundamentals, practical aspects and analytical applications. *Journal of the Brazilian Chemical Society*, **14**, 198–219.

Pasquini, C. (2018). Near infrared spectroscopy: A mature analytical technique with new

perspectives – A review. *Analytica Chimica Acta*, **1026**, 8–36.

Peng, Y. & Wang, W. (2015). Application of Near-infrared Spectroscopy for Assessing Meat Quality and Safety. *Infrared Spectroscopy - Anharmonicity of Biomolecules, Crosslinking of Biopolymers, Food Quality and Medical Applications*, 137–163.

Prieto, N., Andrés, S., Giráldez, F.J., Mantecón, A.R. & Lavín, P. (2008). Discrimination of adult steers (oxen) and young cattle ground meat samples by near infrared reflectance spectroscopy (NIRS). *Meat Science*, **79**, 198–201.

Prieto, N., Juárez, M., Larsen, I.L., López-Campos, Zijlstra, R.T. & Aalhus, J.L. (2015). Rapid discrimination of enhanced quality pork by visible and near infrared spectroscopy. *Meat Science*, **110**, 76–84.

Prieto, N., Pawluczyk, O., Dugan, M.E.R. & Aalhus, J.L. (2017). A Review of the Principles and Applications of Near-Infrared Spectroscopy to Characterize Meat, Fat, and Meat Products. *Applied Spectroscopy*, **71**, 1403–1426.

Rahmati, S., Julkapli, N.M., Yehye, W.A. & Basirun, W.J. (2016). Identification of meat origin in food products-A review. *Food Control*, **68**, 379–390.

Reid, L.M., O'Donnell, C.P. & Downey, G. (2006). Recent technological advances for the determination of food authenticity. *Trends in Food Science and Technology*, **17**, 344–353.

Reis, M.M., Beers, R. Van, Al-Sarayreh, M., Shorten, P., Yan, W.Q., Saeys, W., Klette, R. & Craigie, C. (2018). Chemometrics and hyperspectral imaging applied to assessment of chemical, textural and structural characteristics of meat. *Meat Science*, **144**, 100–109.

Rinnan, Å., Berg, F. van den & Engelsen, S.B. (2009). Review of the most common pre-processing techniques for near-infrared spectra. *TrAC - Trends in Analytical Chemistry*, **28**, 1201–1222.

Roggo, Y., Chalus, P., Maurer, L., Lema-martinez, C. & Jent, N. (2007). A review of near infrared spectroscopy and chemometrics in pharmaceutical technologies, **44**, 683–700.

Ruth, S.M. van, Luning, P.A., Silvis, I.C.J., Yang, Y. & Huisman, W. (2018). Differences in fraud vulnerability in various food supply chains and their tiers. *Food Control*, **84**, 375–381.

Savitzky, A. & Golay, M.J.E. (1964). Smoothing and Differentiation of Data by Simplified Least Squares Procedures. *Analytical Chemistry*, **36**, 1627–1639.

Savoia, S., Albera, A., Brugiapaglia, A., Stasio, L. Di, Ferragina, A., Cecchinato, A. & Bittante, G. (2020). Prediction of meat quality traits in the abattoir using portable and hand-held near-infrared spectrometers. *Meat Science*, **161**, 108017.

Sentandreu, M.Á. & Sentandreu, E. (2014). Authenticity of meat products: Tools against fraud. *Food Research International*, **60**, 19–29.

Sjoberg, A.-M.K., Jari, '', Tuominen, P., Kiutamo, T. & Luukkonenuvb, S.M. (1992). Evaluation of a Gas ChromatonraDhic Method for Detection of Irradiation of chicken and a Chicken Meat Product. J Sci Food Agric.

Spink, J. & Moyer, D.C. (2011). Defining the Public Health Threat of Food Fraud. *Journal of Food Science*, **76**.

Statista (2019). World total population from 2009 to 2019: https://www.statista.com/statistics/805044/total-population-worldwide/#statisticContainer. Accessed 22/11/2020.

Surowiec, I., Fraser, P.D., Patel, R., Halket, J. & Bramley, P.M. (2011). Metabolomic approach for the detection of mechanically recovered meat in food products. *Food Chemistry*, **125**, 1468–1475.

Talens, P., Mora, L., Morsy, N., Barbin, D.F., ElMasry, G. & Sun, D.-W. (2013). Prediction of water and protein contents and quality classification of Spanish cooked ham using NIR hyperspectral imaging. *Journal of Food Engineering*, **117**, 272–280.

Valdés, A., Beltrán, A., Mellinas, C., Jiménez, A. & Garrigós, M.C. (2018). Analytical methods combined with multivariate analysis for authentication of animal and vegetable food products with high fat content. *Trends in Food Science and Technology*, **77**, 120–130.

Verbeke, W. & Ward, R.W. (2006). Consumer interest in information cues denoting quality , traceability and origin : An application of ordered probit models to beef labels, **17**, 453–467.

Walker, M.J., Burns, M. & Burns, D.T. (2013). Horse Meat in Beef Products- Species Substitution 2013. *Journal of the Association of Public Analysts (Online)*, **41**, 67–106.

Wang, W., Peng, Y., Sun, H., Zheng, X. & Wei, W. (2018). Spectral Detection Techniques for Non-Destructively Monitoring the Quality, Safety, and Classification of Fresh Red Meat. Food Analytical Methods.

Wei, W., Peng, Y. & Qiao, L. (2016). Development of hand-held nondestructive detection device for assessing meat freshness. *Sensing for Agriculture and Food Quality and Safety VIII*, **9864**, 98640W.

Wiedemair, V., Biasio, M. De, Leitner, R., Balthasar, D. & Huck, C.W. (2018). Application of Design of Experiment for Detection of Meat Fraud with a Portable Near-Infrared Spectrometer. *Current Analytical Chemistry*, **14**, 58–67.

Williams, P. (2006). Near-infrared technology - Getting the best out of light. In: A short course in the practical implementation of near-infrared spectroscopy for the user. Nanaimo, Cananda: PDK Projects, Inc.

Williams P, Antoniszyn J & Manley M (2019) Near-infrared Technology: Getting the Best Out of Light. Stellenbosch: AFRICAN SUN MeDIA, p. 304.

Wise, B.M., Gallagher, N.B., Bro, R., Shaver, J.M., Windig, W. & Koch, R.S. (2006). *PLS_Toolbox Version 4.0 for use with MATLAB ™*. *Eigenvector Research*.

Wold, S. (1976). Pattern recognition by means of disjoint principal components models. *Pattern Recognition*, **8**, 127–139.

Wold, S. (1987). Principal component analysis. *Principal Component Analysis*, **2**, 37–52.

Wold, S. & Sjostrom, M. (2001). <Wold et al - 2001 - PLS-regression, a basic tool of chemometrics.pdf>, 109–130.

Yan, H. & Siesler, H.W. (2018). Hand-held near-infrared spectrometers: State-of-the-art

instrumentation and practical applications. *NIR news*, **29**, 8–12.

Zhang, J., Zhang, X., Dediu, L. & Victor, C. (2011). Review of the current application of fingerprinting allowing detection of food adulteration and fraud in China. *Food Control*.

Zhao, H., Guo, B., Wei, Y. & Zhang, B. (2013). Near infrared reflectance spectroscopy for determination of the geographical origin of wheat. Food Chemistry, **138**, 1902–1907.

Chapter 3

Near infrared (NIR) spectroscopy to differentiate Longissimus thoracis et lumborum (LTL) muscles of game species

Abstract

Near infrared (NIR) spectroscopy was used to differentiate game meat from six different species, i.e., medium-sized (Impala, Blesbok and Springbok) and large sized (Eland, Black wildebeest and Zebra) that were harvested from different farms across South Africa. *Longissimus thoracis et lumborum* (LTL) muscle steaks were removed and scanned with a handheld NIR spectrophotometer in the spectral range of 908 to 1700 nm. Spectra were treated with two different pre-processing combinations: 1) smoothing, standard normal variate and Detrend (SNV-Detrend), and 2) SNV-Detrend and Savitzky-Golay 2nd derivative, explored with principal component analysis (PCA) and classified with linear discriminant analysis (LDA), soft independent modelling by class analogy (SIMCA) and partial least squares discriminant analysis (PLS-DA). For classification purposes, the models were developed within each of the medium- and large-sized groups. LDA delivered good classification accuracies ranging from 68 to 100%, irrespective of the pre-processing combination used. PLS-DA performed well when spectra were treated with SNV-Detrend and Savitzky-Golay 2nd derivative and delivered classification accuracies ranging from 70 to 96%. The prediction results obtained with SIMCA pre-processed with smoothing and SNV-Detrend ranged from 67% (springbok) to 100% (impala and eland). Although models of good accuracy were obtained, they still require improvement where each species should be fully represented with meat samples from different areas, e.g., geographical locations, sex, season and age to develop robust models.

Keywords: Near infrared spectroscopy, Discrimination, Multivariate analysis, Game meat

Published as: Dumalisile, P., Manley, M., Hoffman, L. & Williams, P.J. (2020a). Near-Infrared (NIR) Spectroscopy to Differentiate *Longissimus thoracis et lumborum* (LTL) Muscles of Game Species. *Food Analytical Methods,* **13**, 1220-1233.

Introduction

Meat and meat products represent an important component of the human diet. In addition to proteins, red meat also offers minerals and trace elements, particularly zinc and iron, to the diet. Game meat, also high in proteins (20.0–23.8%), offers a healthy alternative to other red meat as it is known to be much lower in fat (0.8–2.45%) compared to beef (14.2% fat; 19.2% protein) (Hoffman, 2007). South African (SA) game meat is considered an organic food product since the animals are wild and free roaming, in contrast with many game species in other parts of the world that are semi-domesticated (Hoffman *et al.,* 2007). For this reason, SA game meat is a highly priced commodity making it an attractive target for species substitution (Ballin, 2010; Kamruzzaman *et al.,* 2013).

Meat species substitution is a current problem involving economic and safety issues since one cannot easily detect the source of origin or differentiate between species when evaluating meat visually (Kamruzzaman *et al.,* 2013). Beef burgers (produced in Ireland in 2013) were found to contain horse meat, exposing consumers to undeclared animal species in meat products (O'Mahony, 2013; Walker *et al.,* 2013). In South Africa, Cawthorn *et al.* (2013) found species (such as chicken, goat, water buffalo and donkey) that were not declared on the product labelling in beef sausages. Such reports subsequently raised consumers' concern regarding traceability and origin of the food they eat (Verbeke and Ward, 2006). Correct and reliable labelling of meat products is important to allow consumers to make informed choices.

Due to the cost of analytical methods (chromatography, electrophoresis, enzyme-linked immunosorbent assay (ELISA) and DNA based techniques) required for accurate identification of meat species (Cawthorn *et al.,* 2013; Fajardo *et al.,* 2010; Jonker *et al.,* 2008), raw meat products are not tested on a regular basis. To address this shortcoming, near-infrared (NIR) spectroscopy can be used as a rapid screening method (Manley, 2014) for detection of potential substitution of meat species (Ding and Xu, 1999; Cozzolino and Murray, 2004). NIR spectroscopy can be used to quantify and qualify physical, chemical and biological attributes of food samples based on their spectral signature (Manley, 2014).

Visible (400–780 nm) and NIR (780–1100 nm and 1100–2500 nm) spectroscopy has been indicated as an effective test method for meat species identification. NIR spectroscopy works well in combination with chemometrics for more decisive classification of food samples (Reid *et al.,* 2006). Information contained in NIR spectra can be extracted using various multivariate techniques that relate several variables to chemical properties. The most frequently used techniques allow samples with similar characteristics to be grouped, in order to establish classification methods for unknown samples (qualitative analysis) or to perform methods determining some property of unknown samples (quantitative analysis). Ding and Xu (1999), Cozzolino and Murray (2004) and, Mamani-Linares *et al. (*2012) coupled NIR with chemometrics to achieve good classification models of meat species. Visible-near-infrared (vis-NIR) spectroscopy was used in initial studies on meat species classification. Ding & Xu (1999) differentiated beef from kangaroo meat samples with a classification accuracy of 83%. No kangaroo meat samples were misclassified (100% accuracy). Similarly,

Cozzolino & Murray (2004) identified muscles from beef, pork, chicken and lamb with accuracies of more than 85%. Discrimination of cattle, llama and horse meat species was possible with accuracies of 100, 95 and 89%, respectively (Mamani-Linares *et al.,* 2012). Prieto *et al.* (2008) used only the NIR region (1100–2500 nm) to discriminate ground meat samples of adult steers (oxen) from that of young cattle. Using partial least squares discriminant analysis (PLS-DA), an overall classification accuracy of 100% was obtained. Intramuscular fat and water content were shown to be the main sources of variation between these sample groups. Since 2013, the availability of handheld instruments (O'Brien *et al.,* 2013) opened up the opportunity to take the instrument to the sample, in contrast to desktop NIR instruments which require samples to be transported to the laboratory for analysis.

The consumption of game meat is becoming popular all over the world. For example, in Spain approximately one million two hundred thousand hunters, and nine million animals of the main hunted species are hunted each year. In Andalusia, over five million big and small game species were hunted during the 2015 and 2016 season (Moreno-ortega et al., 2018). In Sweden, 70 % of the population including non-hunters are reported to have consumed game meat (Jung *et al.,* 2012). In Africa, among the most hunted species are Springbok (*Antidorcas marsupialis*), Gemsbok (*Oryx gazella*), Impala (*Aepyceros melampus*), Blesbok (*Damaliscus pygargus phillipsi*), Kudu (*Tragelaphus strepsiceros*), Blue Wildebeest (*Connochaetes taurinus*) and Red Hartebeest (*Alcelaphus buselaphus caama*) (Van Schalkwyk and Hoffman, 2016). The South African consumer demand for game meat within the formal market has been considerably lower than for more conventional livestock species such as beef, mutton, and pork. The lower demand can potentially be attributed to limited availability, higher retail prices as well as the naturally darker colour of game meat (Hoffman and Wiklund, 2006; Wassenaar *et al*., 2019). Nonetheless, Saayman *et al*. (2011) investigated the effect of local hunting on the South African economy and found that there was a largely positive economic impact; hunting had a contribution of over 6 billion ZAR to the Gross Domestic Profit (GDP) of the country along with job creation. Van der Waal and Dekker (2000) found approximately 13 700 permanent jobs created as well as extra people being hired temporarily during the hunting season. In a 2018 report, the same authors found that trophy hunting contributed significantly to the national economy and supplied over 17 000 jobs, which could result in areas of lower income becoming more economically stable (Saayman *et al.,* 2018). However, the increase of hunted wild game meat markets all over the world, is however hampered by the lack of a well-structured food chain (Marescotti *et al.,* 2019).

Marketing game meat on species level rather than a collective 'game meat', has been considered. However, some of the game species are more popular and sought after by consumers. Springbok and eland are, e.g. favoured compared to zebra which is deemed less desirable. Game meat is sold in the form of steaks, sausages, biltong and droewors. Therefore, there is a possibility that these meat portions can be mislabelled, and in such cases meat species classification will be required.

In this study, we aim to use NIR spectroscopy coupled with various discriminant and classification methods to differentiate between longissimus thoracis et lumborum (LTL) muscle steaks of selected game species.

Materials and Methods

Meat samples

A total of 118 animals of the following game species was obtained: 33 Impala (Aepyceros melampus), 26 Blesbok (*Damaliscus pygargus phillipsi*), 13 Springbok (Antidorcas marsupialis), 15 Eland (*Taurotragus oryx*), 9 Black wildebeest (*Connochaetes gnou*) and 22 Zebra (*Equus quagga*). The game species originated from different areas and were hunted during different seasons as shown in Table 3.1. The animals were free-roaming and grazed on natural vegetation. All animals were hunted according to the standard operating procedure with ethical clearance (approval number: SU-ACUM14-001SOP; Stellenbosch University (SU) Animal Care and Use Committee). The animals were eviscerated at abattoirs according to the South African red meat regulations (DAFF, 2004; Van Schalkwyk and Hoffman, 2010), and transported chilled to the meat research laboratory at the Department of Animal Sciences, SU. After 24 to 48 h post-mortem, the *longissimus thoracis et lumborum* (LTL) muscle were removed at the 6th rib of each carcass.

Near infrared (NIR) spectral acquisition

Each LTL muscle was cut into a 2.0 to 2.5 cm thick steak and allowed to bloom for 30 min at ambient temperature. NIR spectra were collected from each muscle with a MicroNIR™ OnSite spectrophotometer and spectral acquisition software (Viavi Solutions®, San Jose, CA, USA). The illumination source comprised of two integrated vacuum tungsten lamps coupled to a linear variable filter and a 128-pixel Indium Gallium Arsenide (InGaAs) photodiode array detector. The reflectance spectra were recorded from 908 to 1680 nm at 6.2 nm intervals, resulting in 125 data points. The InGaAs detector was used to achieve a resolution of 30 µm x 250 µm / 50 µm (<12.5 nm resolution). A 2 mm thick Steriplan glass Petri dish was placed on top of the meat samples to prevent direct contact of the spectrophotometer with surface moisture. Triplicate spectra were collected through the glass surface, at three different positions for each sample. A sample spectrum was recorded in about 0.25 to 0.5 sec. Each spectrum was the average of 100 scans. The external white and dark references were scanned every 10 min during sample collection.

Table 3.1 Description of game species (blesbok, impala, springbok, black wildebeest, eland and zebra), number of samples, provenance and harvest season

Species	Total number of animals (n)	Sex		Average weight (kg)	Provenance (n)	Harvest season due to availability
		Female	Male			
Blesbok	26	14	12	51.2	Witsand (15)	May 2016
					Witsand (11)	May 2017
Impala	33	11	22	37.1	Bredasdorp (11)	February 2017
					Modimolle (22)	February 2017
Springbok	13	8	5	38.3	Witsand (10)	May 2017
					Witsand (3)	September 2017
Black wildebeest	9	3	6	141	Bredasdorp (9)	September 2017
Eland	15	7	8	337.3	Bredasdorp (15)	June 2016
Zebra	22	5	17	323.7	Bredasdorp (10)	July 2017
					Wellington (12)	January 2018

Moisture, protein and fat analysis

Moisture, protein and fat content of the game meat steaks were determined as described by Neethling *et al.* (2014). The moisture content (g/100g) of each species was determined by drying the homogenized muscles at 100 °C for 24h, according to the Association of Official Analytical Chemist's Standard Techniques (AOAC method 934.01.30). For protein content determination, dried and defatted meat samples were ground to a fine powder. The crude protein was analysed using the LECO combustion method also known as the Dumas combustion method (AOAC method 992.15). Approximately 0.15 g sample was weighed and inserted into a foil wrap designed for a Leco protein analyser (LECO FP-528 Nitrogen Analyzer, Leco Corporation). An ethylene diamine tetra-acetic acid (EDTA) calibration sample (Part number 502-092) was analysed with each batch of samples to ensure accuracy and recovery rate. The protein content was determined as nitrogen (% N) content multiplied by a factor of 6.25. The fat content was determined by homogenising the samples in a blender, followed by chloroform: methanol (2:1) extraction (Lee *et al.,*1996).

Multivariate data analysis

The spectral data were imported into and analysed with The Unscrambler® X version 10.5 (CAMO Software, Oslo, Norway) and PLS_Toolbox (Version 8.6.2, Eigenvector Research, Inc., Manson, WA USA) data analysis software packages. Triplicate spectra were averaged, to obtain one spectrum per sample. The data was converted to absorbance with the following formula:

$$A = -\log(R)$$

Where:

A = absorbance
Log = log base 10
R = reflectance

Spectral pre-processing

Two combinations of pre-processing (mathematical transformation) techniques were applied to reduce potential scattering effects, baseline shifts and noise in the data (Rinnan *et al.,* 2009; Engel *et al.,* 2013). Firstly (Combination 1), spectra were smoothed with a seven-point moving average to remove noise followed by standard normal variate (SNV) and de-trending (Barnes *et al.,*1989). SNV was applied to remove the scattering effects by centering and scaling each spectrum and de-trending was applied to reduce the baseline shift and curvature. Secondly (Combination 2), spectra were treated with SNV and de-trending (SNV-Detrend), followed by Savitzky-Golay 2nd derivative, 2nd order polynomial and seven-point smoothing. Savitzky-Golay 2nd derivative was applied to smooth noise fluctuations without introducing distortions and to enhance peaks not clearly visible in the original spectra (Savitzky and Golay, 1964). In the end also a mean centering step was performed.

Principal component analysis

Principal component analysis (PCA) was computed in The Unscrambler®. PCA (Cowe and McNicol, 1985), decomposes the raw data matrix (X) into scores and loadings, according to the following equation:

$$\mathbf{X} = \mathbf{t_1 p_1^t + t_2 p_2^t + \ldots\ldots\ldots\ldots + t_k p_k^t + E}$$

where:

X = raw data matrix

t = scores vector

p = loadings vector

E = residuals

k = must be less than or equal to the smaller dimension of **X**

In this equation, E is that part of the original data (X) not explained by the model. The explainable part ($\mathbf{t_1 p_1^t + t_2 p_2^t + \ldots\ldots\ldots\ldots + t_k p_k^t}$), captures the essential patterns in the data and is known as the principal components (PCs). The first PC accounts for as much of the variability in the data as possible, and each succeeding component accounts for the remaining variance. Thus, in a 3-component model, PC1 will have the largest explained variance, PC2 the second most and PC3 the least. The explained variance, similar to the eigenvalues, indicates the portion of variability captured by a PC (Wold, 1987). The larger the eigenvalue, the greater the amount of the variance the PC explains.

Calibration and validation sets

Calibration and validation (test) sets were obtained from the original data using the Kennard-Stone (KS) algorithm (Kennard and Stone, 1969). This algorithm allows to design model set uniformly, i.e., samples are selected into a model set by including samples that represent the most different sources of variability. Thus, it employs distance calculations and selects samples based on their spectral features (Pasquini, 2018). The algorithm was employed on the full data set to split it into a calibration set comprised of 83 samples (70% of the original data set) and the remaining 35 (30%) were used for validation. Table 3.2 illustrates the number of samples used for calibration and validation.

Classification methods

Classification models were developed using hard and soft modelling methods. Here were used popular techniques such as linear discrimination analysis (LDA) (Fisher, 1936), partial least squares discriminant analysis (PLS-DA) (Barker and Rayens, 2003) and soft independent modelling of class analogy (SIMCA) (Wold, 1976; Brereton, 2011). The different species were grouped according to size, medium-sized (impala, blesbok and springbok) and large-sized (eland, black wildebeest and zebra) species and models were developed within each of these groups.

Table 3.2 Calibration and validation (tests) sets obtained by Kennard-Stone algorithm

Species	Calibration (70%) = 83	Validation (30%) = 35
Impala	23	10
Blesbok	21	5
Springbok	10	3
Black wildebeest	5	4
Eland	10	5
Zebra	14	8

For the PLS-DA approach, groups of classes were modelled simultaneously using one PLS-2 model. Cross-validation based on venetian blinds was applied during the calibration process to determine the optimum number of latent variables (LVs) and all models were independently validated. For all algorithms, class modelling was set to “Class Predict Strict” in the PLS_Toolbox (Version 8.6.2, Eigenvector Research, Inc., Manson, WA USA). In this approach, each sample belongs to a given class if the probability is greater than a threshold value for that class. If no class has a probability greater than the threshold, or if more than one class has a probability exceeding it, the sample is assigned to class zero (0) indicating no class could be assigned. Confusion matrices were used to evaluate the performance of the individual models. To interpret the confusion matrix results, classification accuracy was calculated using the following equation (Oliveri and Downey, 2012):

$$\%Accuracy = \frac{TP+TN}{TP+TN+FP+FN} \times 100\%$$

where,

TP = True positive (when samples belonging to the class being modelled are correctly predicted to be inside the boundary of that class) e.g. for a blesbok class model, true positive samples are blesbok samples predicted as such,

FN = False negative (when samples belonging to the class being modelled are incorrectly predicted to be outside the boundary of the class), e.g. in a blesbok class model, false negative samples are blesbok samples that are misclassified

FP = False positive (when samples not belonging to the class being modelled are incorrectly predicted to be inside the boundary of the class), e.g. in a blesbok class model, false positive samples are samples not being blesbok, predicted as blesbok

TN = True negative (when samples not belonging to the class being modelled are correctly predicted to be outside the boundary of the class), e.g. in a blesbok class model, true negative samples are samples not being blesbok, predicted as such

Results and discussion

Proximate analysis

Proximate analysis was done to support the spectral interpretation of the species, and these are presented in Table 3.3. The moisture content of game meat usually varies between 70 and 77% (Hoffman, 2007). In this study, the moisture content was between 75.30 and 75.60%, with no major differences between the species. As expected, the protein content was within the range (20.0–23.8%) reported by Hoffman (2007), with blesbok the lowest (21.53%) and eland the highest (22.96%). The fat content was within the reported limits (0.8–2.45%), except blesbok with a fat content of 2.48%. This was higher than the 1.7% reported by Von la Chevallerie (1972). The zebra's composition was similar results to that reported by Hoffman et al. (2016).

Table 3.3 Average proximate chemical composition (moisture, fat and protein) (%) of the LTL muscles of blesbok, impala, eland and zebra

Species	Moisture (%)	Protein (%)	Fat (%)
Blesbok	75.30	21.53	2.48
Impala	75.37	22.65	1.61
Eland	75.59	22.96	1.21
Zebra	75.60	22.33	1.76

Characterisation of NIR spectra

Mean spectra (raw and pre-processed) of the medium-sized antelopes and the large-sized game species are shown in Figs. 3.1 and 3.2, respectively. The raw spectra (Figs. 3.1a and 3.2a) show three broad absorption bands typical of red meat samples. The bands at 976 and 1434 nm are related to third and second overtone stretching of the O-H bond (Barbin *et al.,*2012; Elmasry *et al.,* 2011) associated with the moisture content of the samples. Water is the main component of meat (ca. 75%) (Table 3.3). In addition to these, the wavelength band at 1186 nm corresponds to the second overtone of a C-H stretching bond, associated with intramuscular fat (Cozzolino and Murray, 2004; Ding and Xu, 2000; Osborne *et al.,* 1993).

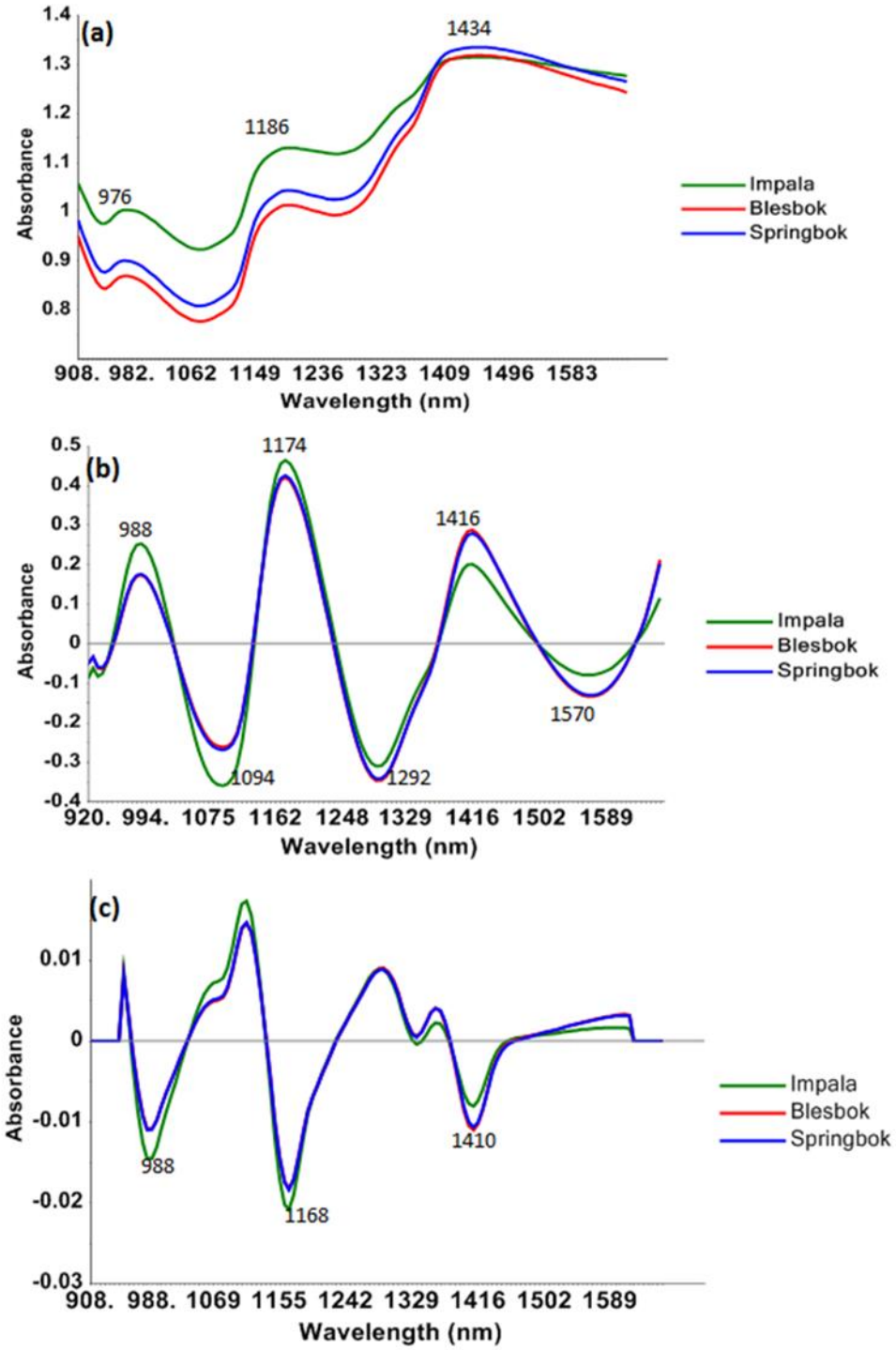

Figure 3. 1 Mean spectra of samples of the medium-sized antelopes (impala, blesbok and springbok species) with (a) raw spectra, (b) Combination 1 pre-processed spectra and (c) Combination 2 pre-processed spectra. Wavebands 976–988 nm and 1410–1434 nm are associated with moisture and wavebands 1168–1186 nm with fat

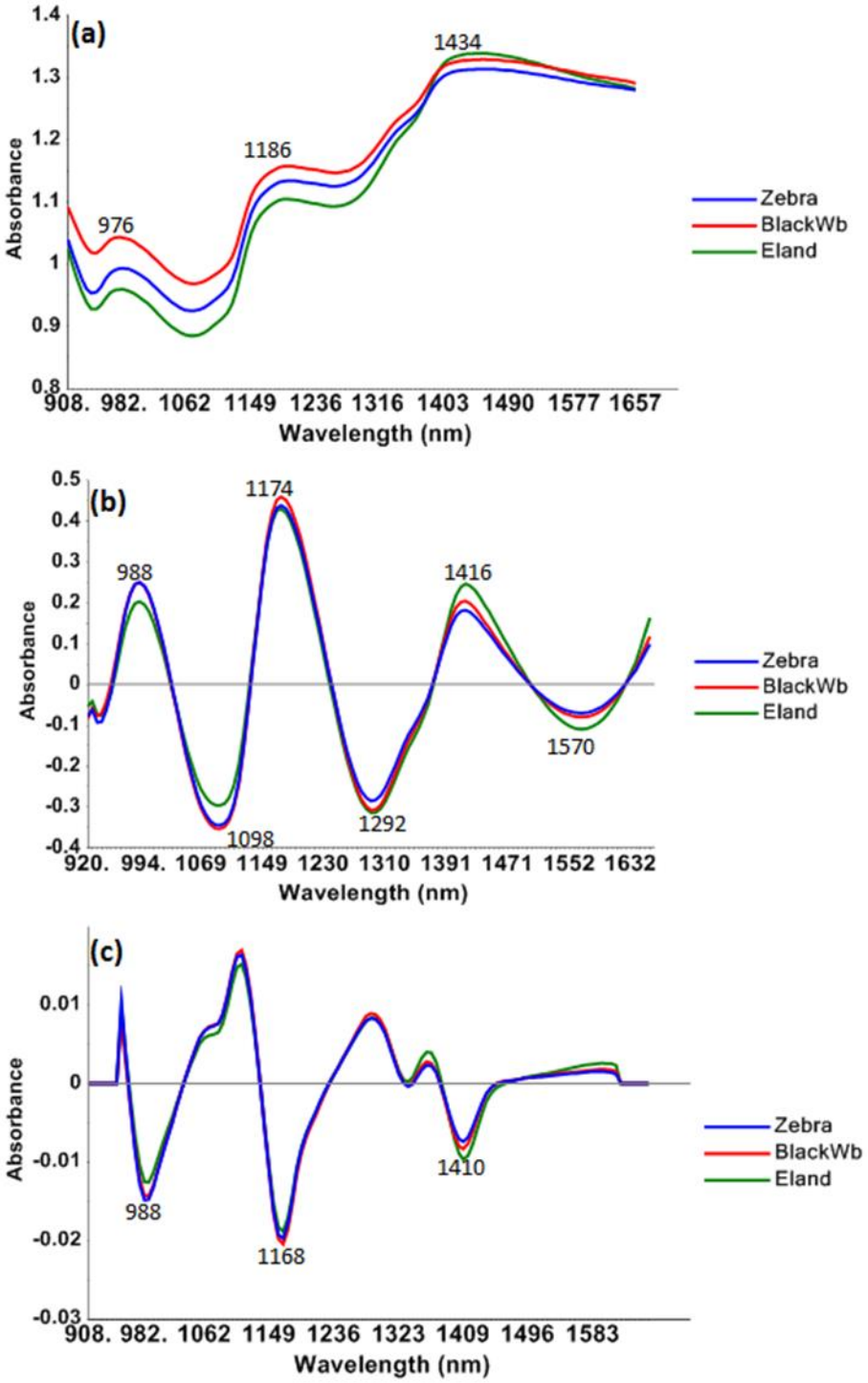

Figure 3.2 Mean spectra of the samples of the samples of the large-sized game species (black wildebeest, eland and zebra) with (a) raw spectra, (b) Combination 1 pre-processed spectra and (c) Combination 2 pre-processed spectra. Wavebands 976–988 nm and 1410–1434 nm are associated with moisture and wavebands 1168–1186 nm with fat.

Pre-processing enhanced the differences between the respective species at these wavelengths (Figs. 3.1b & c and 3.2b & c). The average spectra of blesbok and springbok seemed to be more similar than that of impala. The average spectra of the large-sized species showed differences in absorbance values between all three species, especially at the bands associated with moisture. The large-sized species seemed to be more similar in terms of fat. Due to the broad bands observed in NIR spectra, it was not always possible to distinguish between the different species based on visual inspection of the raw or pre-processed spectra. Further analysis such as exploratory data analysis and classification model development are required to effectively determine the potential of NIR spectroscopy to distinguish between game meat muscles.

Principal component analysis (PCA)

The PCA scores plot (PC1 vs. PC3) of all six species, pre-processed with Combination 1 transformation and accounted for 94% of the total explained, is shown in Fig. 3.3a. Two clear clusters separated the medium-sized antelopes from the large-sized game species. The loading line plot of PC3 (Fig. 3.3b) indicates a waveband at ca. 1372 nm, associated with fat, accounting for the separation between the medium- and large-sized game species. This is evident from the difference in average fat content of blesbok and impala (2.05%) compared to that of eland and zebra (1.49%) (Table 3.3).

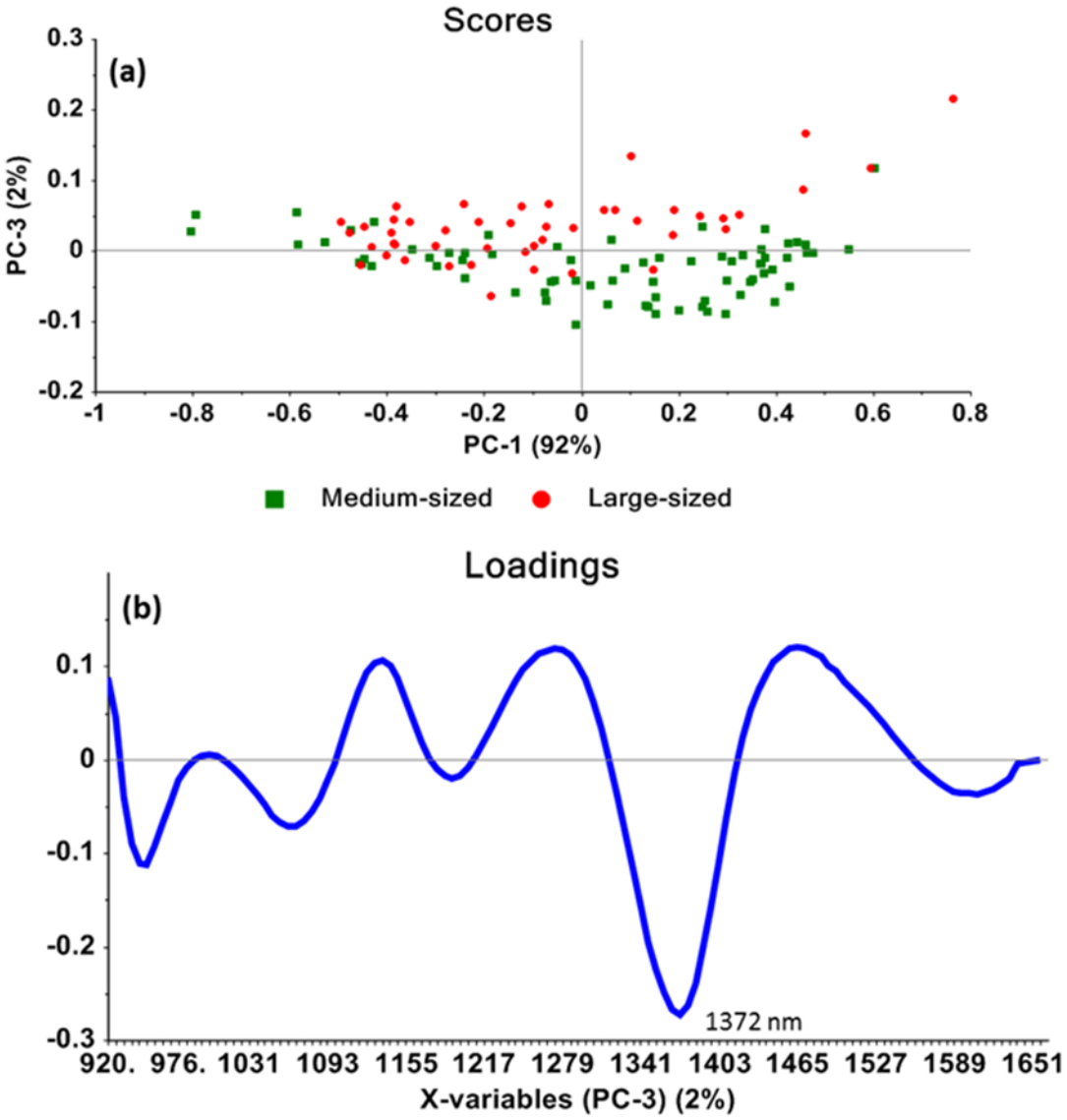

Figure 3.3 (a) PCA scores plot (Combination 1 pre-processed spectra; smoothing and SNV-Detrend) of PC1 vs. PC3 (94% explained variance) illustrating separation of the medium-sized antelopes (impala, blesbok and springbok) from the large-sized game species (black wildebeest, eland and zebra) samples in the direction of PC3 (b) PC3 loadings line plot, with the waveband at ca. 1372 nm (associated with fat) contributing to the separation of the meat samples from the medium-sized antelopes and large-sized game species

Fig. 3.4 and Fig. A3.1 of the Appendix depict the PCA scores plots of the medium-sized antelopes, pre-treated with Combination 1 (smoothing and SNV-Detrend) and Combination 2 (SNV-Detrend and 2nd derivative) pre-processing, respectively. The first two principal components (PCs) explain 98% of the total variance when the spectra were pre-processed with Combination 1 and 95% when pre-processed with combination 2. The PCA scores plots shows separation in both cases, in the direction of PC1, between the impala muscles and those of springbok and blesbok. The PC1 loadings line (Fig. 3.4b), for the data pre-processed with combination 1, shows prominent wavebands at 982 and 1416 nm (O-H bonds) and 1093 and 1570 nm (N-H bonds), associated with moisture and protein, respectively (Osborne et al., 1993). When the data was pre-processed with Combination 2, wavebands at 976 nm (moisture) and, 1155 and 1366 nm (fat) were contributing to the separation.

The similar spectral characteristics observed between the springbok and blesbok samples is probably because they were harvested from the same farm, during the same season and grazing on the same pasture/fodder. Van Zyl, and Ferreira (2004) reported a distinct chemical difference between springbok, blesbok and impala harvested from different regions. In addition, Neethling *et al.* (2018) noted that springbok from three farm locations differed significantly in their proximate composition and sensory attributes. Based on these findings, it appears that the geographical origin of the species has a meaningful impact on their chemical composition. The lack of geographic variation in our study is evident.

The PCA scores plots of the large-sized species pre-processed with Combination 1 (smoothing and SNV-Detrend) and Combination 2 (SNV-Detrend and 2nd derivative), are shown in Fig. A3.2 of the Appendix and Fig. 3.5, respectively. Fig. A3.2a of the Appendix shows the scores of PC1 vs. PC2 (95% explained variance) illustrating separation of zebra muscles from eland and black wildebeest in the direction of PC1. The wavelength bands (982 and 1422 nm (O-H) and 1087 and 1570 nm (N-H)) responsible for this separation are shown in the PC1 loadings line plot (Fig. A3.2b of the Appendix). The O-H bands are related to third and second overtone stretching of the O-H bond (Barbin *et al.,* 2012), associated with the moisture content of the samples, while the N-H bands are associated with the second overtone stretching related to NH2 compounds (proteins) (Osborne et al., 1993). In the direction of PC2, eland muscles are separated from black wildebeest and the accompanying loadings line plot (Fig. A3.2c of the Appendix) indicates 1174 nm as the responsible waveband. This C-H, second overtone stretching bond is associated with fat (Cozzolino and Murray, 2004). Hoffman *et al.,* (2009) reported that black wildebeest harvested in spring (regardless of sex), to have a low-fat content. Thus, it seems possible that the difference in fat content between the eland and black wildebeest muscles are due to the fact that the black wildebeest species were harvested in spring (Table 3.1).

Fig. 3.5a displays the scores plot of PC1 vs. PC3 (78% explained variance) showing clustering of the three groups of large-sized species. The PC1 loadings line plot (Fig. 3.5b) reveals the main wavelength bands responsible for the grouping as those located at 970, 1155 and 1366 nm, which correspond to the moisture and fat, respectively. The loadings line plot for PC3 (Fig. 3.5c)

shows prominent bands at 1112 and 1366 nm (both CH bands), responsible for the separation of eland and black wildebeest.

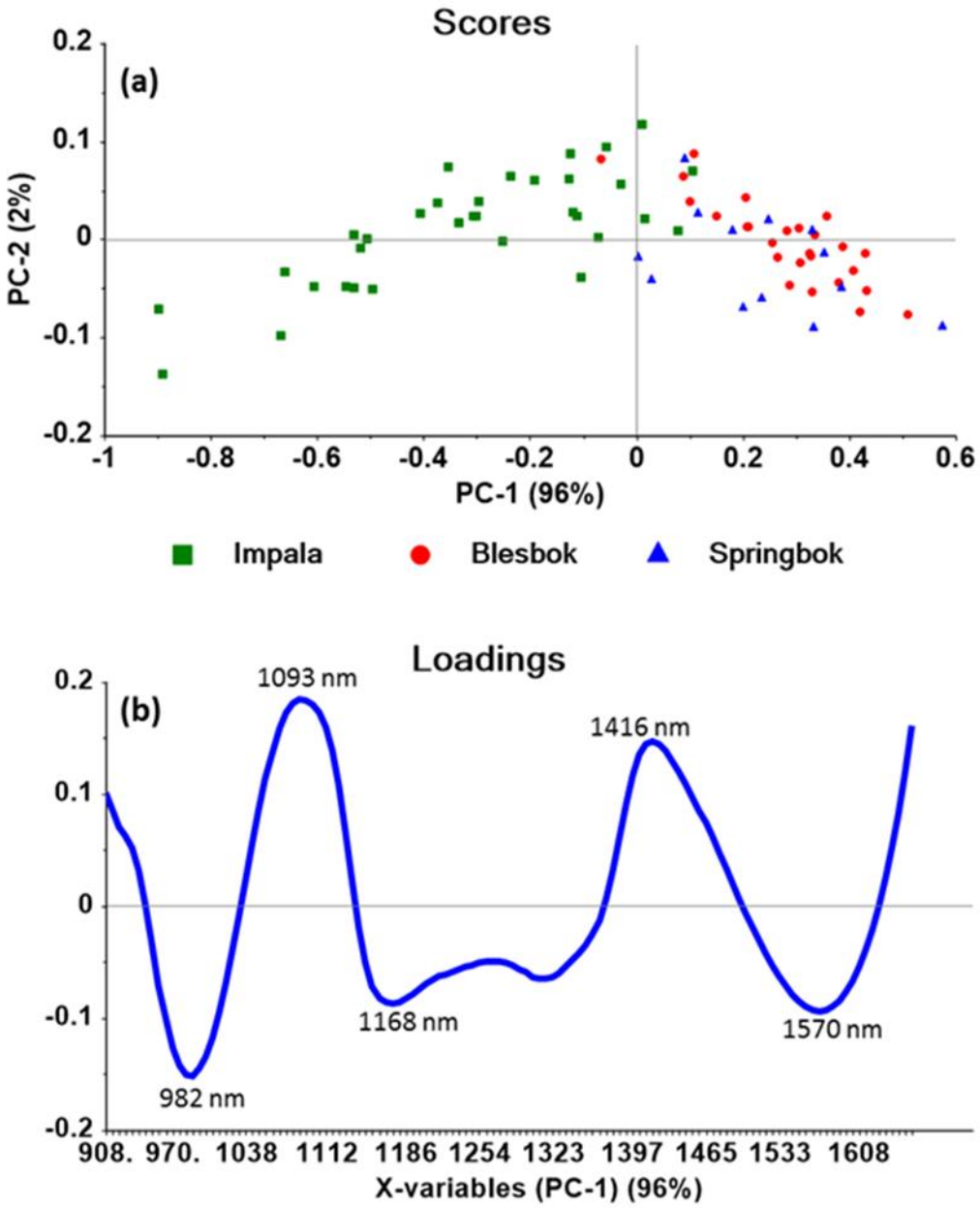

Figure 3.4 (a) PCA scores plot (smoothing and SNV-Detrend pre-processed spectra) of PC1 vs. PC2 (98% explained variance) illustrating separation of the impala meat muscles from those of blesbok and springbok in the direction of PC1 (b) PC1 loadings line plot, depicting wavebands associated with protein (1093 and 1570 nm) and moisture (982 and 1416 nm) mainly contributing to the separation of impala from blesbok and springbok

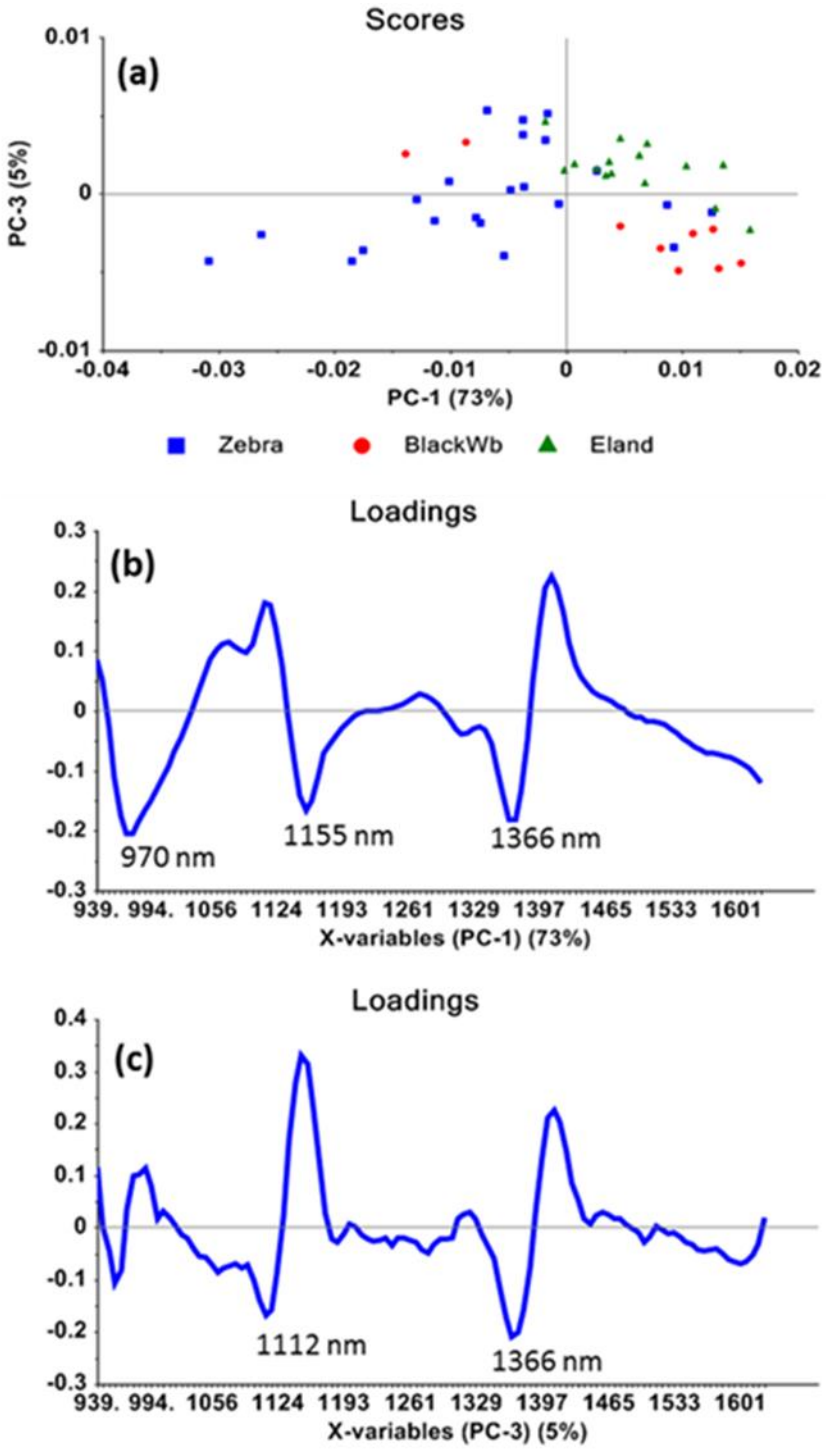

Figure 3.5 (a) PCA scores plot (SNV-Detrend and 2nd derivative pre-processed spectra) of PC1 vs. PC3 (78% explained variance) showing the grouping of the zebra, black wildebeest and eland muscles (b) PC1 loadings line plot, showing the wavebands associated with the separation of most of the zebra samples from those of eland and black wildebeest (970 nm = moisture; 1155 and 1366 nm = fat) (c) PC3 loadings line plot depicts the separation of the samples of eland and black wildebeest due to difference in fat (1112 and 1366 nm)

Classification methods

Because of the separation observed in the PCA scores plot (Fig. 3.3a), the two groups (medium-sized antelopes and the large-sized game species) were classified with PLS-DA and a 96% classification accuracy was obtained (Fig. A3.3 of the Appendix). The model showed one medium-sized antelope (impala) sample misclassified as a large-sized game species, while two large-sized game species (zebra) were misclassified as medium-sized antelopes. Based on these results, subsequent classification models were developed within these two groups.

Table 3.4 shows the classification accuracies of models developed with LDA, PLS-DA and SIMCA for both pre-processing combinations. When combination 1 was used, LDA delivered overall prediction results above 68% with 100% accuracy for the impala meat samples. The PLS-DA models gave the lowest classification accuracies ranging from 47 to 91%. Regardless of the low accuracy (57%) obtained for zebra species, the overall classification accuracy for large-sized species was 77%. SIMCA models yielded classification accuracies ranging from 67%, up to 100% for impala and eland meat samples. However, when pre-processing combination 2 was used for spectral treatment of SIMCA models, the lowest accuracies were obtained (50 to 84%); this highlights the importance of the pre-processing method used and concurs with Rinnan, van den Berg, and Engelsen (2009). The LDA model generated the best prediction results across all categories with classification accuracies ranging from 72 to 95%. The PLS-DA model also gave good accuracies, ranging from 70 to 96%. With respect to the medium-sized antelopes category, impala samples gave outstanding results across the models. This was already evident in the spectral features (Fig. 3.1). In the case of the large-sized species, the calibration and prediction accuracies of eland samples were outstanding for PLS-DA models compared to the others (LDA & SIMCA). In contrast, when SIMCA was used for classification, the lowest accuracies were achieved for the eland samples. Classification accuracies of up to 82% were obtained for the zebra samples, despite the difference between the two batches (Table 3.1). This indicates that as much variation as possible is needed from each species to build a robust model.

Table 3.5 illustrates the confusion matrix of the calibration sets. A notable result was obtained with PLS-DA pretreated with combination 2 for springbok samples, where 50% were misclassified (false negatives). Springbok meat samples had the highest misclassification rate, and were misclassified as blesbok (Fig. A3.4 of the Appendix). This is likely because both species were harvested from the same farm in the same season, feeding on the same pasture (Table 3.1) (Neethling et al., 2014). A noteworthy model for the large-sized species was obtained with SIMCA pre-treated with combination 1. Eland had a 50% misclassification rate, while the other classes (True negatives) were correctly classified. Thus, this model was capable of identifying all the other classes as a group. Even though the eland had the lowest classification accuracy (75%), in contrast to black wildebeest (90%) and zebra (78%), the model had a validation accuracy of 100% (Table 3.4). This should be approached with caution though as only 5 eland samples were in the validation set.

Table 3.4 Calibration (Cal) and validation (Val) accuracy (%) results of LDA, PLS-DA and SIMCA models, for classification of meat from medium-sized antelopes and large-sized species using pre-processed spectral data (Combinations 1: smoothing and SNV-Detrend; Combination 2: SNV-Detrend and 2nd derivative)

		LDA		PLS-DA		SIMCA	
Category	**Species**	**Cal (%)**	**Val (%)**	**Cal (%)**	**Val (%)**	**Cal (%)**	**Val (%)**
Combination 1							
Medium-sized antelopes	Blesbok	91	**72**	**84**	**66**	**91**	**70**
	Impala	94	100	89	84	98	100
	Springbok	78	90	73	47	70	67
Large-sized species	Black wildebeest	88	68	100	83	90	96
	Eland	90	87	82	91	75	100
	Zebra	86	82	72	57	78	69
Combination 2							
Medium-sized antelopes	Blesbok	89	86	90	70	57	60
	Impala	98	95	90	89	85	80
	Springbok	80	93	72	77	65	80
Large-sized species	Black wildebeest	88	72	90	71	78	84
	Eland	83	83	87	96	50	50
	Zebra	83	82	75	76	71	57

Table 3.5 Confusion matrix obtained for LDA, PLS-DA and SIMCA classification models for medium-sized antelopes and large-sized species

Classification Method	Class	True positive	False positive	True negative	False negative
Smoothing (7 points) and SNV-Detrend pre-processed spectral data (Combination 1)					
Medium-sized antelopes					
LDA	Blesbok	95	12	88	5
	Impala	96	6	94	4
	Springbok	70	20	80	30
PLS-DA	Blesbok	71	3	97	29
	Impala	78	0	100	22
	Springbok	50	5	95	50
SIMCA	Blesbok	80	0	100	19
	Impala	96	0	100	4
	Springbok	40	0	100	60
Large-sized species					
LDA	Black wildebeest	89	13	88	11
	Eland	100	16	84	0
	Zebra	86	13	87	14
PLS-DA	Black wildebeest	100	0	100	0
	Eland	80	16	84	20
	Zebra	50	7	93	50
SIMCA	Black wildebeest	80	0	100	20
	Eland	50	0	100	50
	Zebra	57	0	100	43
SNV-Detrend and 2nd derivative (7 points) pre-processed spectral data (Combination 2)					
Medium-sized antelopes					
LDA	Blesbok	95	15	85	5
	Impala	96	0	100	4
	Springbok	80	20	80	20
PLS-DA	Blesbok	86	6	94	14
	Impala	83	3	97	17
	Springbok	50	7	93	50

SIMCA	Blesbok	14	0	100	86
	Impala	70	0	100	30
	Springbok	30	0	100	70
Large-sized species					
LDA	Black wildebeest	89	8	92	11
	Eland	90	21	79	10
	Zebra	79	13	87	21
PLS-DA	Black wildebeest	80	0	100	20
	Eland	80	5	95	20
	Zebra	57	7	93	43
SIMCA	Black wildebeest	60	4	96	40
	Eland	0	0	100	100
	Zebra	43	0	100	57

When pre-processed with combination 2, none of the eland samples were correctly classified. This further emphasises the importance of choice of pre-processing method.

The confusion matrix results are best visualised graphically, as illustrated in Fig. A3.4 of the Appendix where the PLS-DA (pre-processed with combination 2) predictions are shown for the medium-sized antelope. In the blesbok model, two samples were misclassified as springbok while four springbok samples were misclassified as blesbok, which also concurs with the overlapping spectral features discussed in Section 3.1 (Fig. 3.1). For the impala model, one sample was misclassified, and one springbok sample was classified as impala. Finally, for the springbok model, three springbok samples were misclassified as blesbok and, three blesbok and four impala samples were misclassified as springbok.

Conclusions

To date, this is the first reported study to discriminate different South African game meat species using NIR spectroscopy in combination with multivariate data analysis. From this study, it was attested that it is possible to differentiate game meat with classification accuracies of 67 up to 100%. However, it is too early for the models to be used in the industry, based on the limited dataset. Moreover, the three discrimination methods applied have proven to discriminate meat samples from the two groups (medium-sized antelopes and large-sized species) of game species. In general, impala, black wildebeest and eland gave the best classification results while blesbok and springbok were not good due to spectral similarities. Furthermore, it was observed, especially with the PLS-DA and the SIMCA models, that the classification accuracy of a model is influenced by the pre-processing method. In this study, SIMCA models performed better when treated with smoothing and SNV-Detrend while PLS-DA models gave better accuracies with SNV-Detrend and Savitzky-Golay 2nd.

References

AOAC International. (2002). Dumas Combustion method. AOAC Official Method 992.15. In: *Official methods of analysis*, ed. Arlington, Virginia, USA: Association of Official Analytical Chemists Inc.

AOAC International. (2002). Loss on drying (moisture) at 95 – 100°C for feeds. AOAC Official 17th Method 934.0. In: *Official methods of analysis*, ed. Arlington, Virginia, USA: Association of Official Analytical Chemists Inc.

Ballin, N. Z. (2010). Authentication of meat and meat products. *Meat Science*, ***83***(3), 577-877.

Barbin, D., Elmasry, G., Sun, D. W., & Allen, P. (2012). Near-infrared hyperspectral imaging for grading and classification of pork. *Meat Science*, ***90(***1), 259–268.

Barker, M. & Rayens, W. (2003). Partial least squares for discrimination. *Journal of Chemometrics,* **17,** 166–173.

Barnes, R. J., Dhanoa, M. S., & Lister, S. J. (1989). Standard normal variate transformation and de-trending of near-infrared diffuse reflectance spectra. *Applied Spectroscopy, **43**,* 772–777.

Brereton, R. G. (2011). One-class classifiers. *Journal of Chemometrics*, ***25(***5), 225–246.

Cawthorn, D. M., Steinman, H. A., & Hoffman, L. C. (2013). A high incidence of species substitution and mislabelling detected in meat products sold in South Africa. *Food Control*, ***32(***2), 440–449.

Cowe, A., & McNicol, J. W. (1985). The use of principal components in the analysis of near infrared spectra. *Applied Spectroscopy, **39***(2)*,* 257-266.

Cozzolino, D., & Murray, I. (2004). Identification of animal meat muscles by visible and near infrared reflectance spectroscopy. *LWT - Food Science and Technology*, ***37***(4), 447–452.

DAFF (Department of Agriculture, Forestry and Fisheries). 2004. Meat Safety Act (Act No. 40 of 2000), Red meat regulations (No. R. 1072 of 17 September 2004) (Regulation Gazette No. 8056). Government Printing Offices, South Africa.

Ding, H. B., & Xu, R. J. (1999). Differentiation of beef and kangaroo meat by visible/near-infrared reflectance spectroscopy. *Journal of Food Science*, ***64***(5), 814–817.

Ding, H. B., & Xu, R. J. (2000). Near-infrared spectroscopic technique for detection of beef hamburger adulteration. *Journal of Agricultural and Food Chemistry*, ***48***(6), 2193–2198.

Elmasry, G., Iqbal, A., Sun, D. W., Allen, P., & Ward, P. (2011). Quality classification of cooked, sliced turkey hams using NIR hyperspectral imaging system. *Journal of Food Engineering*, ***103***(3), 333–344.

Engel, J., Gerretzen, J., Szymańska, E., Jansen, J. J., Downey, G., Blanchet, L., & Buydens, L. M.

C. (2013). Breaking with trends in pre-processing? *TrAC - Trends in Analytical Chemistry*, ***50*****,** 96–106.

Fajardo, V., González Isabel, I., Rojas, M., García, T., & Martín, R. (2010). A review of current PCR-based methodologies for the authentication of meats from game animal species. *Trends in Food Science and Technology*, ***21*****(**8), 408–421.

Fisher R. A. (1936). The use of multiple measurements in taxonomic problems. *Annals of Eugenics, **7**,* 179–188.

Hoffman, L. C. (2007). The meat we eat: are you game? *Inaugural Addess.* Stellenbosch University, Western Cape, South Africa.

Hoffman, L. C., Geldenhuys, G., & Cawthorn, D. M. (2016). Proximate and fatty acid composition of zebra *(Equus quagga burchellii)* muscle and subcutaneous fat. *Journal of the Science of Food and Agriculture, **96**:* 3922–3927.

Hoffman, L. C., Kroucamp, M., & Manley, M. (2007). Meat quality characteristics of springbok *(Antidorcas marsupialis).* 2: Chemical composition of springbok meat as influenced by age, gender and production region. *Meat Science*, ***76***(4), 762–767.

Hoffman, L. C., Muller, M., Schutte, D. W., Calitz, F. J., & Crafford, K. (2005). Consumer expectations , perceptions and purchasing of South African game meat. *South African Journal of Wildlife Research*, ***35*****(**1), 33–42.

Hoffman, L. C., van Schalkwyk, S., & Muller, N. (2009). Effect of season and gender on the physical and chemical composition of black wildebeest (*Connochaetus gnou*) meat. *South African Journal of Wildlife Research*, ***39*****(**October), 170–174.

Hoffman, L. C., & Wiklund, E. (2006). Game and venison - meat for the modern consumer. *Meat Science*, ***74*****(**1), 197–208.

Jonker, K. M., Tilburg, J. J. H. C., Hagele, G. H., & de Boer, E. (2008). Species identification in meat products using real-time PCR. *Food Additives & Contaminants. Part A, Chemistry, Analysis, Control, Exposure & Risk Assessment*, ***25***(5), 527–533.

Kamruzzaman, M., Sun, D. W., ElMasry, G., & Allen, P. (2013). Fast detection and visualization of minced lamb meat adulteration using NIR hyperspectral imaging and multivariate image analysis. *Talanta*, ***103***, 130–136.

Kennard, R. W., & Stone, L. A. (1969). Computer aided design of experiments. *Technometrics, **11** (1),* 137-148.

Lee, C. M., Trevino, B., & Chaiyawat, M. (1996). A simple and rapid solvent extraction method for determining total lipids in fish tissue. *Journal of AOAC International, **79*****(**2), 48-492.

LJung, P. E., Riley, S. J., Heberlein, T. A., & Ericsson, G. R. (2012). Eat Prey and Love : Game-Meat Consumption and Attitudes Toward Hunting, *Wildlife Society Bulletin*. ***36***(4), 669–675.

Mamani-Linares, L. W., Gallo, C., & Alomar, D. (2012). Identification of cattle, llama and horse meat by near infrared reflectance or transflectance spectroscopy. *Meat Science, **90**,* 378 - 385.

Manley, M. (2014). Near-infrared spectroscopy and hyperspectral imaging: Non-destructive analysis of biological materials. *Chemical Society Reviews*, ***43***(24), 8200–8214.

Marescotti, M. E., Caputo, V., Demartini, E., & Gaviglio, A. (2019). Discovering market segments for hunted wild game meat, ***149***(November 2018), 163–176.

Moreno-ortega, A., Morales, J. S., Moreno-ortega, A., Angel, M., Lopez, A., Casas, A. A., Amaro, M. A. (2018). Game meat consumption by hunters and their relatives : A probabilistic Game meat consumption by hunters and their relatives : a probabilistic approach. *Food Additives & Contaminants: Part A*, ***00***(00), 1–10.

Mostert, R., & Hoffman, L. C. (2007). Effect of gender on the meat quality characteristics and chemical composition of kudu (*Tragelaphus strepsiceros)*, an African antelope species. *Food Chemistry*, ***104*****(**2), 565–570.

Neethling, J., Britz, T. J., & Hoffman, L. C. (2014). Impact of season on the fatty acid profiles of male and female blesbok *(Damaliscus pygargus phillipsi)* muscles. *Meat Science*, ***98***(4), 599–606.

Neethling, J., Hoffman, L. C., & Britz, T. J. (2014). Impact of season on the chemical composition of male and female blesbok (*Damaliscus pygargus phillipsi*) muscles. *Journal of the Science of Food and Agriculture*, ***94***(3), 424–431.

Neethling, J., Muller, M., van der Rijst, M., & Hoffman, L. C. (2018). Sensory quality and fatty acid content of springbok (*Antidorcas marsupialis*) meat: influence of farm location and sex. *Journal of the Science of Food and Agriculture*, ***98***(7), 2548–2556.

O'Brien, N., Hulse, C. A., Pfeifer, F., & Siesler, H. W. (2013). Near infrared spectroscopic authentication of seafood. *Journal of Near Infrared Spectroscopy*, ***21***(4), 299–305.

O'Mahony, P. J. (2013). Finding horse meat in beef products-a global problem. *Qjm*, ***106*****(**6), 595–597.

Oliveri, P., & Downey, G. (2012). Multivariate class modeling for the verification of food-authenticity claims. *TrAC - Trends in Analytical Chemistry*, ***35*****,** 74–86.

Osborne, B. G., Fearn, T., & Hindle, P. H. (1993). Practical NIR spectroscopy with applications in food and beverage analysis, 2nd edn.*Longman Scientific & Technical, Essex*

Pasquini, C. (2018). Near infrared spectroscopy: A mature analytical technique with new perspectives – A review. *Analytica Chimica Acta*, ***1026*****,** 8–36.

Prieto, N., Andrés, S., Giráldez, F. J., Mantecón, A. R., & Lavín, P. (2008). Discrimination of adult steers (oxen) and young cattle ground meat samples by near infrared reflectance spectroscopy (NIRS). *Meat Science*, ***79*****(1)**, 198–201.

Reid, L. M., O'Donnell, C. P., & Downey, G. (2006). Recent technological advances for the determination of food authenticity. *Trends in Food Science & Technology*, **17**, 344–353.

Rinnan, Å., Berg, F. van den, & Engelsen, S. B. (2009). Review of the most common pre-processing techniques for near-infrared spectra. *TrAC - Trends in Analytical Chemistry*, ***28***(10), 1201–1222.

Savitzky, A., & Golay, M. J. E. (1964). Smoothing and differentiation of data by simplified least squares procedures. *Analytical Chemistry*, ***36***(8), 1627–1639.

Van Schalkwyk, D. L., & Hoffman, L. C. (2010). *Guidelines for the harvesting of game for meat export*. Windhoek, Namibia: Printech cc 71pp.

Van Zyl, L., & Ferreira, A. V. (2004). Physical and chemical carcass composition of springbok (Antidorcas marsupialis), blesbok (Damaliscus dorcas phillipsi) and impala (Aepyceros melampus). *Small Ruminant Research*, ***53*****(**1–2), 103–109.

Varmuza, K., & Filzmoser, P. (2009). Chemoinformatics-chemometrics-statistics. *In Introduction to multivariate statistical analysis in chemometrics* (pp. 1–26). Boca Raton, FL: CRC Press Taylor and Francis Group.

Verbeke, J., & Ward, R. W. (2006). Consumer interest in information cues denoting quality, traceability and origin: An application of ordered probit models to beef labels. *Food Quality and Preference, **17**,* 453-467.

Von la Chevallerie, M. (1972). Meat quality of seven wild ungulate species. *South African Journal of Animal Science, **2**,* 101–103.

Walker, M. J., Burns, M., & Burns, D. T. (2013). Horse meat in beef products- Species Substitution 2013. *Journal of the Association of Public Analysts (Online)*, ***41*****,** 67–106.

Wold, S. (1976). Pattern recognition by means of disjoint principal components models. *Pattern Recognition*, ***8***(3), 127–139.

Wold, S. (1987). Principal component analysis. *Chemometrics and Intelligent Laboratory Systems*, ***2*****,** 37–52.

Chapter 4

Discriminating muscle type of selected game species using near infrared (NIR) spectroscopy

Abstract

In this study near infrared (NIR) spectroscopy was used to discriminate between different muscle types within each species of selected game animals, and to classify species regardless of the muscle. Muscle steaks from *longissimus thoracis et lumborum* (LTL) located at the 6th rib of the carcasses, *infraspinatus* (IS) and *supraspinatus* (SS) located on the forequarter, and *biceps femoris* (BF), *semitendinosus* (ST) and *semimembranosus* (SM) located on the hindquarter of impala and eland species; and samples from fan fillet (FF), big drum (BD), triangle steak (TS), moon steak (MS) and rump steak (RS) of ostrich species were scanned with a handheld NIR spectrophotometer in the spectral range of 908–1700 nm. Spectra were pre-treated with different pre-processing methods and classification models were developed using partial least squares discriminant analysis (PLS-DA). Classification accuracies were higher when the muscles were grouped according to their anatomical location in the carcass, than attempting to classify them separately. Classification accuracies ranging from 85.0 to 100% were achieved throughout, with forequarter muscles yielding the highest classification accuracy rate for both impala and eland species. Furthermore, when the species were discriminated regardless of muscles, PLS-DA models pre-treated with SNV-Detrend and Savitzky-Golay 1st derivative yielded accuracies of 97, 81 and 92% for eland, impala and ostrich, respectively. These results indicate that NIR spectroscopy can be used for the authentication of game meat, specifically impala, eland and ostrich. Furthermore, it was easier to discriminate species regardless of the muscle used than different muscles within each species.

Keywords: Near infrared spectroscopy; Discrimination; Multivariate analysis; Muscle types; Game meat; Food fraud

Published as: Dumalisile, P., Manley, M., Hoffman, L. & Williams, P.J. (2020). Discriminating muscle type of selected game species using near infrared (NIR) spectroscopy. *Food Control*, **110**, 106981.

Introduction

The deception of consumers by retailers selling substituted food products for economic gain is illegal (Department of Health, 2010), and in the food industry it is termed food fraud. As tempting as it may be to retailers or suppliers, the consequences of food fraud are destructive and may include damaging the company's reputation (Van Ruth *et al.*, 2018). Food fraud is defined by Spink and Moyer (2011) as a collective term used to encompass the deliberate and intentional substitution, addition, tampering, or misrepresentation of food, food ingredients, or food packaging; or false or misleading statements made about a product, for economic gain.

Meat and meat products are often targets of food fraud, and are currently leading the top 5 list of EU food categories of illegal import fraud examples (Soon & Manning, 2018). Finding horse meat in beef burgers produced in Ireland in 2013 showed that consumers are undoubtedly encountering undeclared animal species in meat products (O'Mahony, 2013; Walker, Burns, & Burns, 2013). In South Africa, Cawthorn *et al.* (2013) found species in beef sausages that were not declared on the product labelling. Thus, the reported and unreported incidents of undeclared labelling of meat products have subsequently raised the consumers' awareness of quality, traceability and origin of the food they eat (Verbeke and Ward, 2006).

Consumers are very aware of the different muscle types (cuts) and their retail value, mainly due to quality differences. When a customer decides which meat species to buy, the next decision is to choose the muscle type. In most cases tenderness and selling price tend to influence this decision. It is then disappointing and fraudulent to purchase what is thought to be a tender expensive muscle, only to discover it is tough and likely a low-priced muscle. Thus, mislabelling of food products is a serious issue that can even potentially affect the country of origin, in the case of exported products. Proper labelling of meat products is important to help fair trade and to enable consumers to make informed choices (Department of Health, 2010; Department of Agriculture, 2015). In South Africa, there are regulatory bodies governing food legislation. The Foodstuff, Cosmetics and Disinfectant Act, under the Department of Health (DoH), controls the labelling and advertising guidelines of meat and meat products to ensure consumers are not misled and given false information (DoH, 2010). As much as there are regulations in place to protect consumers, the food products need to be verified (authenticated). Food authentication is a procedure that verifies that food complies with its label description (Danezis *et al.,* 2016).

Authenticity issues associated with substitution of meat and its products are identified by a variety of standard analytical methods (chromatography, electrophoretic separation of proteins, enzyme-linked immunosorbent assay (ELISA). However, all of these are tedious, costly, require complicated laboratory procedures and hazardous solvents, need skilled personnel and sample preparation, with most of them also including a destructive step that damages or lowers the quality of the product being tested (Kamruzzaman *et al.*, 2013; Manley, 2014). Therefore, there is a need of a rapid, chemical-free method and near infrared (NIR) spectroscopy offers this.

Kamruzzaman *et al.* (2011) used NIR hyperspectral imaging to discriminate lamb muscles (*Semitendinosus* (ST), *Longissimus dorsi* (LD) and *Psoas major* (PM)) in a wavelength range of 900–1700 nm. They used principal component analysis (PCA) for wavelength reduction and linear discriminant analysis (LDA) (Fisher, 1936) to build classification models. The results showed that it was possible to discriminate between the three lamb muscles with an overall accuracy of 100%. Similarly, Sanz *et al.* (2016) discriminated lamb muscles using hyperspectral imaging in the wavelength range of 380–1028 nm, in a follow-up to the conclusions of Kamruzzaman *et al.* (2011) by including an additional muscle type and using more samples. In their work, they used four different muscle types (LD, ST, PM and *Semimembanosus* (SM)) from 30 animals of a different breed to that Kamruzzaman *et al.* (2011) used and found that the Linear Least Mean Squares (LMS) classifier gave the best classification accuracy of 96.67%. They also found that the inclusion of an additional muscle (SM) made the classification problem more complex. Furthermore, Alomar *et al.* (2003) segregated different types of bovine meat and predicted several chemical fractions from two breeds and three muscles (LD, ST and *Supraspinatus* (SS)) using NIR spectroscopy in a wavelength range of 400–2500 nm. The results showed the two breeds were correctly classified with 78.8% accuracy and the three muscle types yielded 97.8 (LD), 97.7 (SS) and 89.5% (ST) classification accuracy.

Game meat offers a healthy alternative to red meat consumers, as it contains low fat and high protein levels (Hoffman, 2007). It is known that within an animal, different muscles have diverse textural and chemical properties (Van Ba *et al.*, 2014). Moreover, different muscle types differ in their retail price as their quality is not the same, for example fillet is more expensive than sirloin steak. To date, no study has been done on rapid techniques to support the authenticity of different muscle types within species of South African game meat. Therefore, the aim of this study was to investigate the ability of NIR spectroscopy in discriminating selected game muscle types and, to discriminate different species irrespective of the muscle used.

Table 4.1 The total number (females and males) of impala, eland and ostrich species and their average weight (kg)

Species	Total number	Sex		Average Weight (kg)
		Females	Males	
Impala	12	0	12	37.1
Eland	15	7	8	337.3
Ostrich	15	4	11	85.9

Material and Methods

Meat samples

Meat samples were obtained from carcasses of three different game species. A total of 42 animals from the following species were harvested from farms in Bredasdorp and Oudtshoorn, South Africa: 12 Impala (*Aepyceros melampus*), 15 Eland (*Taurotragus oryx*) and 15 Ostrich (*Struthio camelus*). All of these species were harvested in winter. The ostriches were semi-domesticated hence their age could be determined (10 months old), whereas eland and impala were free roaming feeding/ grazing on natural vegetation hence their age could not be determined at the time of slaughter. The sex of all animals was known and is illustrated in Table 4.1. All animals were harvested according to the standard operating procedure (Van Schalkwyk & Hoffman, 2010) with ethical clearance (approval number: SU-ACUM14-001SOP; Stellenbosch University Animal Care and Use Committee). The animals were eviscerated at abattoirs according to the South African red meat regulations (DAFF, 2004; Van Schalkwyk & Hoffman, 2010), and transported chilled to the meat laboratory at the Department of Animal Sciences, Stellenbosch University. After 24 to 48 h post-mortem, the six muscles were removed from the impala and eland carcasses. These were *longissimus thoracis et lumborum* (LTL) located at the 6th rib of the carcasses; *infraspinatus* (IS) and *supraspinatus* (SS) located in the forequarter; and *biceps femoris* (BF), *semitendinosus* (ST) and *semimembranosus* (SM) located in the hindquarter of the carcass. For the ostrich, only five commercially important muscles, (fan fillet (*Muscularis iliotibialis cranialis)*, big drum *(Muscularis femorolibialis medium)*, triangle steak *(Muscularis iliofibularis)*, moon steak *(Muscularis flexor crusis lateralis)* and rump steak *(Muscularis iliotibialis lateralis*), were removed from the leg of the birds. It is important to note that, within the ostrich species there were three genotypes (South African Black, Zimbabwean Blue and Kenyan Red). Identification of the muscles was done by an experienced animal physiologist and verified online (http://bovine.unl.edu/). This information was in turn used to create categories for each muscle type and dummy variables, zero or one, were used to indicated presence or absence during PLS-DA modelling. For example, for category LTL, all LTL muscles would be assigned a one (belonging) and all other muscles a zero (not belonging).

NIR spectroscopy spectral acquisition

From each carcass, fresh muscles of approximately 2.0–2.5 cm thick steaks were scanned with a portable MicroNIR™ OnSite spectrophotometer (Viavi Solutions®, San Jose, CA, USA) over the NIR range of 908–1700 nm. The illumination source of the spectrophotometer included two joined vacuum tungsten lamps coupled to a linear variable filter and a 128-pixel Indium Gallium Arsenide (InGaAs) photodiode array detector. The InGaAs detector was used to achieve a resolution of 30 µm x 250 µm / 50 µm (<12.5 nm resolution). And, the reflectance spectra were recorded at 6.2 nm intervals, resulting in 125 data points. Each muscle steak was scanned in triplicate at different positions at ambient temperature after allowing a minimum bloom period of 30 min. When scanning,

a 2 mm thick glass Steriplan petri dish was placed on top of the meat samples to prevent direct contact of the meat surface moisture with the instrument. Each spectrum was the average of 100 scans, thus a sample spectrum was recorded in about 0.25 to 0.5 seconds. An external white and dark reference standards were scanned every 10 min during sample collection. The total number of impala samples scanned were 72 muscles (12 carcasses X 6 different muscles), while the eland's total samples were 90 (15 carcasses X 6 muscles). For ostrich the total number of samples scanned were 75 muscles (15 birds X 5 different muscles).

Chemical analysis

Moisture, protein and fat content of the game meat steaks were determined as described by Neethling, Hoffman, & Britz, (2014).

Warner Bratzler shear force (WBSF)

After scanning, the muscle steaks were placed individually into plastic bags that were then submerged into a pre-heated water bath (maintained at 80°C) for 60 min and then cooled at 4°C overnight. Once cooled, the samples were then removed from the plastic bags and blotted dry using absorbent paper to remove excess moisture. The cooled cooked meat samples were then used to determine the tenderness using a 3345 model Instron Universal Testing Machine (Apollo Scientific cc, Alberta, Canada) fitted with a Warner-Bratzler blade. Two scalpels fixed at 1 cm from each other were used to cut through the 2 cm thick steaks to produce a rectangular prism of 1 cm x 1 cm x 2 cm that ran parallel with the muscle fibres. Six pieces were removed from each muscle steak and sheared perpendicular to the fibres' longitudinal orientation with a Warner Brazler blade. The average of six measurements was calculated and the value was used to determine the Warner-Bratzler shear force (N) of the muscle, with a greater force being associated with tougher meat (Honikel, 1998).

Multivariate data analysis

The Unscrambler® X version 10.5 (CAMO Software, Oslo, Norway) and PLS_Toolbox (Version 8.6.2, Eigenvector Research, Inc., Manson, WA USA) data analysis software packages were used to analyse the spectra. The spectral range was reduced from 908–1700 nm to 908–1680 nm to remove the spectral noise segments. As each muscle was scanned three times at different points, spectra were averaged to obtain one spectrum per sample.

Spectral pre-processing

Different pre-processing methods were applied to reduce the scattering effects, baseline shifts and background information (noise) in the data. For impala, ostrich and the combined species, spectra

were first treated with standard normal variate (SNV) to remove the scatter effects by centering and scaling each individual spectrum. Detrend transformation was then applied to reduce the baseline shift and curvature in the spectroscopic data (Barnes *et al.,* 1989). Subsequently, for impala and ostrich, SNV-Detrend was followed by Savitzky-Golay 2nd derivative, 2nd order polynomial, with five smoothing points; while for combined species, 1st derivative was used. Savitzky-Golay 1st and 2nd derivative were applied to smooth the noise fluctuations without introducing distortions to the data, and to expose the peaks that were not clearly visible (Savitzky & Golay, 1964). For the eland muscles, the spectra were only treated with SNV and Savitzky-Golay 2nd derivative, 2nd order polynomial, with five smoothing points.

Principal Component Analysis

Principal component analysis (PCA) was performed to explore the spectral data and to get an overview of correlations among the muscle types (Cowe & McNicol, 1985; Wold, 1987; Esbensen *et al.,* 2002). For muscle type discrimination, each species was analysed separately; and then later the different species were collectively analysed regardless of the muscles used.

Calibration and validation (test set) samples

The Kennard-Stone (KS) algorithm was applied to separate the data into a calibration and validation set (Kennard & Stone, 1969). In this approach, a subset of samples providing uniform coverage across the entire data set, including samples on the periphery, are selected. The method begins by finding the two samples which are farthest apart using geometric distance, usually Euclidean distance. To add more samples to the selection set, the algorithm selects from the remaining samples those with the greatest separation distance from the previously selected samples. This process is repeated until the required number of samples, k, have been added to the selection set. In this study, the calibration set was 70% of the original data set and the remaining 30% was used for validation.

Classification

Partial least squares discriminant analysis (PLS-DA) was used to develop models for differentiating the muscle types and species, based on the categories created and the dummy variables assigned, irrespective of muscle used (Barker and Rayens, 2003; Chevallier *et al.,* 2006; Varmuza *et al.,* 2009). Venetian blinds cross-validation was applied to select the optimum number of latent variables (LVs). Subsequently, the models developed were then used to predict unknown samples. When the forequarter, hindquarter and ostrich leg muscles were combined as one class, class modelling was set to "Class Predict Strict". In the PLS_Toolbox (Version 8.6.2, Eigenvector Research, Inc., Manson, WA USA) software, the option "strictthreshold" specifies the "predict strict" classification approach and has a default value of 0.5. This technique reveals only one class that the model is confident to assign each sample. If no class could be assigned to a sample, because the sample's probability is less than the specified threshold, then the sample will be assigned to class zero (0). Afterwards, confusion matrices were used to evaluate the individual models. To interpret the confusion matrix results, percentage classification accuracy was calculated using the following equation (Oliveri and Downey, 2012):

$$\% \text{ Accuracy} = \frac{TP+TN}{TP+TN+FP+FN} \text{ X } 100\%$$

Where:

TP = True positive (samples belonging to the modelled class, if they are correctly predicted to be inside the boundary of that class) e.g. for an LTL class model, true positive samples are LTL samples predicted as such.

FP = False positive (when samples not belonging to the modelled class are incorrectly predicted to be inside the boundary of that class) e.g. in an LTL class model, false positives are samples that are not LTL predicted as LTL.

TN = True negative (samples not belonging to the modelled class, if they are correctly predicted to be outside the boundary of that class) e.g. in an LTL class model, true negatives are samples that are not LTL, predicted as such.

FN = False negative (when samples belonging to the class being modelled are incorrectly predicted to be outside the boundary of that class), e.g. in an LTL class model, false negatives are LTL samples that are misclassified.

Results and discussion

Physico-chemical analysis

The proximate chemical composition analysis was done to support the spectral interpretation of the species, and the results are presented in Table 4.2. For the ostrich samples, only the shear force values were analysed from the samples scanned, the proximate analysis values were from a previous study by Majewska *et al.* (2009) for comparison purposes.

In this study, a moisture content difference of approximately 2% was observed throughout the muscle types of the same species. For impala the moisture ranged from 74.9–76.3% where the highest moisture content was obtained from the IS muscle; for eland the moisture ranged from 75.6–77.8% where the highest was obtained from the BF muscle. Majewska *et al.* (2009) reported a moisture difference across the ostrich muscles ranging from 75.6–77.2%. In general, the moisture variation of these species between 70–77% is supported by Hoffman (2007), even though the eland BF muscle was slightly higher than the other muscles. Likewise, a noticeable protein variation across the muscle types in both impala and eland species was observed. However, there was less variation in fat as compared to other analysis.

It was observed from the eland and impala muscles and also confirmed from the literature (Neethling *et al.,* 2016; Van Heerden, 2018), that the IS muscle is the most tender. Tenderness is a considerable technological parameter used for evaluating the eating quality of meat from a consumer's perception (Cheng *et al.,* 2017). Neethling *et al.* (2016) reported the SM muscle as the toughest of all, and that was confirmed with the impala muscles (Table 4.2), with the exception of the eland muscles that showed LTL as the toughest. Regarding the ostrich muscles, FF showed to be the most tender and MS was the toughest.

Characterisation of NIR spectra

The average NIR spectra of impala selected muscles (BF, IS, LTL, SM, SS and ST) are shown in Figure 4.1. The raw spectra (Figure 4.1a) of the different muscles adhere to a similar shape even though there are absorbance differences, which could be the associated to differences amongst the muscle types.

In Figure 4.1a, two broad absorption bands are observed at 976 and 1422 nm, the bands are related to third and second overtone stretching of the O-H bond (Barbin *et al.*, 2012; Elmasry *et al.*, 2011) that is associated with the water content of the samples. Water is the main component of meat (Table 4.2). In addition to these, there is a band at 1186 nm that corresponds to the second overtone C-H stretching bond representing the intramuscular fat (Cozzolino and Murray, 2004; Ding and Xu, 2000; Osborne *et al.*, 1993). It is also observed in the raw spectra that IS and SS (forequarter) muscles overlap throughout the wavelength range, while SM and ST (hindquarter) muscles overlap only at 1422 nm. A possible explanation for the overlapping of these muscles might be that they are close in their anatomical location and functions. Neethling *et al.* (2014b) reported similar findings on the effect of season on the chemical composition of male and female blesbok IS and SS muscles.

Table 4.2 Proximate chemical composition (moisture, fat and protein) (%) and shear force (WBSF) (N) of impala, eland and ostrich muscles

Species	Muscle	Moisture (%)	Fat (%)	Protein (%)	WBSF (N)
Impala	LTL	75.5	1.2	22.9	36.9
	BF	75.4	1.6	23.1	44.4
	SM	74.9	1.4	23.5	45.9
	ST	76.1	1.1	22.6	33.6
	IS	76.3	1.9	21.6	28.8
	SS	76.1	1.3	22.1	33.7
Eland	LTL	75.6	1.2	23.0	97.6
	BF	77.8	1.8	20.3	91.5
	SM	76.0	1.6	22.4	78.7
	ST	77.2	1.4	21.3	77.5
	IS	77.3	1.3	21.2	65.5
	SS	77.2	1.6	20.8	89.2
Ostrich	FF	75.6*	1.36*	20.6*	35.8
	RS	76.2*	1.21*	21.4*	56.3
	BD	77.0*	0.95*	20.8*	51.9
	MS	75.8*	1.44*	21.5*	71.0
	TS	77.2*	1.1*	20.7*	46.8
Standard error of laboratory (SEL)	-	0.2	0.27	1.6	8.6

Abbreviations: LTL= *longissimus thoracis et lumborum*, BF= *biceps femoris*, SM= *semimembranosus*, ST= *semitendinosus,* IS= *infraspinatus*, SS= *supraspinatus*, FF= fan fillet, RS= rump steak, BD= big drum, MS= moon steak, TS= triangle steak, WBSF= Warner Bratzler shear force

*Majewska *et al.* (2009)

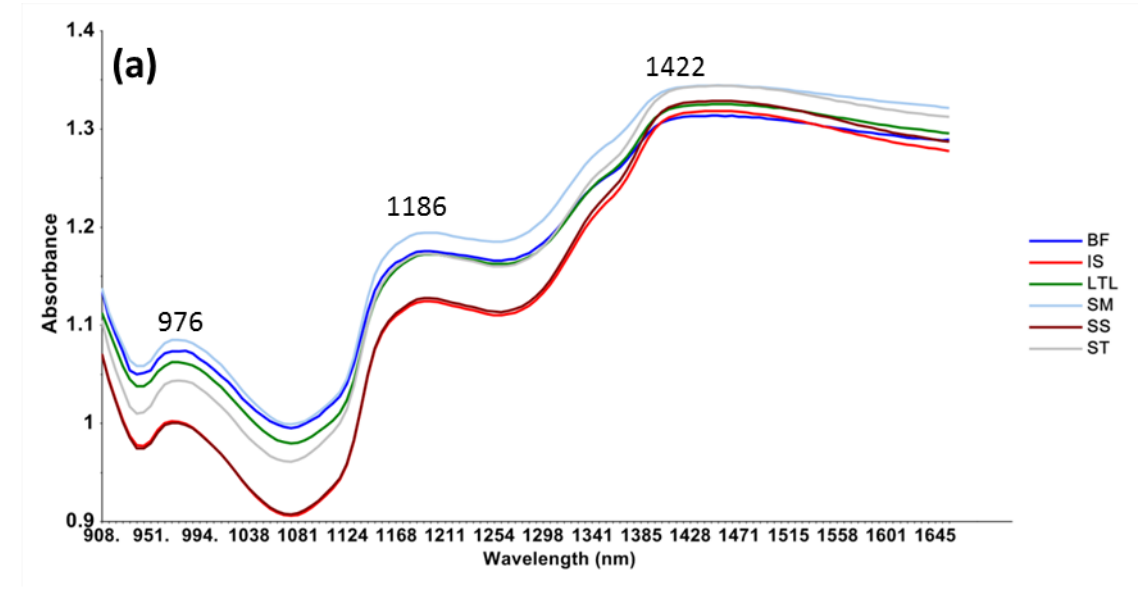

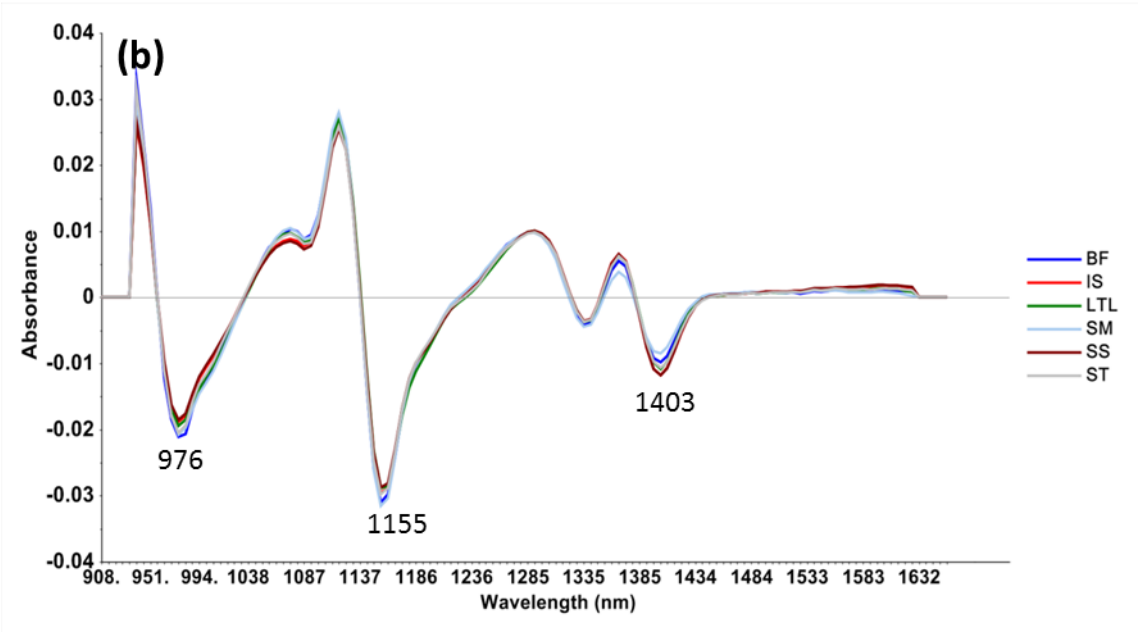

Figure 4.1 Mean spectra of impala selected muscles (BF, IS, LTL, SM, SS and ST) showing the wavelength bands of (a) raw spectra, (b) SNV-Detrend and 2nd derivative pre-processed spectra Abbreviations: LTL= longissimus thoracis et lumborum, BF= biceps femoris, SM= semimembranosus, ST= semitendinosus, IS= infraspinatus, SS= supraspinatus

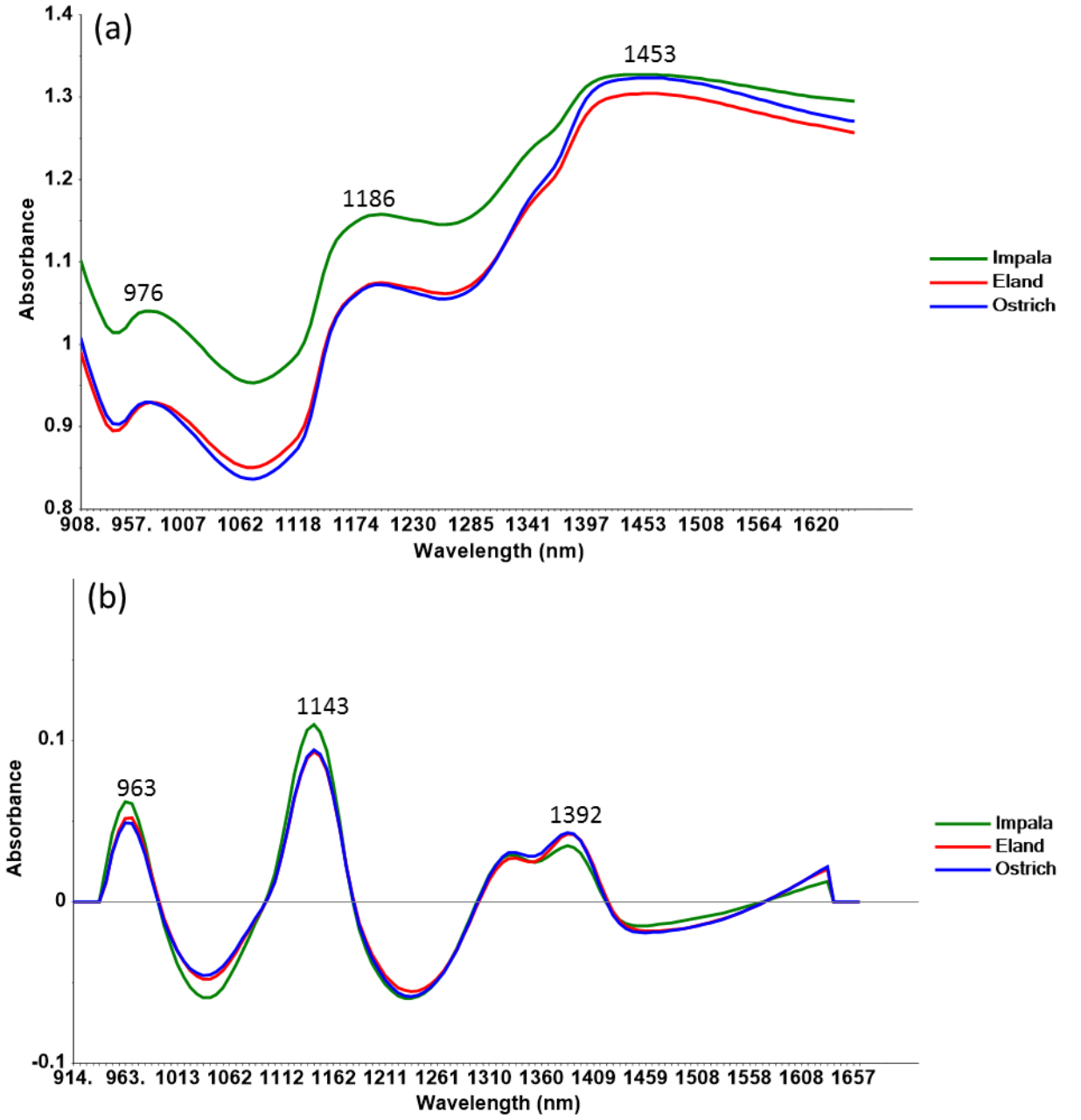

Figure 4.2 Mean spectra of impala, eland and ostrich species showing the wavelength bands of (a) raw spectra, (b) SNV-Detrend and 1st derivative pre-processed spectra.

Furthermore, there were noticeable variations between forequarter and hindquarter muscles throughout the spectra. In Figure 4.1b (SNV-Detrend, 2nd derivative pre-processed spectra), there are no prominent differences between the muscle types observed at bands located at 976, 1155 and 1403 nm. That is contrasting what was observed by Dumalisile *et al.* (2019) when different species were compared.

The mean spectra of selected muscle types of eland (BF, IS, LTL, SM, SS and ST) and ostrich (BD, MS, FF, RS and TS) are presented in the Appendix, Figures A4.1 and 2 respectively. The spectra of eland muscles were very similar to that of impala muscles regarding the shape, absorption bands and the fact that the IS and SS muscles were overlapping. Furthermore, the spectra of ostrich muscles also followed a similar pattern as the impala muscles, except that ostrich had different muscle types. In addition, there was a noticeable difference between the BD and TS muscles. It should be noted that all ostrich muscles are from the leg, unlike other species with muscles from different anatomical locations.

Regarding the mean spectra of impala, eland and ostrich when all muscles were used, Figure 4.2 illustrates that there is a visible difference amongst impala and the other two species. Furthermore, some overlapping between eland and ostrich at different wavelengths was evident in both the raw (Figure 4.2a) and SNV-Detrend and 1st derivative pre-processed spectra (Figure 4.2b). The impala muscles had prominent bands situated at 963 and 1143 nm. The 963 nm band is related to the third overtone stretching of an O-H bond (Barbin *et al.,* 2012) associated with the moisture content, and the 1143 nm band corresponds to the second overtone C-H stretching bonds representing the intramuscular fat (Cozzolino and Murray, 2004). Numerous researchers conducting studies on proximate chemical composition of game meat have revealed that the male animals have lower fat and higher moisture contents than females (Von la Chevallerie, 1972; Neethling *et al.*, 2014a; Neethling *et al.*, 2018). Therefore, the difference in intramuscular fat and moisture content of impala meat compared to the other species might have been caused by the fact that only male impala animals were slaughtered in this study (Table 4.1). Moreover, the eland and ostrich muscles had an overlapping prominent band situated at 1392 nm, which is associated with the second overtone C-H stretching bond (Cozzolino and Murray, 2004) that is related to the fat content of the samples. Thus, it was easier to observe the differences in spectral features of the different species (Figure 4.2b) than to differentiate the spectral features of different muscles within the same species (Figure 4.1b).

Principal Component Analysis

Figure 4.3a shows the PCA scores plot of ostrich muscles (BD, FF, MS, RS and TS) pre-treated with SNV-Detrend and 2nd derivative. The first two principal components (PCs) that explained 93% of the variation, revealed separation only between BD and TS muscles in the direction of PC1. From the PC1 loadings line plot (Figure 4.3b), the bands that were most influential for the grouping of these muscles are shown. The wavelength bands at 1149 and 1366 nm represent the C-H bond that corresponds to the fat (Osborne *et al.,* 1993). According to Majewska *et al.* (2009), BD has the lowest fat content (0.95%) versus TS (1.1 %) with higher fat content, which explains the variation between the two muscles. Another band that contributes to the clustering is 976 nm which is related to the third overtone stretching of the O-H bond (Barbin *et al.,* 2012; Elmasry *et al.*, 2011) associated with the moisture content of the samples.

Regarding the impala muscles (BF, IS, LTL, SM, SS and ST), the PCA scores plot of PC1 (73%) versus PC3 (4%), treated with SNV-Detrend and 2nd derivative pre-processing (Appendix, Figure 4.3a), showed two clusters separating the muscles. Clustering was according to their anatomical locations. The forequarter (SS and IS) muscles had negative score values, the back (LTL) muscles had positive scores and, the hindquarter (BF, ST and SM) muscles were clustered around the origin; all in the direction of PC3. It was also observed that there was overlapping of SS and IS muscles, which was also noticed in the spectra (Figure 1a). PC3 loadings line plot (Appendix, Figure 3b) shows the main wavelength band responsible for the clustering as 1360 nm. This band, the C-H bond, corresponds to the fat (Cozzolino and Murray, 2004). The PCA scores plot and the loadings line plot of eland muscles (Appendix, Figure A4.4) follow the same sequence and explanation as impala, except that the clustering is in the direction of PC1.

Finally, the PCA scores plot presenting all impala, eland and ostrich muscles regardless of the muscle type is shown in Figure 4.4. PC1 and PC3 explained 90% of the total variance. Impala samples had positive score values in the direction of PC1, while eland and ostrich had negative and positive score values, respectively, in the direction of PC3. The bands responsible for the clustering of impala muscles are shown in PC1 loadings line plot (Figure 4.4b). The main band at 1131 nm represents the C-H bond corresponding to the fat (Osborne *et al.,* 1993), while the 957 nm band represents an O-H bond associated with moisture content. In contrast, PC3 loadings plot (Figure 4.4c) shows the major bands contributing to the clustering of the eland and ostrich muscles. The 1323 nm band was responsible for the clustering of ostrich samples, while the 1397 nm band was for the eland samples. Both bands represented the C-H bond associated with the intramuscular fat (Osborne *et al.,* 1993). Additionally, there was some minor overlapping observed between species.

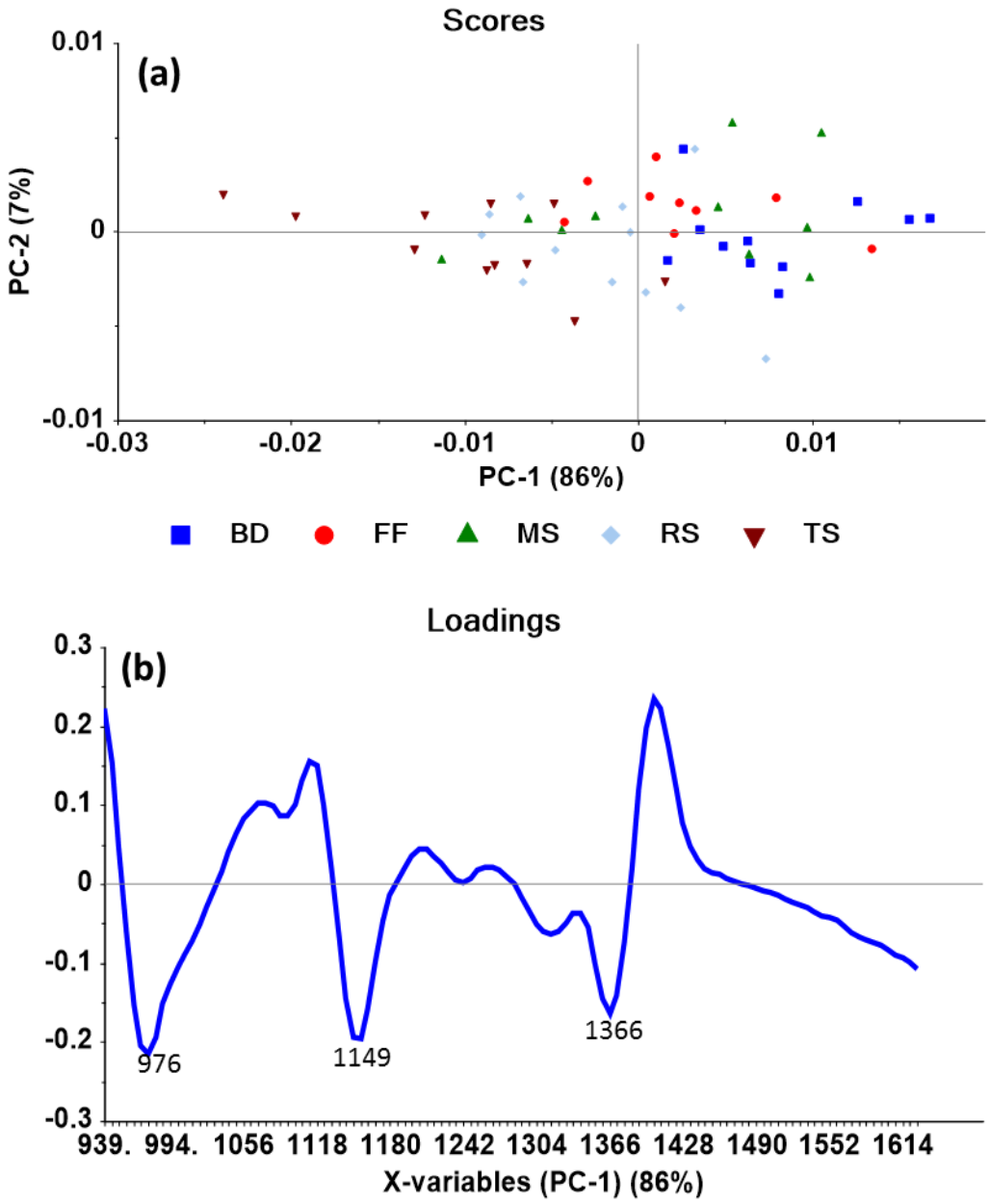

Figure 4.3 (a) PCA scores plot of PC1 vs. PC2 contributing 93% explained variance of the model showing the clustering of the ostrich muscle types (SNV-Detrend and 2nd derivative pre-processed spectra). (b) PC1 loadings line plot showing the bands responsible for the clustering of muscle types. Abbreviations: FF= fan fillet, RS= rump steak, BD= big drum, MS= moon steak, TS= triangle steak

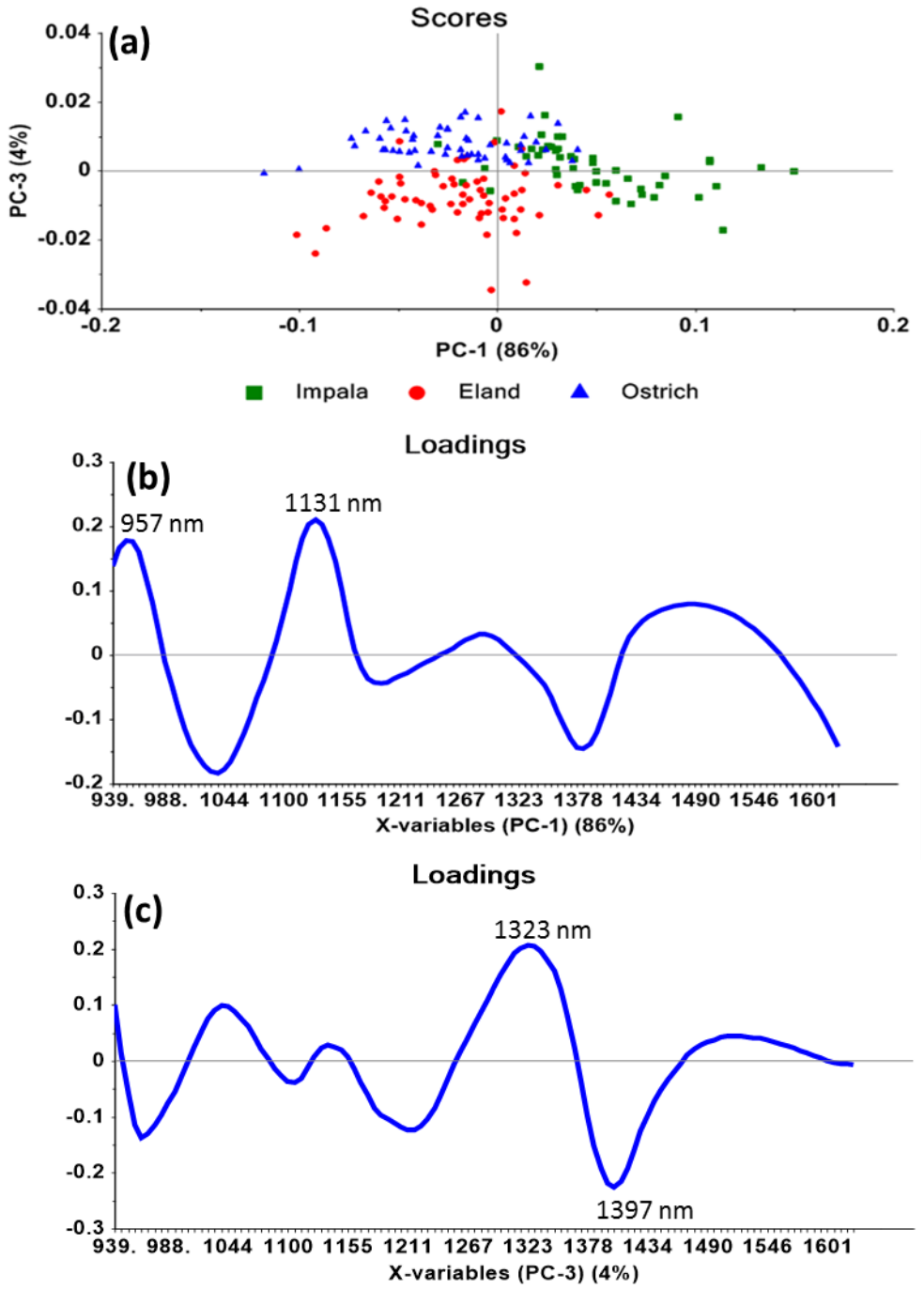

Figure 4.4 (a) PCA scores plot of PC1 vs. PC3 contributing 90% of the model showing the clustering of all impala, eland and ostrich muscles irrespective of the type (SNV-Detrend and 1st derivative pre-processed spectra). (b) PC1 and (c) PC3 loadings line plots showing the bands responsible for the clustering of the muscles of these species.

Classification methods

Figure 4.5 shows the PLS-DA scores plot of the impala muscles (BF, IS, LTL, SM, SS and ST), pre-treated with SNV-Detrend and 2nd derivative. Based on cross-validation, five LVs were selected for model calibration with an explained Y variance of 95.6%. For the BF muscle class, six out of nine samples were correctly classified, while two ST and one from each class of LTL, SM, IS and SS muscles were misclassified as BF. For the ST class, six out of seven muscles were correctly classified, whilst three BF (also a hindquarter muscle) samples were misclassified as ST. Misclassification of muscles from the same anatomical location was also observed in the SM class; where one BF muscle was misclassified as SM muscles that were 100% correctly classified. The same misclassification occurred for the forequarter (SS and IS) muscles. However, none was noticed for the LTL class which had a different anatomical location. From the confusion matrix table (Table 4.3), it is apparent that 100% of the IS muscles were misclassified as SS muscles. This misclassification contributed to the high percentage error of the model that resulted in the 50% classification accuracy for the IS muscles (Table A4.1, Appendix) of the impala model. The same transpired for the hindquarter (BF, ST and SM) muscles. Misclassification between the hindquarter muscles resulted in a low percentage of correctly predicted (true positive) BF muscles (33%) (Table 4.3), and low prediction (57.1%) of ST muscles (Table A4.1, Appendix). This means the model cannot be used as a reliable tool to authenticate these muscles. Similarly, Sanz *et al.* (2016) reported difficulty in discriminating multiple muscles (four types) of lamb with hyperspectral imaging. In contrast, Kamruzzaman *et al.* (2011) managed to discriminate fewer (three) muscle types of lamb meat and obtained 100% classification accuracy. The muscle types that Kamruzzaman *et al.* (2011) used in their study were also from different anatomical locations. From these results and previous findings from other researchers, it was decided to combine the forequarter (IS and SS) muscles into one class and the hindquarter (BF, ST and SM) muscles into another.

Figure 4.6 displays the prediction plot of impala muscle when hindquarter and forequarter muscles were combined. The first four LVs explained 93.9% of the Y variation and was used for model calibration. For the hindquarter muscles, one ST muscle was misclassified as LTL, and one LTL muscle was misclassified as a hindquarter muscle. This is confirmed by the confusion matrix table (Table 4.6). Furthermore, none of the forequarter muscles were misclassified. The best classification accuracies obtained for these models ranged from 92.9 to 100% (Table 4.4). These models were validated externally, with samples that were not part of the calibration model and gave excellent results ranging from 79.2–100% accuracy. Figure 4.5 in the Appendix illustrates the PLS-DA scores plot of eland muscle types pre-treated with SNV-2nd derivative pre-processing. Similar to the impala muscles, the eland model could correctly classify the forequarter, hindquarter and LTL muscles with a classification accuracy rate ranging from 85.5–92.2% (Table 4.4). When assessing the classification accuracies of these two species, it was noted that eland is lower than impala. This could have been caused by the fact that, for this study, there was no variation in sex for impala

samples; hence the higher accuracies compared to eland that had almost equal number of sexes (Table 4.1). This effect of sex needs further investigation.

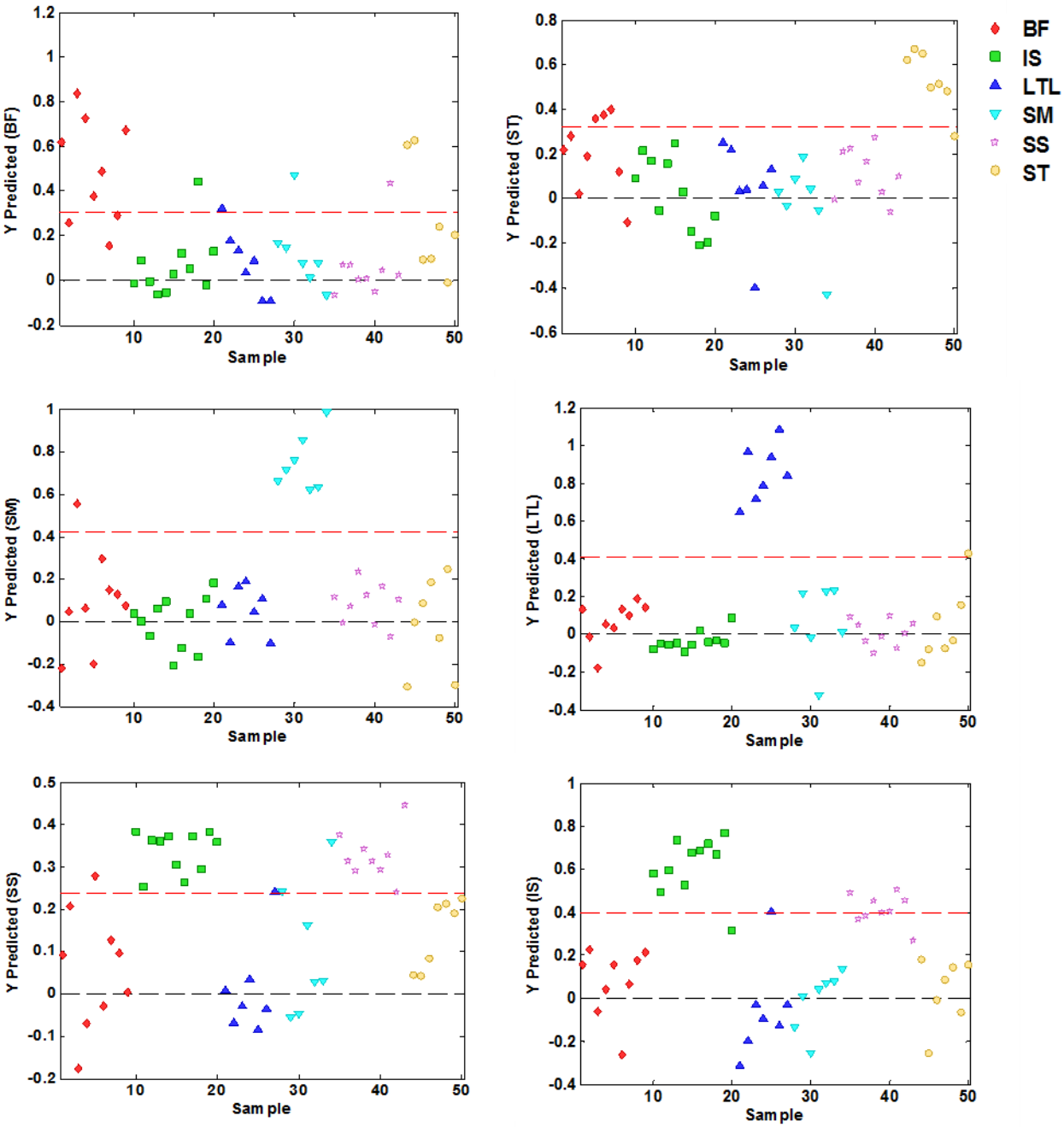

Figure 4.5 Score plot obtained by PLS-DA pre-treated with SNV-Detrend and 2nd derivative pre-processing method showing the segregation of impala muscle types. The red dotted line represents the discrimination line. Any sample that is above the red dotted line is regarded as predicted class and any sample that is below the red line is regarded as the other classes not predicted.

Table 4.3 Confusion matrix obtained with PLS-DA (pre-treated with SNV-Detrend and 2nd derivative) showing muscle types of impala. The true positives, false positives, true negatives, false negatives and the total number of muscle type used for the calibration model are presented

Class	True + (%)	False + (%)	True - (%)	False - (%)	n
BF	33.0	0.0	100.0	66.7	9
IS	0.0	0.0	100.0	100.0	11
LTL	57.1	2.3	97.7	42.9	7
SM	57.1	0.0	100.0	42.9	7
SS	33.3	2.4	97.6	66.7	9
ST	57.1	2.3	97.7	42.9	7

Abbreviations: LTL= *longissimus thoracis et lumborum*, BF= *biceps femoris*, SM= *semimembranosus*, ST= *semitendinosus,* IS= *infraspinatus*, SS= *supraspinatus*, + = positive, - = negative

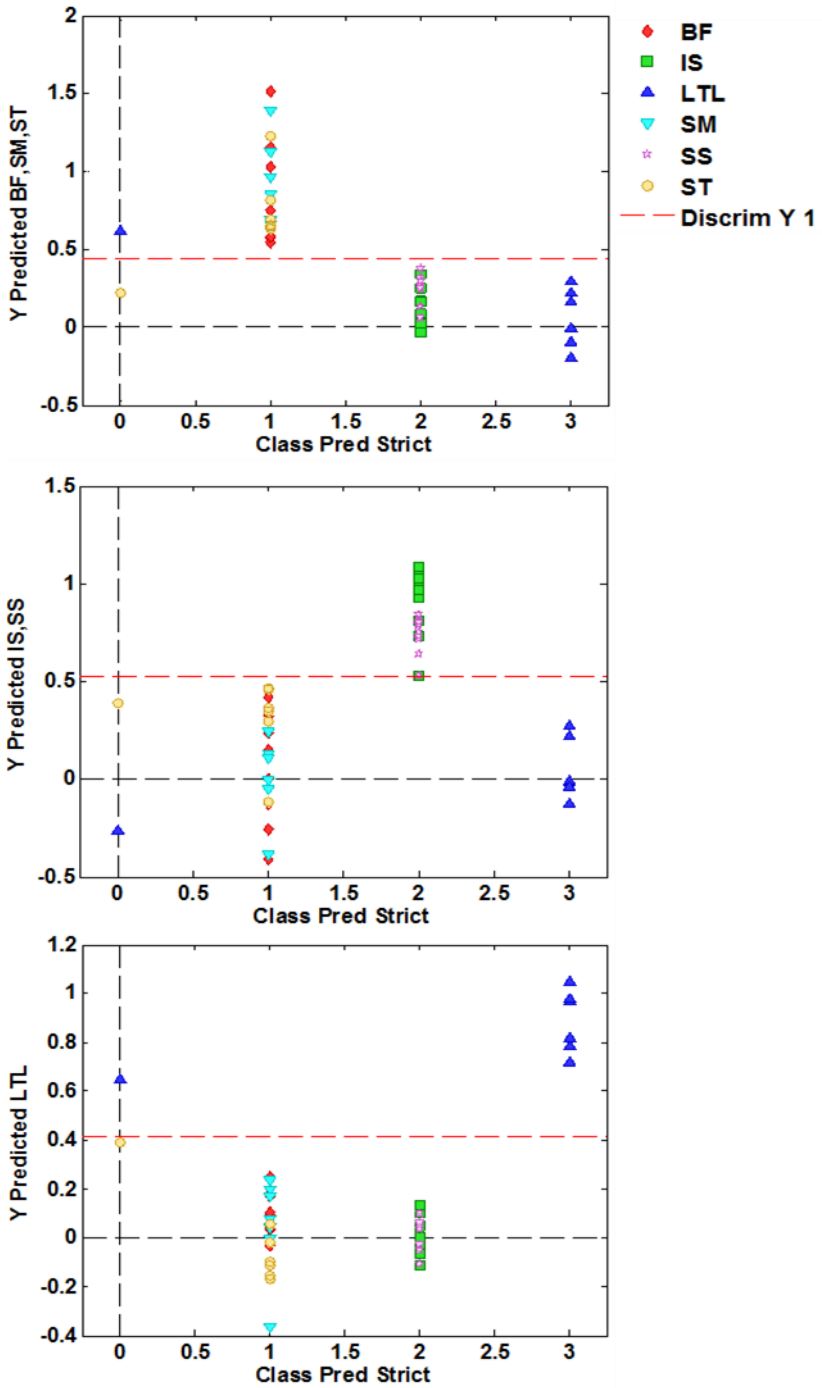

Figure 4.6 Class predict strict plot obtained by PLS-DA pre-treated with SNV-Detrend and 2nd derivative pre-processing method showing the segregation of impala muscle types (BF, SM, ST, IS, SS and LTL) when hindquarter muscles are combined as one class, and so as the forequarter muscles. The red dotted line represents the discrimination line. Any sample that is above the red dotted line is regarded as the predicted class and those below the red line are regarded as the other classes not predicted. Samples located at 0 are unassigned samples.

Abbreviations: LTL= *longissimus thoracis et lumborum*, BF= *biceps femoris*, SM= *semimembranosus*, ST= *semitendinosus,* IS= *infraspinatus*, SS= *supraspinatus*

Table 4.4 Classification accuracy of PLS-DA models, calibration (Cal) and validation (Val), for discriminating muscles (when hindquarter (BF, SM and ST), forequarter (IS and SS) and ostrich leg (RS and TS) muscles are combined according to their anatomical locations) of impala and ostrich species (SNV-Detrend and 2nd derivative pre-processing) and eland (SNV-2nd derivative pre-processing)

Species	Class	Cal (%)	Val (%)
Impala	BF, SM, ST	98	85
	IS, SS	100	79
	LTL	93	100
Eland	BF, SM, ST	86	76
	IS, SS	92	90
	LTL	89	68
Ostrich	BD	96	75
	MS	89	55
	FF	85	70
	RS, TS	88	90

Abbreviations: LTL= *longissimus thoracis et lumborum*, BF= *biceps femoris*, SM= *semimembranosus*, ST= *semitendinosus,* IS= *infraspinatus*, SS= *supraspinatus*, FF= fan fillet, RS= rump steak, BD= big drum, MS= moon steak, TS= triangle steak

The PLS-DA scores plot presenting the ostrich muscle types (BD, FF, MS, RS and TS) pre-treated with SNV-Detrend and 2nd derivative technique is shown in Figure 4.6 of the Appendix. Based on cross-validation, six LVs were selected for model calibration with an explained Y variance of 98.1%. From the RS muscle class model, it was observed that the majority of TS muscles were misclassified as RS muscles. The misclassification of TS muscles contributed to the lowest percentage of correctly predicted (true positive) TS samples (18.2%) (Table 4.2, Appendix). Subsequently, that resulted to the lowest classification accuracy (56.7%) of the TS class of the model (Table A4.1, Appendix). Anatomically, TS and RS muscles are both in the same category of the silver side muscles of the ostrich thigh. It was then decided to classify these muscles as the same category, and the class predict strict plot shown in Figure 4.7 is the improved model for ostrich muscles. An explained Y variance of 97.7% described the model calibration selected by six LVs based on cross-validation. In the BD class model, no BD muscles were misclassified. It was observed that only one sample from the MS class was misclassified as the RS/TS class. The same sample from the MS class was detected again in all other class models. In general, no samples were misclassified as other classes, rather they were unassigned (sample either allocated in more than one class or not assigned in any class) with the exception of this MS muscle. Thus, the MS class was the only class with the lowest prediction accuracy (55.3%). The confusion matrix shows no samples were misclassified as BD, FF and MS muscles, however, only 3.3% of other muscles were misclassified as RS/TS (Table A4.3, Appendix). The classification accuracy obtained for the ostrich model ranged from 85.0 to 95.5% (Table 4.4). The different ostrich genotypes did not show any visible groupings, hence did not have any influence on the muscle type results. However, the misclassification of the ostrich muscle types might have been caused by the fact that all of these muscles are from the leg, thus similar anatomical locations.

Finally, the three (impala, eland and ostrich) species were discriminated regardless of their muscles and the class predict strict plot pre-treated with SNV-Detrend, 1st derivative pre-processing is shown in Figure 4.8. An explained Y variance of 95.3% described the model calibration with five LVs. In all of these class models, there is one similarity; one impala sample was misclassified as eland, one impala was misclassified as ostrich and two ostrich samples were misclassified as impala. As much as there was no class model that attained a 100% classification accuracy, it is however apparent that the models attained good classification accuracies ranging from 85 to 94% (Table 4.5). In contrast to Dumalisile *et al.* (2020), where selected game species were discriminated using only the LTL muscles, the overall classification accuracies obtained ranged from 70 to 96%. Thus, it has been demonstrated that NIR spectroscopy can discriminate game meat species irrespective of the muscles used. It was expected that there would be a substantial difference when the different muscles were used, since the muscles within each species differ in their anatomical locations and function (Neethling *et al.,* 2016; Van Heerden, 2018).

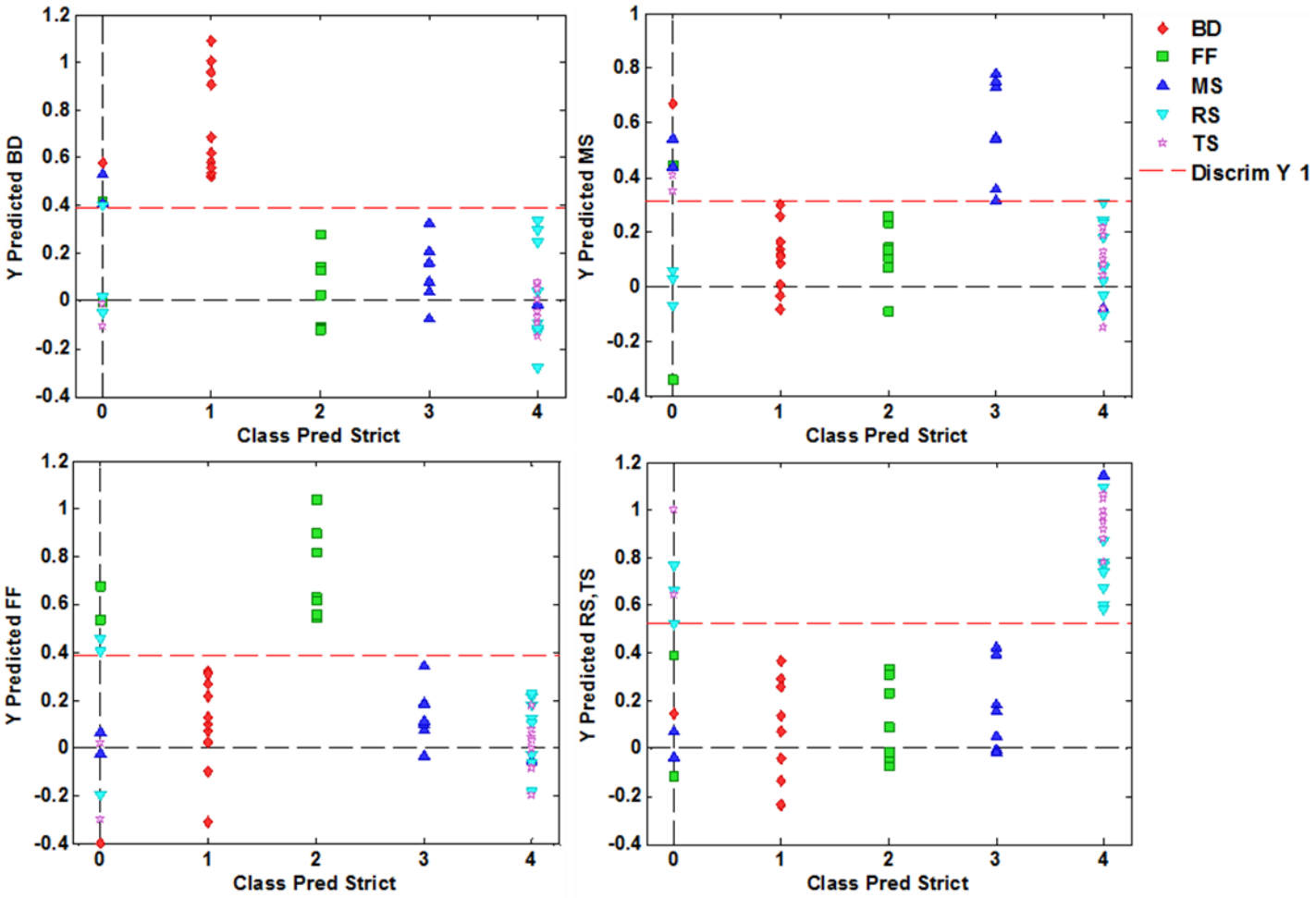

Figure 4.7 Class predict strict plot obtained by PLS-DA pre-treated with SNV-Detrend and 2nd derivative pre-processing method showing the segregation of ostrich muscle types (BD, FF, MS, RS and TS) when RS and TS are combined as one class. The red dotted line represents the discrimination line. Any sample that is above the red dotted line is regarded as the predicted class and those below the red line is regarded as the other classes not predicted. Samples located at 0 are unassigned.

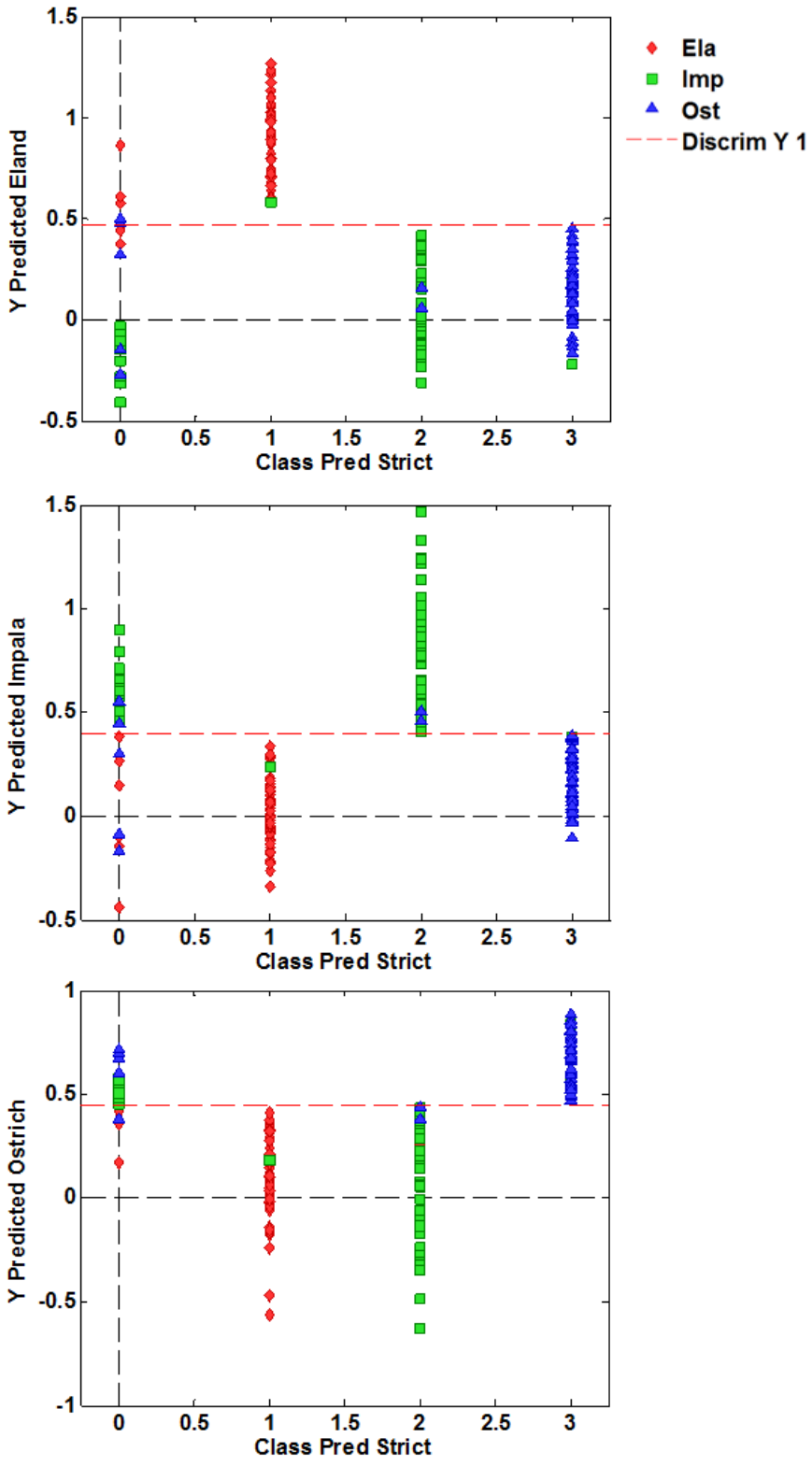

Figure 4.8 Class predict strict plot obtained by PLS-DA pre-treated with SNV-Detrend, 1st derivative pre-processing method showing the segregation of all impala, eland and ostrich different muscles. The red dotted line represents the discrimination line. Any sample above the discrimination line is regarded as the predicted class and those below the red line are regarded as the other classes not predicted. Samples located at 0 are unassigned.

Table 4.5 Percentage accuracy results of PLS-DA models, calibration (Cal) and validation (Val), for classification of all eland, impala and ostrich muscles regardless of the muscle type used (SNV-Detrend and 1st derivative, pre-processing)

		PLS-DA	
Species	**Class**	**Cal (%)**	**Val (%)**
Different species using all muscles	Eland muscles	94	97
	Impala muscles	85	81
	Ostrich muscles	93	92

Table 4.6 Confusion matrix obtained by PLS-DA showing impala muscle types (pre-treated with SNV-Detrend and 2nd derivative) and different species using all muscles (pre-treated with SNV-detrend and 1st derivative). The true positives, false positives, true negatives, false negatives and the total number of muscles of the models are presented.

Category	**Class**	**True + (%)**	**False + (%)**	**True - (%)**	**False - (%)**	**n**
Impala muscle types	BF, SM, ST	95.7	0.0	100	4.3	23
	IS, SS	100.0	0.0	100	0.0	20
	LTL	85.7	0.0	100	14.3	7
Different species regardless of the muscles	Eland	88.9	1.0	99.0	11.1	63
	Impala	72.0	2.6	97.4	28.0	50
	Ostrich	86.8	1.8	98.2	13.2	53

+ = positive, - = negative
Abbreviations: LTL= *longissimus thoracis et lumborum*, BF= *biceps femoris*, SM= *semimembranosus*, ST= *semitendinosus,* IS= *infraspinatus*, SS= *supraspinatus*

Conclusions

From this study it was confirmed that it is possible to discriminate muscle types of game species with classification accuracies ranging from 85 to 100% using NIR spectroscopy. From this study, the possibility to discriminate muscle types of game species using NIR spectroscopy was attested with classification accuracies ranging from 85 to 100%.

However, the muscles were discriminated successfully when they were grouped according to their anatomical locations (forequarter, back and hindquarter regions), and when observing within the species. It was also noted that, muscles that are in the same anatomical location e.g. IS and SS, can be easy targets for fraudsters since it is not easy to distinguish them from one another with NIR spectroscopy. Furthermore, it was easier to classify the different species regardless of the muscle used than to classify the different muscles within the same species. Nevertheless, that was expected as the different species also differ in their DNA structure. These results reveal the development of classification methods based on NIR analysis for the authentication of impala, eland and ostrich muscles. These results bring to light the likelihood of authenticating impala, eland, and ostrich muscles with the developed classification models based on NIR analysis.

References

Alomar, D., Gallo, C., Castañeda, M., & Fuchslocher, R. (2003). Chemical and discriminant analysis of bovine meat by near infrared reflectance spectroscopy (NIRS). *Meat Science*, ***63***(4), 441–450.

Barbin, D., Elmasry, G., Sun, D. W., & Allen, P. (2012). Near-infrared hyperspectral imaging for grading and classification of pork. *Meat Science*, ***90***(1), 259–268.

Barker, M., & Rayens, W. (2003). Partial least squares for discrimination. *Journal of Chemometrics*, ***17***(3), 166–173.

Barnes, R. J., Dhanoa, M. S., & Lister, S. J. (1989). Standard normal variate transformation and de-trending of near-infrared diffuse reflectance spectra. *Applied Spectroscopy, **43**,* 772–777.

Cawthorn, D. M., Steinman, H. A., & Hoffman, L. C. (2013). A high incidence of species substitution and mislabelling detected in meat products sold in South Africa. *Food Control*, ***32***(2), 440–449.

Cheng, J. H., Nicolai, B., & Sun, D. W. (2017). Hyperspectral imaging with multivariate analysis for technological parameters prediction and classification of muscle foods: A review. *Meat Science*, ***123***, 182–191.

Chevallier, S., Bertrand, D., Kohler, A. & Courcoux, P. (2006). Application of PLS-DA in multivariate image analysis. *Journal of Chemometrics*, **20,** 221-229.

Cowe, A., & McNicol, J. W. (1985). The use of principal components in the analysis of near infrared spectra. *Applied Spectroscopy, **39***(2)*,* 257-266.

Cozzolino, D., & Murray, I. (2004). Identification of animal meat muscles by visible and near infrared reflectance spectroscopy. *LWT - Food Science and Technology*, ***37***(4), 447–452.

DAFF (Department of Agriculture, Forestry and Fisheries). 2004. Meat Safety Act (Act No. 40 of 2000), Red meat regulations (No. R. 1072 of 17 September 2004) (Regulation Gazette No. 8056). Government Printing Offices, South Africa.

Danezis, G. P., Tsagkaris, A. S., Camin, F., Brusic, V., & Georgiou, C. A. (2016). Food authentication: Techniques, trends & emerging approaches. *TrAC - Trends in Analytical Chemistry*, ***85*****,** 123–132.

Ding, H. B., & Xu, R. J. (2000). Near-infrared spectroscopic technique for detection of beef hamburger adulteration. *Journal of Agricultural and Food Chemistry*, ***48***(6), 2193–2198.

DoA (Department of Agriculture). 2015. Agricultural Product Standards Act, 1990 (Act 119 of 1990): Regulations regarding the classification and marking of meat intended for sale in the Republic of South Africa (R. 55/2015). Government Printing Offices, South Africa.

DoH (Department of Health). 2010. Foodstuffs, Cosmetics and Disinfectants Act, 1972 (Act 54 of 1972): Regulations relating to the labelling and advertising of foods: R. 146 of 2010, As amended up to and including R.45 of 2012. Government Printing Offices, South Africa.

Dumalisile, P., Manley, M., Hoffman, L. & Williams, P.J. (2020a). Near-Infrared (NIR) Spectroscopy to differentiate *Longissimus thoracis et lumborum* (LTL) Muscles of Game Species. *Food Analytical Methods,* **13**, 1220-1233.

Elmasry, G., Iqbal, A., Sun, D. W., Allen, P., & Ward, P. (2011). Quality classification of cooked, sliced turkey hams using NIR hyperspectral imaging system. *Journal of Food Engineering*, ***103***(3), 333–344.

Esbensen, K. H., Guyot, D., Westad, F., & Houmoller, L. P. (2002). Principal Component Analysis (PCA) - Introduction Multivariate data analysis - In practice: An introduction to multivariate data analysis and experimental design (pp.19–74): Camo ASA

Fajardo, V., González Isabel, I., Rojas, M., García, T., & Martín, R. (2010). A review of current PCR-based methodologies for the authentication of meats from game animal species. *Trends in Food Science and Technology*, ***21***(8), 408–421.

Fisher R. A. (1936). The use of multiple measurements in taxonomic problems. *Annals of Eugenics,* ***7,*** 179–188.

Hoffman, L. C. (2007). The meat we eat: are you game? *Inaugural Addess.* Stellenbosch University, Western Cape, South Africa.

Honikel, K. O. (1998). Reference methods for the assessment of physical characteristics of meat. *Meat Science*, ***49*****(**4), 447–457.

Jonker, K. M., Tilburg, J. J. H. C., Hagele, G. H., & de Boer, E. (2008). Species identification in meat products using real-time PCR. *Food Additives & Contaminants. Part A, Chemistry, Analysis, Control, Exposure & Risk Assessment*, ***25***(5), 527–533.

Kamruzzaman, M., Elmasry, G., Sun, D. W., & Allen, P. (2011). Application of NIR hyperspectral imaging for discrimination of lamb muscles. *Journal of Food Engineering*, ***104***(3), 332–340.

Kamruzzaman, M., Sun, D. W., ElMasry, G., & Allen, P. (2013). Fast detection and visualization of

minced lamb meat adulteration using NIR hyperspectral imaging and multivariate image analysis. *Talanta*, ***103*****,** 130–136.

Kennard, R. W., & Stone, L. A. (1969). Computer aided design of experiments. *Techno- metrics, **11** (1),* 137-148.

Majewska, D., Jakubowska, M., Ligocki, M., Tarasewicz, Z., Szczerbińska, D., Karamucki, T., & Sales, J. (2009). Physicochemical characteristics, proximate analysis and mineral composition of ostrich meat as influenced by muscle. *Food Chemistry*, ***117***(2), 207–211.

Manley, M. (2014). Near-infrared spectroscopy and hyperspectral imaging: Non-destructive analysis of biological materials. *Chemical Society Reviews*, ***43***(24), 8200–8214.

Nakyinsige, K., Man, Y. B. C., & Sazili, A. Q. (2012). Halal authenticity issues in meat and meat products. *Meat Science*, ***91***(3), 207–214.

Neethling, J., Britz, T. J., & Hoffman, L. C. (2014a). Impact of season on the fatty acid profiles of male and female blesbok (Damaliscus pygargus phillipsi) muscles. *Meat Science*, ***98***(4), 599–606.

Neethling, J., Hoffman, L. C., & Britz, T. J. (2014b). Impact of season on the chemical composition of male and female blesbok (*Damaliscus pygargus phillipsi*) muscles. *Journal of the Science of Food and Agriculture*, ***94*****(**3), 424–431.

Neethling, J., Hoffman, L. C., & Muller, M. (2016). Factors influencing the flavour of game meat: A review. *Meat Science*, ***113*****(**November), 139–153.

Neethling, J., Muller, M., van der Rijst, M., & Hoffman, L. C. (2018). Sensory quality and fatty acid content of springbok (Antidorcas marsupialis) meat: influence of farm location and sex. *Journal of the Science of Food and Agriculture*, ***98*****(**7), 2548–2556.

O'Mahony, P. J. (2013). Finding horse meat in beef products-a global problem. *Qjm*, *106*(6), 595–597.

Oliveri, P., & Downey, G. (2012). Multivariate class modeling for the verification of food-authenticity claims. *TrAC - Trends in Analytical Chemistry*, ***35*****,** 74–86.

Osborne, B. G., Fearn, T., & Hindle, P. H. (1993). Practical NIR spectroscopy with applications in food and beverage analysis, 2nd edn.*Longman Scientific & Technical, Essex*

Sanz, J. A., Fernandes, A. M., Barrenechea, E., Silva, S., Santos, V., Gonçalves, N., Melo-Pinto, P. (2016). Lamb muscle discrimination using hyperspectral imaging: Comparison of various machine learning algorithms. *Journal of Food Engineering*, ***174*****,** 92–100.

Savitzky, A., & Golay, M. J. E. (1964). Smoothing and Differentiation of Data by Simplified Least Squares Procedures. *Analytical Chemistry*, ***36***(8), 1627–1639.

Soon, J. M., & Manning, L. (2018). Food smuggling and trafficking: The key factors of influence. *Trends in Food Science and Technology*, ***81***(May), 132–138.

Spink, J., & Moyer, D. C. (2011). Defining the Public Health Threat of Food Fraud. *Journal of Food Science*, ***76***(9), 157-163.

Van Ba, H., Park, K., Dashmaa, D., & Hwang, I. (2014). Effect of muscle type and vacuum chiller

ageing period on the chemical compositions, meat quality, sensory attributes and volatile compounds of Korean native cattle beef. *Animal Science Journal*, ***85***(2), 164–173.

Van Heerden, A.M. (2018). Profiling the meat quality of blue wildebeest (Connochaetes taurinus), Dissertation presented for the degree of Master of Science (Animal Science), Stellenbosch University, Stellenbosch.

Van Ruth, S. M., Luning, P. A., Silvis, I. C. J., Yang, Y., & Huisman, W. (2018). Differences in fraud vulnerability in various food supply chains and their tiers. *Food Control*, ***84*****,** 375–381.

Van Schalkwyk, D. L., & Hoffman, L. C. (2010). *Guidelines for the harvesting of game for meat export*. Windhoek, Namibia: Printech cc 71pp.

Von la Chevallerie, M. (1972). Meat quality of seven wild ungulate species. South African Journal of Animal Science **2,** 101-103.

Varmuza, K., & Filzmoser, P. (2009). Chemoinformatics-chemometrics-statistics. *In Introduction to multivariate statistical analysis in chemometrics* (pp. 1–26). Boca Raton, FL: CRC Press Taylor and Francis Group.

Verbeke, J., & Ward, R. W. (2006). Consumer interest in information cues denoting quality, traceability and origin: An application of ordered probit models to beef labels. *Food Quality and Preference, **17**,* 453-467.

Walker, M. J., Burns, M., & Burns, D. T. (2013). Horse Meat in Beef Products- Species Substitution 2013. *Journal of the Association of Public Analysts (Online)*, ***41*****,** 67–106.

Wold, S. (1987). Principal component analysis. *Chemometrics and Intelligent Laboratory Systems*, ***2***, 37–52.

Chapter 5

Effect of ageing on the near infrared (NIR) spectra of selected game species' muscles

Abstract

Near infrared (NIR) spectroscopy was used to differentiate between ageing periods of blesbok, eland and ostrich muscles. *Longissimus thoracis et lumborum* (LTL) muscle steaks obtained from blesbok and eland, and fan fillet (FF) muscle steaks of ostrich were portioned, vacuum packed and aged at 4°C for different lengths of time. At each ageing period, the muscle steaks were scanned with a handheld NIR spectrophotometer in the spectral range of 908 to 1700 nm. In addition, Warner-Bratzler shear force (WBSF), pH and CIELab colour ordinates were collected. Spectral data were treated with different pre-processing methods, preceding the development of models. Subsequently, the pre-processed spectral data was explored with principal component analysis (PCA) and later classified with partial least square discriminant analysis (PLS-DA). Prediction accuracy obtained with cross-validated PLS-DA models ranged from 66 to 95%, 56 to 71% and 52 to 68% for the different ageing periods of blesbok, eland and ostrich, respectively. As the predicted samples were not robust enough, it was concluded that the models were too inaccurate for acceptance. It is suggested that some other parameters (e.g. enzyme protease, desmin degradation and sarcomere length) not characterized by the spectral data in the NIR range of 908 to 1700 nm could be responsible for the ageing of meat. Thus, the results from this study did not support the use of a handheld NIR spectrophotometer as a reliable prediction tool for aged game meat.

Introduction

Meat ageing is a popular method used for decades with the purpose of increasing and enhancing tenderness (Dransfield, 1994). This is done by storage of the meat under controlled refrigeration for extended periods of time (Dransfield, 1994; Starkey *et al.*, 2015; Bhat *et al.*, 2018). Ageing without packaging (also known as dry ageing) is widely used (Djenane *et al.*, 2016) however, to achieve consistent quality it requires appropriate environmental control practices. An alternative to dry ageing is vacuum packaging (wet ageing), which has become prevalent due to the advantage of reducing microbial growth and less refrigeration space being used (Hoffman, 2004).

Proteolysis, catalysed by proteases, degrade complex proteins during meat ageing which results in increased palatability and tenderness (Dransfield, 1994). The myofibrillar, cytoskeletal and sarcoplasmic proteins maintain the structural integrity of myofibrils that contribute to the toughness of meat (Koohmaraie *et al.,* 2002). Degradation of these proteins by proteolytic enzymes cause weakening of the myofibrils and thus tenderization.

From a consumer's perspective, tenderness is used in evaluation of the eating quality of meat (Cheng *et al.,* 2017). A number of studies indicate that consumers can differentiate between tough and tender meat, and are willing to pay a premium price for a guaranteed tender steak (Rhee *et al.*, 2004; Koohmaraie and Geesink, 2006; Hildrum *et al.*, 2009; ElMasry and Sun, 2010; Konda Naganathan *et al.*, 2015). It would be beneficial for consumers if aged meat products are labelled as 'aged' for a specified period of time (Moran *et al.*, 2018). However, to gain consumer trust, the ageing period and/or the tenderness and quality of the final product should be able to be authenticated.

Traditionally, sensory analysis and/or Warner-Bratzler shear force (WBSF) are used to verify the level of tenderness in aged game meat (Shackelford *et al.*, 1995). Both these methods are destructive, slow, expensive and require sample preparation, complex laboratory procedures and skilled personnel (Cheng *et al.*, 2017). Therefore, a rapid alternative method is needed to authenticate aged game meat products. Near infrared (NIR) spectroscopy is a rapid and non-destructive method (Cen and He, 2007; Manley, 2014), which has been used for decades in a wide range of applications (Prieto *et al.*, 2008; Elmasry *et al.*, 2011; Kamruzzaman *et al.*, 2011; Williams *et al.*, 2012; Barbin *et al.*, 2015) including meat ageing authentication (Prieto *et al.*, 2015; Moran *et al.*, 2018).

In support of NIR spectroscopy as an efficient technique to evaluate meat ageing and tenderness, initial research has been successful. In a preliminary study, Moran *et al.* (2018) investigated the prediction of the ageing time of beef steaks to assess visible and NIR spectroscopy (Vis-NIR; 400-2400 nm) as an authentication tool. The steaks were aged for 3, 7, 14 and 21 days postmortem. They applied partial least squares discriminant analysis (PLS-DA) to classify steaks based on the number of days aged. They achieved overall correct classifications ranging from 94.2 to 100%, which indicated the ability of the Vis-NIR instrument to discriminate the steaks based on different ageing periods. Furthermore, Prieto *et al.* (2015) studied the rapid discrimination of enhanced quality pork with Vis-NIR spectroscopy in the wavelength range of 350-2500 nm and used

PLS-DA to predict the ageing days. They correctly classified 94 and 97% of aged samples for the 2nd and 14th ageing days, respectively. Elmasry *et al.* (2012) in their study to predict colour, pH, and tenderness changes of fresh beef over time, they managed to predict tenderness after 14 days of ageing, using NIR hyperspectral imaging in the wavelength of 900-1700 nm. They developed partial least squares regression (PLSR) models, and the beef tenderness shear force values were predicted with a coefficient of determination (R^2_{CV}) of 0.83 and a root mean square error estimated by cross-validation (RMSECV) of 40.75 N.

To our knowledge, there are no studies investigating the ageing of South African game (blesbok, eland, and ostrich) meat using NIR spectroscopy. NIR spectroscopy has been shown to be effective in detecting changes in meat during aging, and in this study, it will be used to distinguish between meat groups with different ageing days. Hence, the aim of this study was to determine whether NIR spectroscopy can be used to distinguish between different ageing periods of blesbok, eland, and ostrich muscles.

Material and Methods

Meat samples

Fresh game meat samples from three different species were used. Meat samples were obtained from Blesbok *(Damaliscus pygargus phillipsi)*, Eland (*Taurotragus oryx*) and Ostrich (*Struthio camelus*) from three genotypes (South African Black, Zimbabwean Blue and Kenyan Red), harvested from Witsand, Bredasdorp and Oudtshoorn farms, South Africa, respectively. All ostrich birds were of the same age (10 months old); while for the other two species, the age could not be determined at the time of slaughter. The average weight and sex of the animals were determined at the time of slaughter (Table 5.1). All animals were harvested according to the standard operating procedure with ethical clearance (approval number: SU-ACUM14-001SOP; Stellenbosch University Animal Care and Use Committee). The animals were eviscerated at abattoirs according to the South African red meat regulations (DAFF, 2004; Van Schalkwyk & Hoffman, 2010), and transported chilled to the meat laboratory at the Department of Animal Sciences, Stellenbosch University. After 24 to 48 h post-mortem, the *longissimus thoracis et lumborum* (LTL) muscles were removed from the blesbok and eland, while the fan fillet (FF) was removed from the ostrich. Each muscle was cut perpendicular to the longitudinal axis of the muscle fibres to give approximately 2.0 to 2.5 cm thick steaks. Each meat steak was then randomly allocated to be analysed after five different ageing periods. Blesbok steaks were aged for 4, 10, 13, 17 and 22 days; those of eland for 2, 7, 13, 28 and 35 days; and ostrich steaks for 3, 7, 14, 21 and 28 days. Steaks were individually vacuum packed (Multivac packaging machine, USA) in high-barrier (moisture vapour transfer rate of 2.2 g/m^2 per 24 h at 1 atm, oxygen permeability of 30 cm^3/m^2 per 24 h at 1 atm and carbon dioxide permeability of 105 cm^3/m^2 per 24 h at 1 atm), polyethylene and nylon film vacuum bags (70 µm thickness) and stored at 4°C for the duration of the assigned ageing period. At the end of each time point, the steaks were removed from the vacuum packaging and analysed.

Chemical analysis

Moisture, protein and fat content of the game meat (with the exception of ostrich) steaks were determined as described by Neethling, Hoffman, & Britz, (2014).

Table 5.1 Total number (females and males) and the average weight (kg) of blesbok, eland and ostrich harvested

Species	Total number	Sex		Average Weight ± SD (kg)
		Females	Males	
Blesbok	15	7	8	51.2 ± 5.53
Eland	12	6	6	337.3 ± 57.15
Ostrich	15	4	11	85.9 ± 10.37

Weep loss

Weep loss was measured by weighing the muscle steaks prior to vacuum-packaging to determine their initial mass. The steaks were later weighed at the completion of ageing after being blotted dry with a paper towel to determine moisture loss during ageing. This moisture loss was expressed as a percentage of the initial mass of each muscle steak.

Acidity (pH)

The pH of each muscle was determined at each ageing time point immediately after the meat samples were blotted dry. The pH was measured using a calibrated portable Crison pH25 pH meter with a glass electrode (manufactured by Crison Instruments S.A., Barcelona, Spain; purchased from Lasec SA, Cape Town, South Africa) to monitor the acidity and the alkalinity of meat, as meat with pH < 5.8 is considered normal. Again, meat with pH >5.8 tends to show inconsistent tenderness, and shorter shelf-life as the muscle fibres undergo structural changes at higher pH levels during ageing (Dixit *et al.,* 2021). The electrode was washed with distilled water between the measurements.

Warner Bratzler shear force (WBSF)

Warner Bratzler shear force was determined on each steak per specific ageing period as explained in the Material and Methods of Chapter 4 (Page 73).

Surface colour

After each ageing time point was reached, the muscle steaks were removed from the packaging, blotted dry, then left to bloom for 30 min (Honikel, 1998). The colour ordinates were measured on

five random locations of the meat surface using a Colour-guide 45°/0° colorimeter (BYK-Gardner GmbH, Gerestried, Germany), according to the CIE L* a* b* colour system (Honikel, 1998). Co-ordinates measuring CIE L* (lightness), CIE a* (green-red value) and CIE b* (blue-yellow value) are reported by the colour system.

Sample preparation and near infrared (NIR) spectral acquisition

For each ageing time point, the steaks were removed from the vacuum packaging. After they were blotted dry and bloomed for 30 min, they were scanned with a handheld MicroNIR™ OnSite spectrophotometer and spectral acquisition software (Viavi Solutions®, San Jose, CA, USA) in the wavelength range of 908 to 1700 nm. The reflectance spectra were recorded at 6.3 nm intervals, resulting in 125 data points. The illumination source comprised of two integrated vacuum tungsten lamps coupled to a linear variable filter and a 128-pixel Indium Gallium Arsenide (InGaAs) photodiode array detector. The InGaAs detector was used to achieve a resolution of 30 µm x 250 µm / 50 µm (<12.5 nm resolution).

The steaks were scanned three times at different positions at ambient temperature. While scanning, a 2 mm thick glass Steriplan petri dish was placed on top of the meat samples to prevent direct contact of the meat surface moisture with the instrument. A sample spectrum was recorded in 0.25 to 0.5 sec, with each spectrum being an average of 100 scans. The external white and dark references were scanned every 10 min during sample collection. Reflectance spectra were converted to absorbance.

The total number of blesbok samples scanned were 75 muscles (15 carcasses X 5 ageing days), while the eland total samples were 60 (12 carcasses X 5 ageing days). For ostrich, the total number of samples scanned were 75 muscles (15 birds X 5 ageing days).

Multivariate data analysis

The Unscrambler® X version 10.5 (CAMO Software, Oslo, Norway) and PLS_Toolbox (Version 8.6.2, Eigenvector Research, Inc., Manson, WA USA) data analysis software packages were used to analyse the spectra. The spectral range was reduced from 908-1700 nm to 908-1680 to remove the spectral noise segments. Spectra were first averaged, to obtain one spectrum per sample as each muscle was scanned three times at different locations.

Spectral pre-processing

To minimise the spectral effects related to light scatter and baseline shifts, spectral data were pre-treated with different pre-processing methods which differed for each species analysed, due to their unique spectral signatures (Rinnan *et al.,* 2009; Engel *et al.,* 2013). Several pre-processing methods were evaluated before choosing a technique that delivered the best prediction accuracy results. For ostrich, standard normal variate (SNV) was applied to eliminate the scatter effects by centering and scaling spectra individually. Furthermore, detrend transformation was then applied with SNV to reduce the baseline shift and curvature in the spectroscopic data (Barnes *et al.,* 1989)**.** For eland,

Savitzky-Golay 2nd derivative with a second (2nd) order polynomial and nine smoothing points was applied to smooth the noise oscillations without introducing distortions to the data, and to expose the peaks that were not clearly visible (Savitzky and Golay, 1964). Lastly, for blesbok SNV-Detrend, 2nd derivative, 2nd order polynomial with five smoothing points was applied.

Principal component analysis

Principal component analysis (PCA) (Cowe & McNicol, 1985; Wold *et al.,* 1987) was performed to explore the spectral data and demonstrate the potential clustering of samples based on different ageing days. The results was visualised by means of principal component scores plots (Cozzolino and Murray, 2004; Moscetti *et al.*, 2015). Since the animals in this study were aged for different number of days and had different pre-processing methods applied, each species was analysed separately.

Classification

To develop models for classifying meat samples according to the ageing days, partial least squares discriminant analysis (PLS-DA) (Barker and Rayens, 2003) was applied with each species modelled independently. Cross-validation was used to assess the prediction performance of the models. Venetian blinds (with 10 segments, 1 sample per blind) cross-validation was applied to select the optimum number of latent variables (LVs) and validate the models. For all algorithms, class modelling was set to "Class Predict Strict" in the PLS_Toolbox (Version 8.6.2, Eigenvector Research, Inc., Manson, WA USA). In this approach, each sample belongs to a given class if the probability is greater than a threshold value for that class. If no class has a probability greater than the threshold, or if more than one class has a probability exceeding it, the sample is assigned to class zero (0) indicating no class could be assigned. Thereafter, confusion matrices were used to assess the individual models in terms of percentage correctly classified using the following equation (Oliveri and Downey, 2012):

$$\% \text{ Classification accuracy} = \frac{TP+TN}{TP+TN+FP+FN} \text{ X } 100\%$$

Where:

TP = True positive (samples belonging to the modelled class, if they are correctly predicted to be inside the boundary of that class) e.g., for a Day 2 ageing period class model, true positive samples are Day 2 samples predicted as such.

FP = False positive (when samples not belonging to the modelled class are incorrectly predicted to be inside the boundary of that class) e.g., for a Day 2 ageing period class model, false positives are samples that are not Day 2 predicted as Day 2.

TN = True negative (samples not belonging to the modelled class, if they are correctly predicted outside the boundary of that class) e.g., for a Day 2 ageing period class model, true negatives are samples that are not Day 2, predicted as such.

FN = False negative (when samples belonging to the class being modelled are incorrectly predicted to be outside the boundary of that class), e.g., for a Day 2 ageing period class model, false negatives are Day 2 samples that are misclassified.

Results and discussion

Proximate chemical analysis was performed as supporting information to enable interpretation of the spectral data of the species (Table 5.2). The moisture content ranged between 75.3 and 75.6%, which confirmed the findings by Hoffman (2007). Additionally, the protein and fat content obtained were typical of game meat species, i.e., 20.0–23.8% (protein) and 0.8–2.45% (fat). In a study on proximate analysis and mineral composition of ostrich meat as influenced by muscle, Majewska *et al.* (2009) obtained 75.6, 20.6 and 1.4% for moisture, protein and fat content, respectively.

Table 5.2 Average ± standard deviation of proximate chemical composition (moisture, protein and fat) (%) of the blesbok and eland muscles

Species	Muscle	Moisture (%)	Protein (%)	Fat (%)
Blesbok	LTL	75.3 ± 1.04	21.5 ± 1.00	2.5 ± 0.25
Eland	LTL	75.6 ± 0.81	23.0 ± 0.92	1.2 ± 0.27

Table 5.3 presents the physical composition (pH, surface colour, weep loss and WB shear force) changes occurring in blesbok, eland and ostrich muscles as they aged. There were no noticeable changes in the pH of blesbok and eland muscles during ageing; whereas there was a rapid increase of pH in ostrich muscles until day 14, which was followed by a gradual pH decrease to 6.18 until day 28. The gradual pH decrease is assumed to be attributed to lactic acid production from lactic acid bacteria (Shange *et al.*, 2017).

There was a slight increase in the L* ordinate values of the muscles as the ageing days increased for all three species. Similarly, Liu *et al.* (2003), in their feasibility study to predict colour, texture and sensory characteristics of beef steaks with Vis-NIR spectroscopy, observed an increase in lightness of steaks as the ageing days increased. On the other hand, for the a* and b* ordinates there were no noticeable stable trends. Regarding the weep loss, there was a slight change in moisture lost from blesbok and eland muscles.

In general, game meat particularly eland, tends to be tougher than domestic meat, especially beef (Bartoň *et al.*, 2014). Comparing the meat quality of eland and cattle raised under similar conditions, Bartoň *et al.* (2014) found that after ageing for 14 days, the average Warner-Bratzler shear force (WBSF) values obtained were 63.17 and 47.57 N, respectively. In this study, the average WBSF values show eland to have the toughest muscles of the three species. The average shear force values gradually decreased in all the meat samples of the three species as the ageing days

increased. Although the averaged shear force values were decreasing, a noticeable wide range of variation in the values within each period was observed (Table 5.3). Due to this variation, some overlapping of shear force values across the ageing days was noticed. This wide variation of shear force values was also reported by Rødbotten *et al.* (2000), who were not able to successfully predict beef tenderness using NIR spectroscopy in a wavelength of 1100 to 2500 nm. Smith *et al.* (1978) articulated that most researchers rely on the WBSF instrument for objective estimates of tenderness. However, according to Harris and Shorthose (1988), shear force does not accurately reflect tenderness differences among muscles. The shear force is a mechanical measurement which measures force in Newtons, while tenderness is a biochemical mechanism that involves numerous chemical reactions and changes (Binning *et al.*, 2012).

Characterisation of NIR spectra

The mean NIR spectra of steaks obtained from blesbok, eland and ostrich over the various ageing days are illustrated in Figures 5.1, 5.2 and 5.3, respectively. The raw spectra of blesbok meat (Figure 5.1(a)) illustrates that the meat aged on different days revealed a similar pattern regardless of the ageing day. Furthermore, there is no noticeable variation between the spectra of different ageing days except for samples aged for 4 days that have a higher absorbance throughout the spectra. The raw spectra display three absorption bands, typical of red meat samples. The two broad absorption bands located at 976 and 1440 nm are related to different forms of O-H (Ding and Xu, 1999; Elmasry *et al.*, 2011; Barbin *et al.*, 2012), whose vibrations are associated with water content in the meat samples. Table 5.2 confirms that water is the main component of blesbok meat as it contains 75.3% moisture. Additionally, there is a band at 1186 nm associated with the second overtone C-H stretching bond that characterises fat (Ding and Xu, 2000; Cozzolino and Murray, 2004). Similar results have been reported by Ding and Xu (1999), in a study on differentiation of beef and kangaroo meat by visible/near infrared reflectance spectroscopy.

Table 5.3 Average ± standard deviation physical composition (pH, surface colour and WBSF) of the blesbok, eland and ostrich muscles

Ageing day	pH	Average colour			Weep loss (%)	Average WBSF (N)	WBSF (N) range
		L*	a*	b*			
Blesbok							
4	5.41 ± 0.004	33.2 ± 1.16	14.5 ± 0.85	11.2 ± 0.73	0.0 ± 0.00	56.0 ± 19.94	26.94 - 82.76
10	5.36 ± 0.006	32.2 ± 1.43	16.6 ± 1.67	12.5 ± 1.14	0.0 ± 0.02	30.8 ± 10.91	16.19 - 53.43
13	5.37 ± 0.005	33.6 ± 1.09	16.4 ± 1.91	12.7 ± 0.68	0.0 ± 0.00	25.2 ± 8.94	12.87- 43.02
17	5.40 ± 0.007	33.1 ± 1.68	14.5 ± 0.82	9.8 ± 1.18	0.0 ± 0.03	24.0 ± 6.56	16.46 - 37.65
22	5.41 ± 0.005	33.6 ± 1.25	15.3 ± 0.81	11.4 ± 0.86	0.0 ± 0.00	21.7 ± 5.52	15.37 - 33.84
Eland							
2	5.55 ± 0.012	34.9 ± 1.63	12.0 ± 2.07	10.6 ± 1.13	0.0 ± 0.00	97.3 ± 17.99	61.90 - 119.08
7	5.67 ± 0.032	34.9 ± 1.17	12.5 ± 2.13	11.3 ± 1.16	0.0 ± 0.00	104.7 ± 39.66	56.75 - 162.90
13	5.59 ± 0.008	33.5 ± 2.70	12.1 ± 2.31	10.9 ± 1.73	0.0 ± 0.01	80.9 ± 22.16	47.32 - 122.35
28	5.56 ± 0.015	35.4 ± 2.09	13.5 ± 1.78	12.2 ± 1.05	0.0 ± 0.01	57.0 ± 20.07	31.73 - 83.00
35	5.63 ± 0.010	35.4 ± 2.60	14.3 ± 2.85	11.8 ± 1.62	0.0 ± 0.01	64.9 ± 17.96	42.95 - 100.74
Ostrich							
3	5.93 ± 0.009	30.1 ± 1.95	13.3 ± 0.86	9.5 ± 1.31	1.9 ± 0.96	35.2 ± 7.08	18.74 - 44.57
7	6.21 ± 0.016	30.4 ± 1.65	14.5 ± 1.47	10.8 ± 1.37	2.8 ± 1.58	29.9 ± 6.81	15.84 - 39.33
14	6.23 ± 0.017	33.6 ± 2.09	15.7 ± 0.89	10.3 ± 0.71	2.5 ± 1.16	29.3 ± 9.11	16.94 - 52.76
21	6.20 ± 0.014	33.9 ± 1.76	14.9 ± 1.27	9.7 ± 1.13	3.9 ± 1.35	27.3 ± 7.14	15.18 - 40.76
28	6.18 ± 0.014	30.9 ± 1.81	13.3 ± 1.23	10.5 ± 1.26	2.8 ± 1.42	26.6 ± 7.91	13.83 - 50.02

Abbreviations: WBSF = Warner Bratzler shear force, L* = lightness, CIE a* = green-red value and CIE b* = blue-yellow value

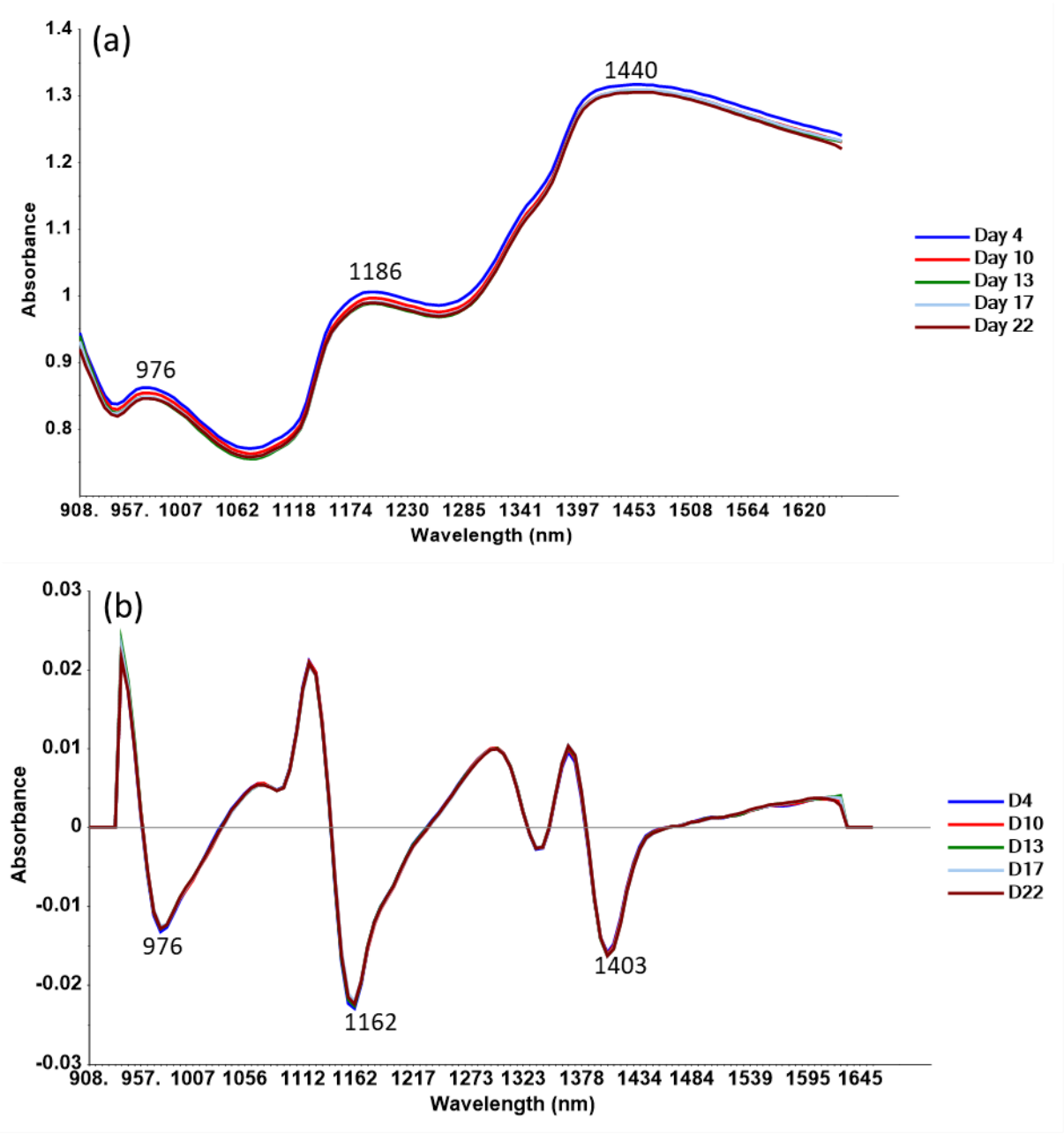

Figure 5.1 Mean spectra of blesbok ageing days (4, 10, 13, 17 and 22) showing the wavelength bands of (a) raw spectra, and (b) SNV-Detrend and 2nd derivative (2nd order polynomial with 5 smoothing points) pre-processed spectra

In contrast, after the blesbok spectra was pre-processed with SNV-Detrend and 2nd derivative, no prominent variation among the ageing days was observed (Figure 5.1(b)). The wide range of Warner Bratzler shear force (WBSF) values supports the overlapping of the spectra of different ageing days within each ageing day (Table 5.3). The wide range of WBSF values within each ageing day was also observed, which resulted in overlapping of the WBSF values across different ageing days. That makes it difficult to differentiate the WBSF values of different ageing periods (Rødbotten *et al.*, 2000; Leroy *et al.*, 2004). Additionally, the three visible bands similar to those of raw spectra, located at the positions (976 and 1403 nm) representing O-H bonds and (1162 nm) C-H bonds were still observed.

The raw mean spectra of eland ageing days shown in Figure 5.2(a) is similar to that of blesbok. However, regarding the variation in ageing days, eland samples aged for 13 days can be differentiated from other ageing days due to higher absorbance values throughout the spectrum. Moreover, when the eland spectral data was pre-treated with the 2nd derivative (Figure 5.2(b)), different results were noticed. There was no variation across the ageing days at the O-H band located at 994 nm. However, the O-H band situated at 1416 nm varied from the other ageing days for the samples aged for 13 days because of their moisture content (Elmasry *et al.*, 2011). This day corresponds to the first noticeable increase of weep loss. Then, at the 1174 nm absorption band which represents the C-H bond, the meat samples aged for 28 days differed from other samples aged on different days because of their fat content (Cozzolino and Murray, 2004). However, there was no noticeable change in classification of ageing days.

The raw mean spectra of ostrich (Figure 5.3 (a)) is similar to the raw spectra of blesbok and eland, where a resemblance between the pattern and absorption bands was observed throughout. Nevertheless, the C-H absorption band located at 1193 nm indicated a difference in samples aged for 14 days from the other samples. This variation might be the result of lipid oxidation, which is due to the long storage period (Jones *et al.*, 2015). High lipid variation was only observed in ostrich muscles compared to other species as the different species age differently. The most intensive absorption bands detected at 976 and 1440 nm were due to water bands. However, when the same spectra were pre-treated with SNV-Detrend (Figure 5.3(b)), different results were obtained. On the pre-treated spectra, the C-H absorption band detected at 1174 nm was responsible for the variation of day 3 against all other ageing days. That implies that lipids again contributed to differentiating day 3 aged meat from all other ageing days of ostrich muscles. Which indicates the variation of the muscle structure during ageing affects the chemical components of muscles, which results in changing the fatty acid composition (Dixit *et al.,* 2021).

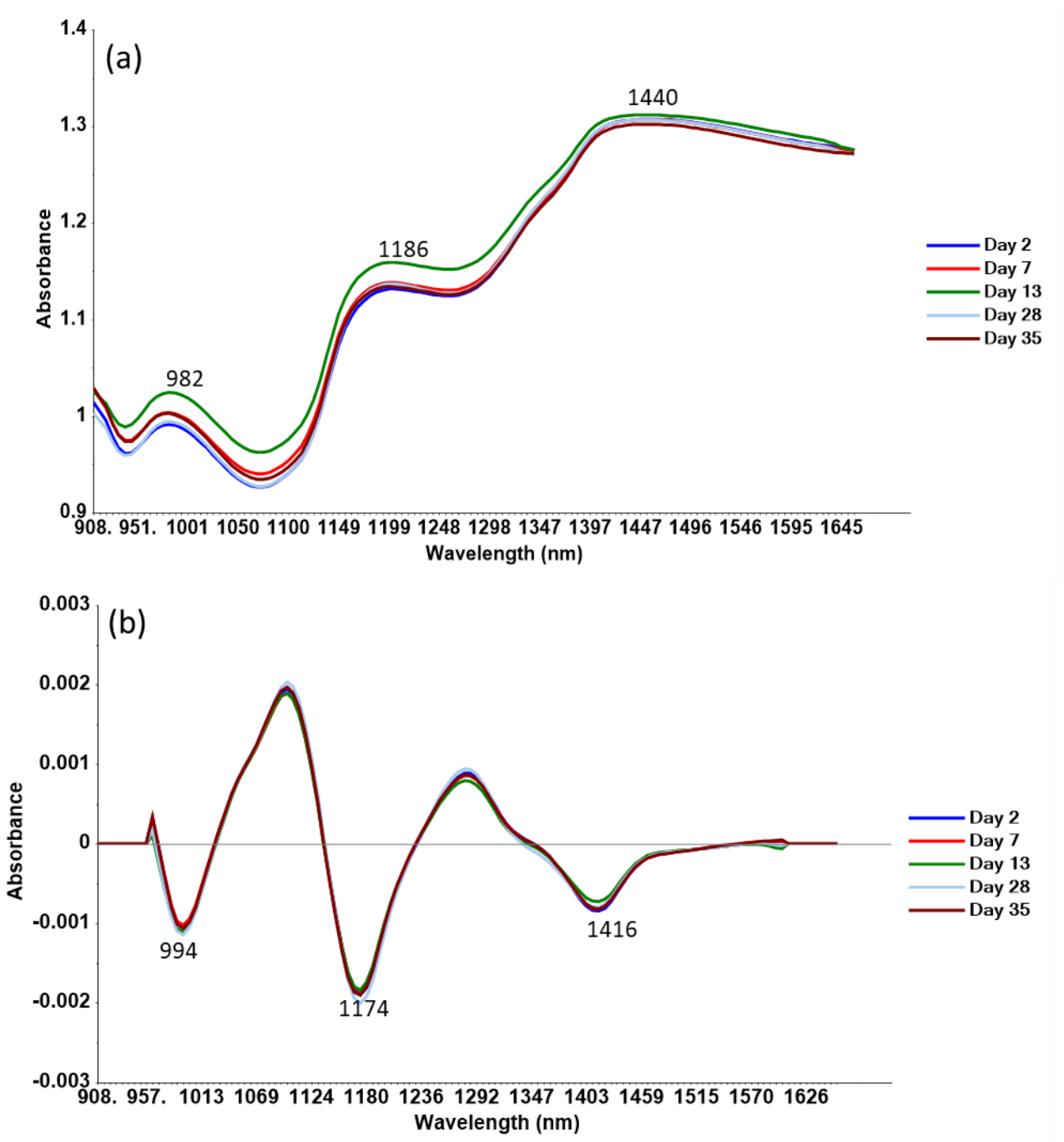

Figure 5.2 Mean spectra of eland ageing days (2, 7, 13, 28 and 35) showing the wavelength bands of (a) raw spectra, and (b) 2nd Derivative (2nd order polynomial with 9 smoothing points) pre-processed spectra

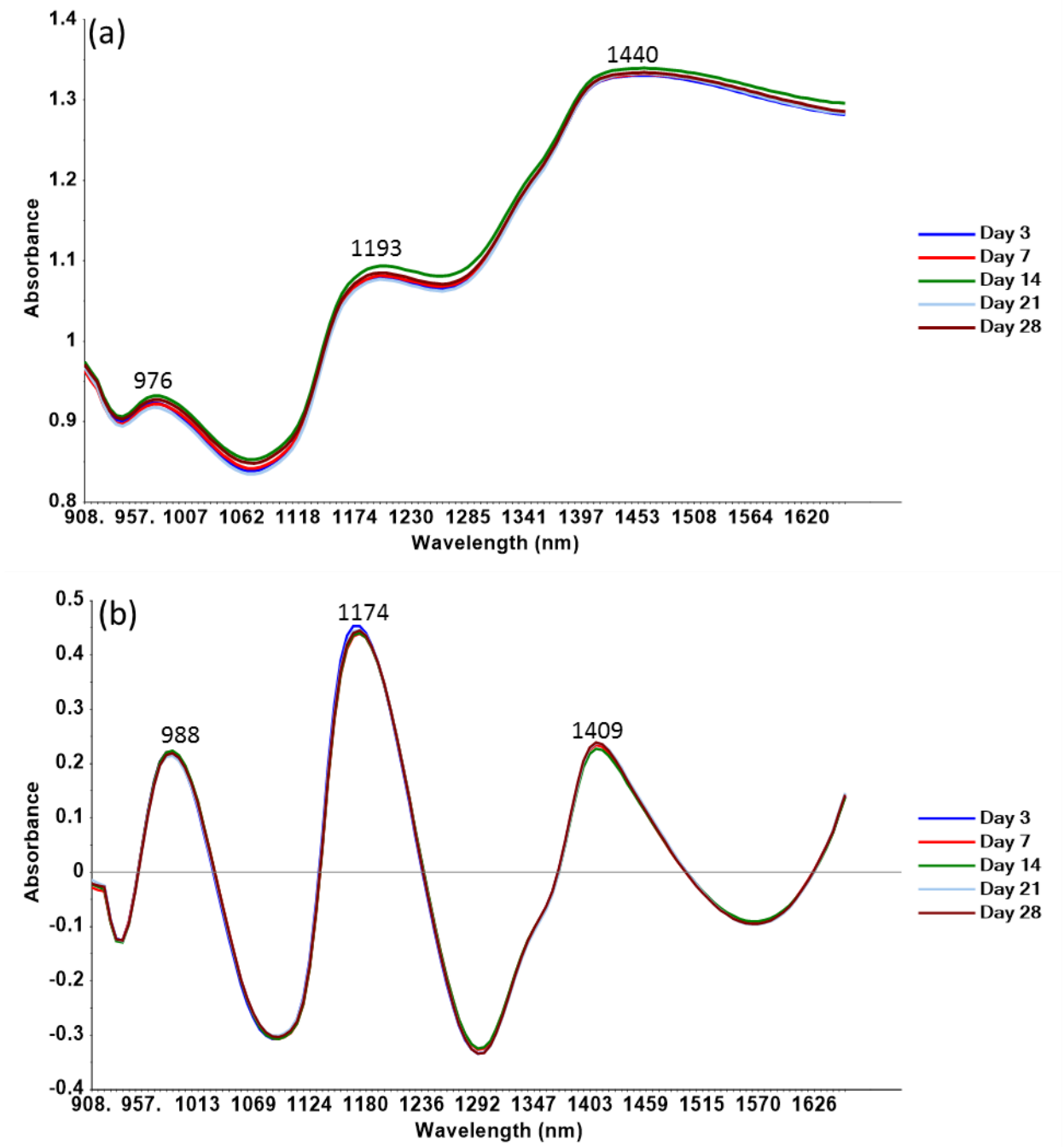

Figure 5.3 Mean spectra of ostrich ageing days (3, 7, 14, 21 and 28) showing the wavelength bands of (a) raw spectra, and (b) SNV-Detrend pre-processed spectra

Principal Component Analysis

A preliminary examination of blesbok meat ageing days (D4, D10, D13, D17 and D22), pre-treated with SNV-Detrend and 2nd derivative shown with a PCA scores plot, is illustrated in Figure 5.4(a). In general, the samples are scattered all over the plot, showing no clear groupings. Nonetheless, in the direction of PC4, there was a slight separation of meat samples aged for 4 days (blue squares) from samples aged for 22 days (brown triangles). The distinction of samples aged for 4 days (blue squares) confirms what the raw spectra illustrated in Figure 5.1(a). Moreover, Figure 5.4(b) shows the PC4 loadings line plot confirming the wavelength band of influence (1385 nm) for the segregation of the steak samples. This absorption band is due to C-H bonds, corresponding to fat (Cozzolino and Murray, 2004; Prieto *et al.*, 2008). Starkey *et al.* (2016), on the question of what really explains variation in tenderness of three ovine muscles, found that the main factors influencing tenderness was intramuscular fat, as well as sarcomere length and desmin degradation.

Figure 5.5(a) shows the PCA scores plot of PC1 vs. PC2 explaining 90% variation of the eland ageing days (D2, D7, D13, D28 and D35) model. Like blesbok, the eland samples are scattered all over, showing no clear groupings. However, in the direction of PC2, there is a slight separation of meat samples aged for 7 days (red circles) from those of 13 days (green triangles). This verifies the observations in the spectral features in Figure 5.2(a). The PC2 loadings line plot (Figure 5.5(b)) illustrates the wavelength band located at 1422 nm, responsible for the separation of ageing days. This band is related to the second overtone stretching of the O-H bond (Elmasry *et al.*, 2011; Barbin *et al.*, 2012), associated with the moisture content of the samples shown by a slight change in weep loss values (Table 5.3) from ageing day 13.

Finally, the PCA scores plot of ostrich meat ageing days (D3, D7, D14, D21 and D28), of spectra pre-treated with SNV-Detrend is shown in Figure 5.6(a). Like blesbok and eland, the samples are all over the plot, showing no distinct groupings. However, the first two PCs that explained 90% of total variation revealed that only samples aged for 3 (blue squares) and 14 days (green triangles) slightly separated in the direction of PC2. The important wavelength band responsible for their separation is the C-H bond located at 1155 nm that corresponds to the fat content (Osborne *et al.,* 1993). The observed PCA scores plots that could not form visible clusters between the ageing days confirmed the overlapping of spectra revealed in Figure 5.3(a), where only day 14 samples (green triangles) differed from the bands located at 1183.

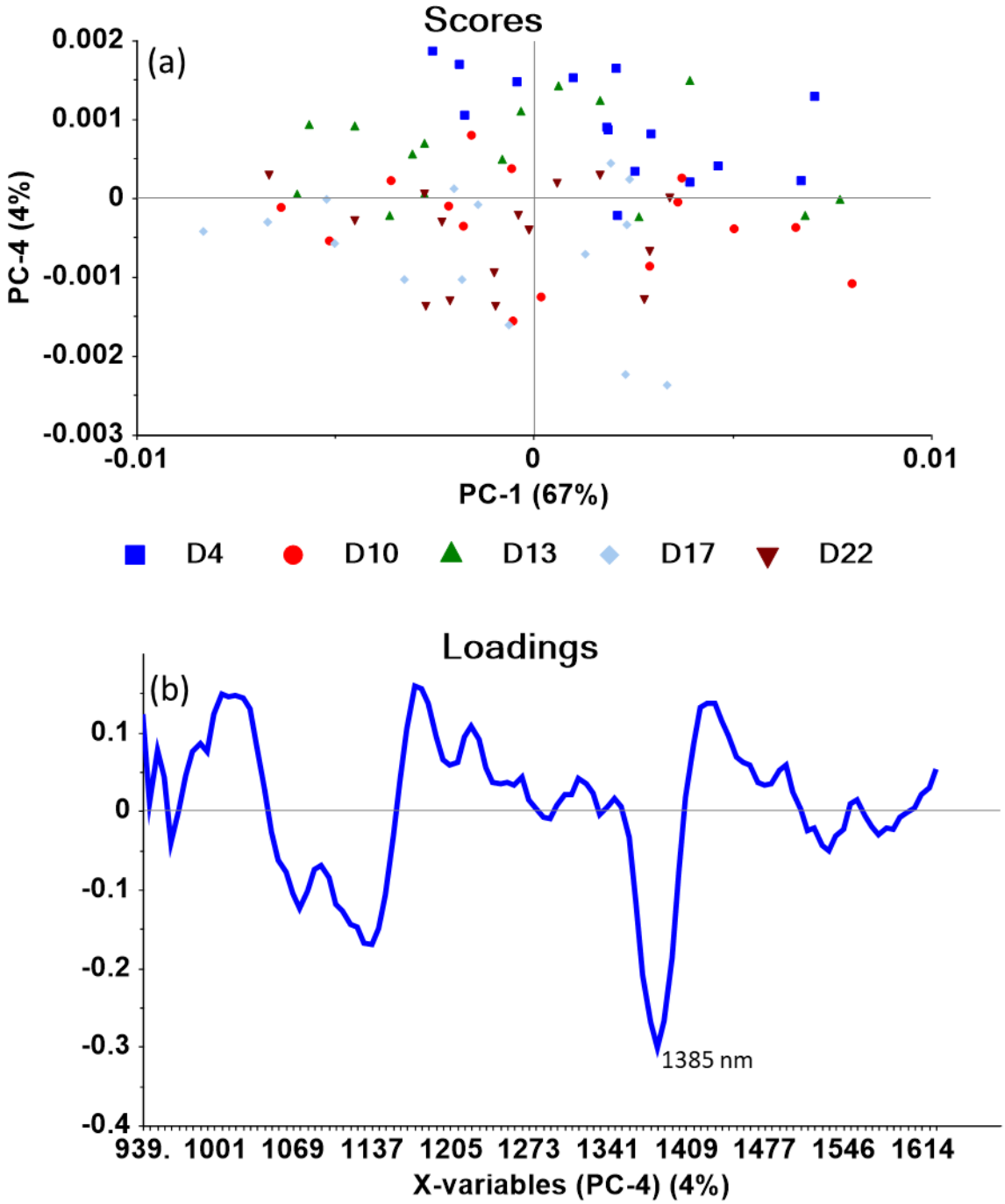

Figure 5.4 (a) PCA scores plot of PC1 vs. PC4 (71% explained variance) showing the separation of samples aged for 4 days (blue squares) from those of 22 days (brown triangles); and scattering of other blesbok ageing days (SNV-Detrend, 2nd derivative (2nd order polynomial with 5 smoothing points) pre-processed spectra). (b) PC4 loadings line plot, illustrating the wavelength band at ca. 1385 nm (associated with fat) responsible for the separation of ageing days.

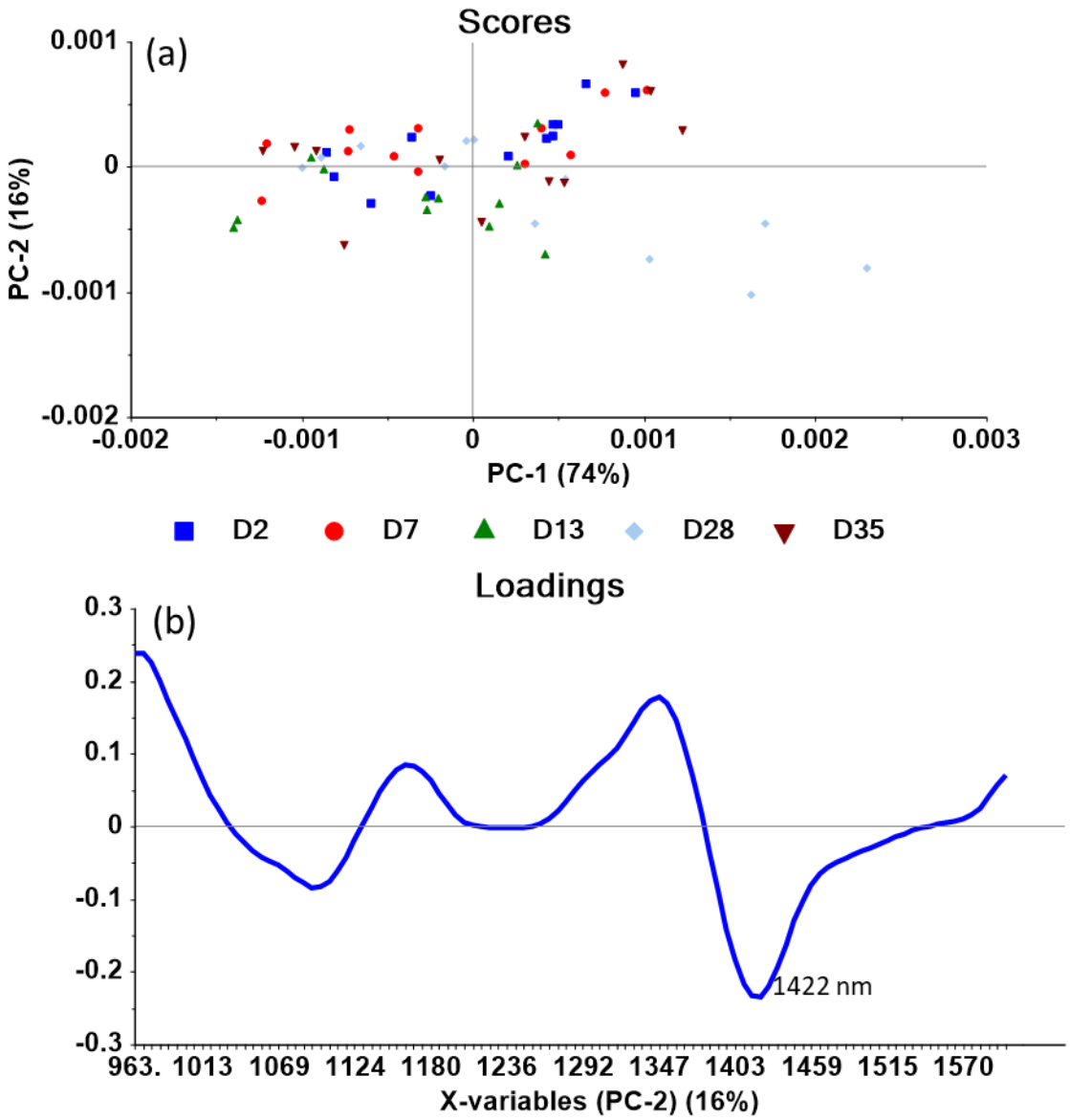

Figure 5.5 (a) PCA scores plot of PC1 vs. PC2 (90% explained variance) shows scattering of eland ageing days (2nd derivative, (2nd order polynomial with 9 smoothing points) pre-processed spectra). (b) PC2 loadings line plot, illustrating the wavelength band at ca. 1422 nm (associated with moisture) responsible for the separation of ageing days.

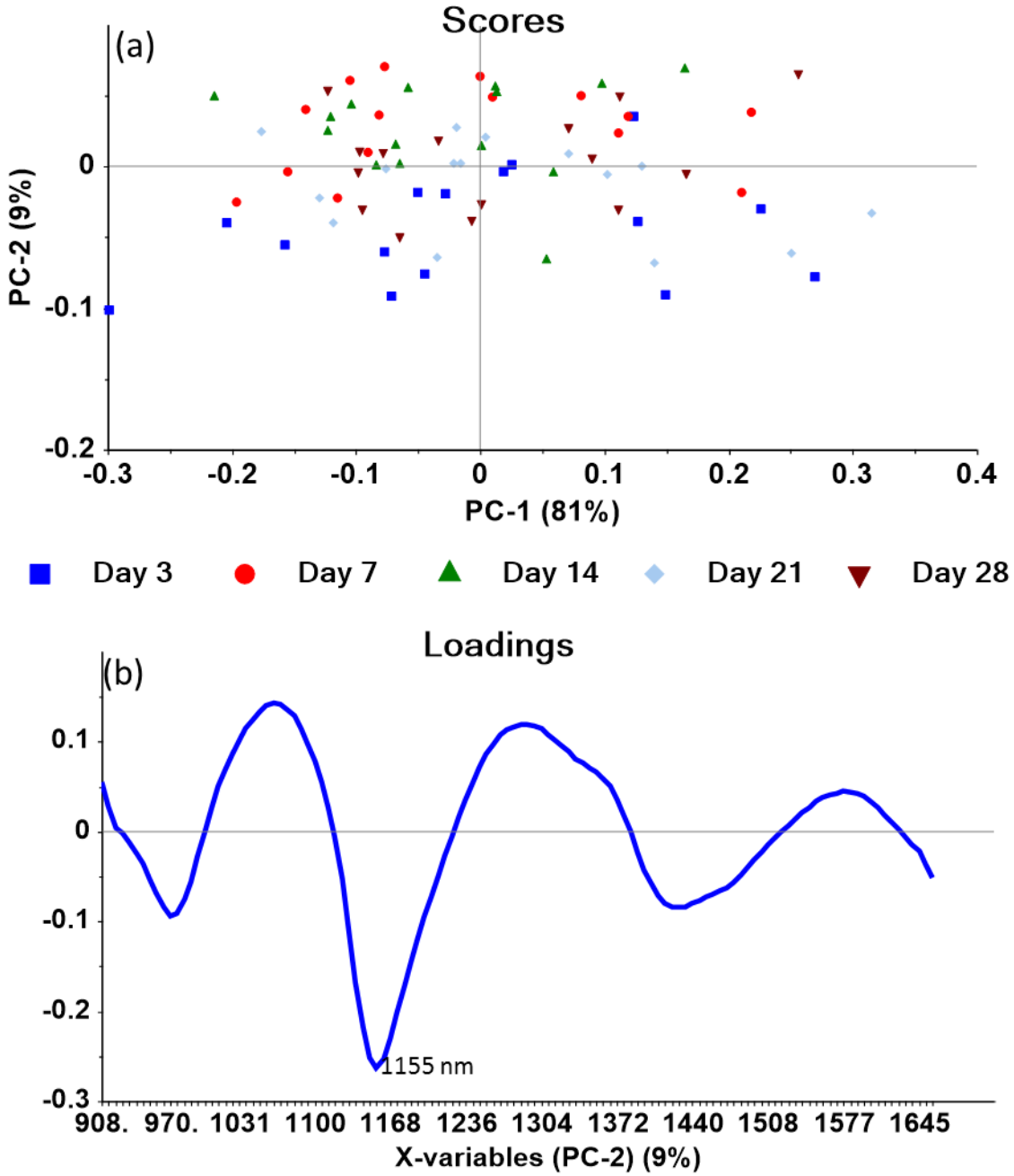

Figure 5.6 (a) PCA scores plot of PC1 vs. PC2 (90% explained variance) showing the separation of samples aged for 3 days (blue squares) from those of 14 days (green triangles); and scattering of other ostrich ageing days (SNV-Detrend pre-processed spectra). (b) PC2 loadings line plot, illustrating the wavelength band at ca. 1155 nm (associated with fat) responsible for the separation of ageing days.

Classification

The scores plot, obtained with PLS-DA pre-treated with SNV-Detrend and 2nd derivative pre-processing methods, illustrating the discrimination of blesbok ageing days (D4, D10, D13, D17 and D22) is presented in Figure 5.7. Based on cross-validation, six LVs were selected for model calibration with an explained Y variance of 96%. All blesbok meat samples aged for 4 days were correctly classified, and 2 samples aged for 13 days were misclassified as day 4 samples. Even though all day 4 samples were correctly classified, it was noted that some samples of this class appeared as false positives in other classes. This means some samples were assigned in more than one class. For example, 2 samples of day 4 were misclassified as day 10, 4 samples misclassified as day 13 and 2 samples misclassified as day 22 (Figure 5.7). The misclassification of some of day 4 aged samples contributed to the lower (76%) classification accuracy (Table 5.4). Thus, the calibration class models presented good classification accuracies ranging from 76 to 97% and the cross-validated class models attained 66 to 95% accuracies. It was also observed that samples aged for 22 days obtained the highest accuracy compared to other days, although this was not reflected in the spectral features and PCA scores plot (Figure 5.1 and 5.4, respectively).

Figure 5.8 presents the score plot obtained with PLS-DA pre-treated with 2nd derivative displaying the discrimination of eland ageing days. Based on the cross-validation, seven LVs were selected for model calibration with an explained Y variance of 99%. The classification accuracies of eland ageing days had a similar explanation as the blesbok. The percentage classification accuracies obtained for the calibration and cross validation models ranged from 64 to 79% and 56 to 71%, respectively (Table 5.4). It was observed that samples aged for 28 days gave the highest prediction accuracy. When Needham *et al*. (2020) studied the optimum ageing day of eland muscles using the same muscle type scanned in this study, he discovered day 28 as the ideal ageing day.

Finally, Figure 5.9 shows the score plot obtained with PLS-DA pre-treated with SNV-Detrend revealing the segregation of ostrich ageing days. An explained Y variance of 99% described the model calibration selected by six LVs based on cross-validation. Percentage classification accuracies obtained for these models ranged from 54 to 80% and 52 to 68% for calibration and cross-validation, respectively (Table 5.4). In these models, no samples from other class models were predicted as day 3, even though some of day 3 samples were misclassified as day 21. There was substantial misclassification between day 7 and day 14 samples, which was also noticed on the pre-processed spectra and PCA score plot (Figure 5.3(b) and 5.6(a), respectively).

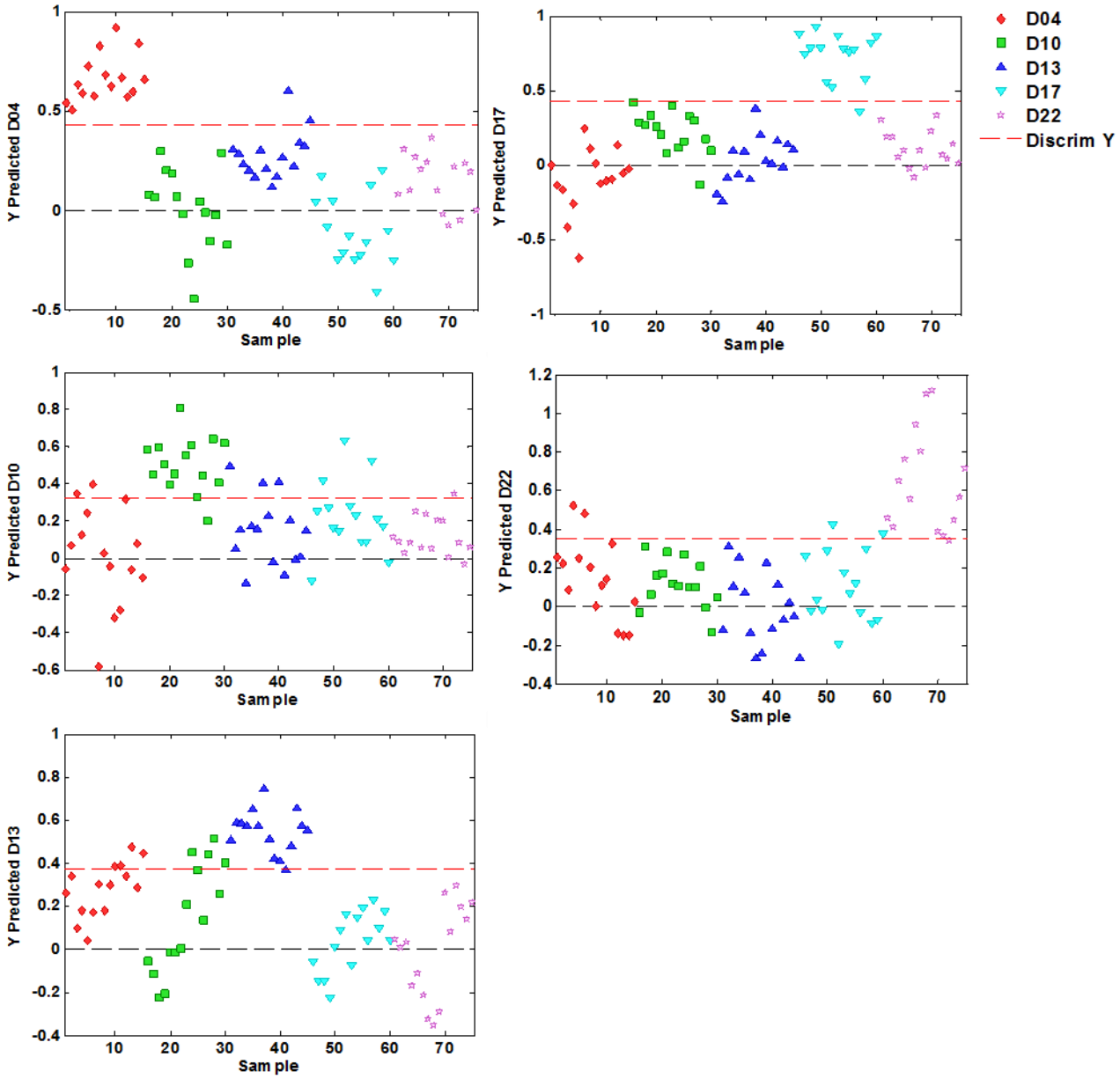

Figure 5.7 PLS-DA model scores plot (spectra pre-treated with SNV-Detrend and 2nd derivative pre-processing) showing the segregation of blesbok ageing days. The red dotted line represents the discrimination line. Samples above the red dotted line are regarded as the predicted class and those below the red line are regarded as other classes not predicted.

There are many reasons that could contribute to the misclassification of aged meat samples which include the breed, age, sex, muscle type, chilling conditions, and the ageing period (Strydom *et al.*, 2016). However, in this investigation attempts were made to take these factors into account. The breed/species were the same (except the three different genotypes of ostrich), the same muscle type was evaluated within species, and the chilling and ageing conditions were standardised. However, sex and the age of the animals were not considered as the age was unknown.

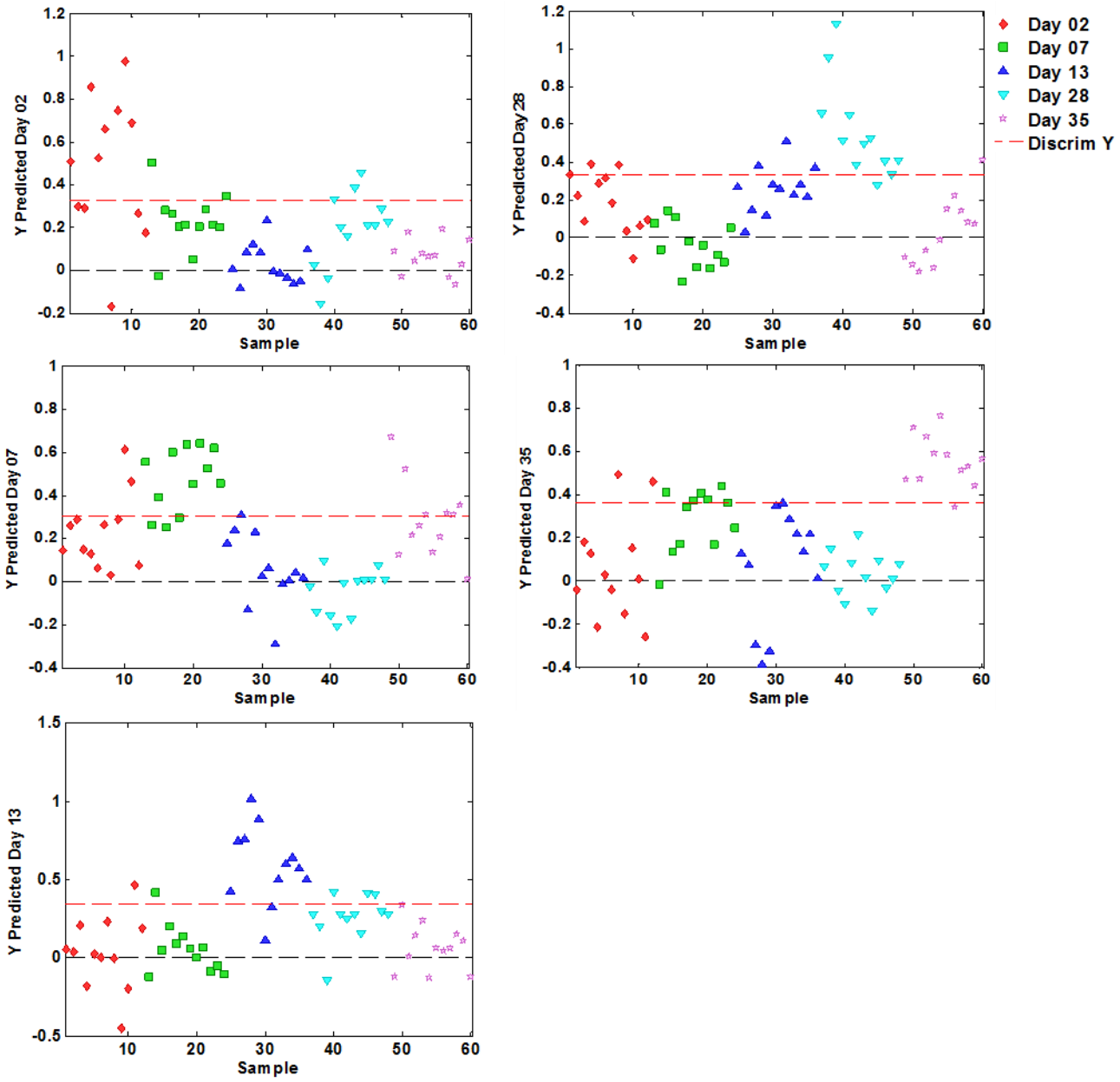

Figure 5.8 PLS-DA model scores plot (spectra pre-treated with 2nd derivative (2nd order polynomial with 9 smoothing points) pre-processing) showing the segregation of eland ageing days. The red dotted line represents the discrimination line. Samples above the red dotted line are regarded as the predicted class and those below the red line are regarded as other classes not predicted.

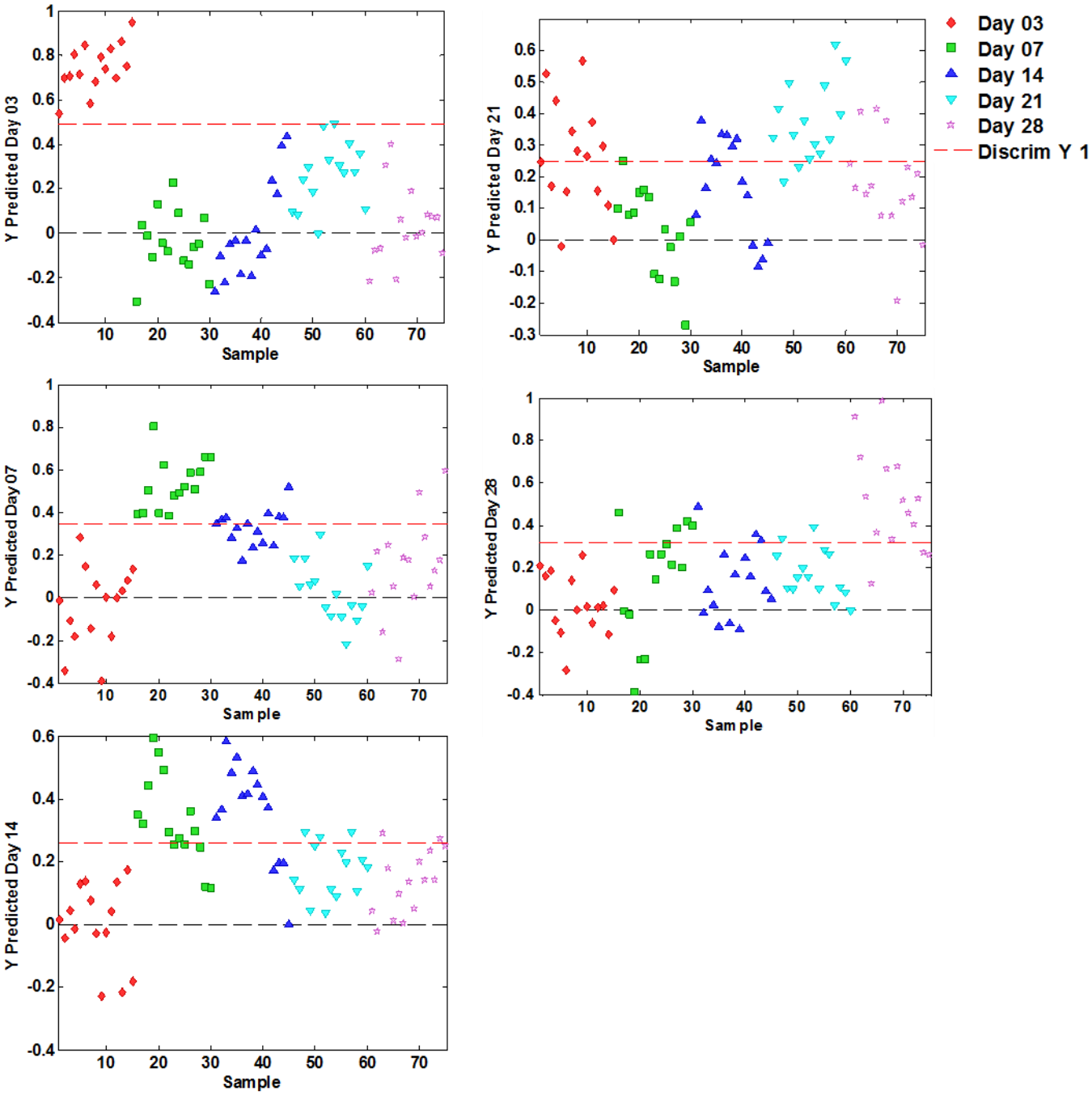

Figure 5.9 PLS-DA model scores plot (spectra pre-treated with SNV-Detrend pre-processing) showing the segregation of ostrich ageing days. The red dotted line represents the discrimination line. Samples above the red dotted line are regarded as the predicted class and those below the red line are regarded as other classes not predicted.

Table 5.4 Calibration and cross-validation (CV) accuracy (%) results of PLS-DA models, for classification of ageing days of blesbok, eland and ostrich species using (i) SNV-Detrend and 2nd derivative (2nd order polynomial with 5 smoothing points), (ii) 2nd derivative (2nd order polynomial with 9 smoothing points) and (iii) SNV-Detrend pre-processed spectra, respectively.

Species	Muscle type	Ageing day	Calibration (%)	CV (%)
SNV-Detrend and 2nd derivative pre-processed				
Blesbok	LTL	4 days	76	66
	LTL	10 days	85	74
	LTL	13 days	83	83
	LTL	17 days	83	77
	LTL	22 days	97	95
2nd derivative pre-processed				
Eland	LTL	2 days	67	56
	LTL	7 days	67	67
	LTL	13 days	74	66
	LTL	28 days	79	71
	LTL	35 days	64	56
SNV-Detrend pre-processed				
Ostrich	FF	3 days	73	63
	FF	7 days	58	52
	FF	14 days	54	53
	FF	21 days	80	64
	FF	28 days	76	68

Abbreviations: LTL= *longissimus thoracis et lumborum*, FF= fan fillet

Figure 5.10 shows the class predicted strict plot obtained with PLS-DA, displaying the predicted samples of blesbok, eland and ostrich ageing days. The samples located at level 0 (at the bottom) in this figure are either unassigned to any class or appearing in classes more than once. For example, for the blesbok model even though all day 4 samples were correctly predicted, day 4 samples that also appear in other classes (Day 10, Day 13 and day 22) are located at level zero.

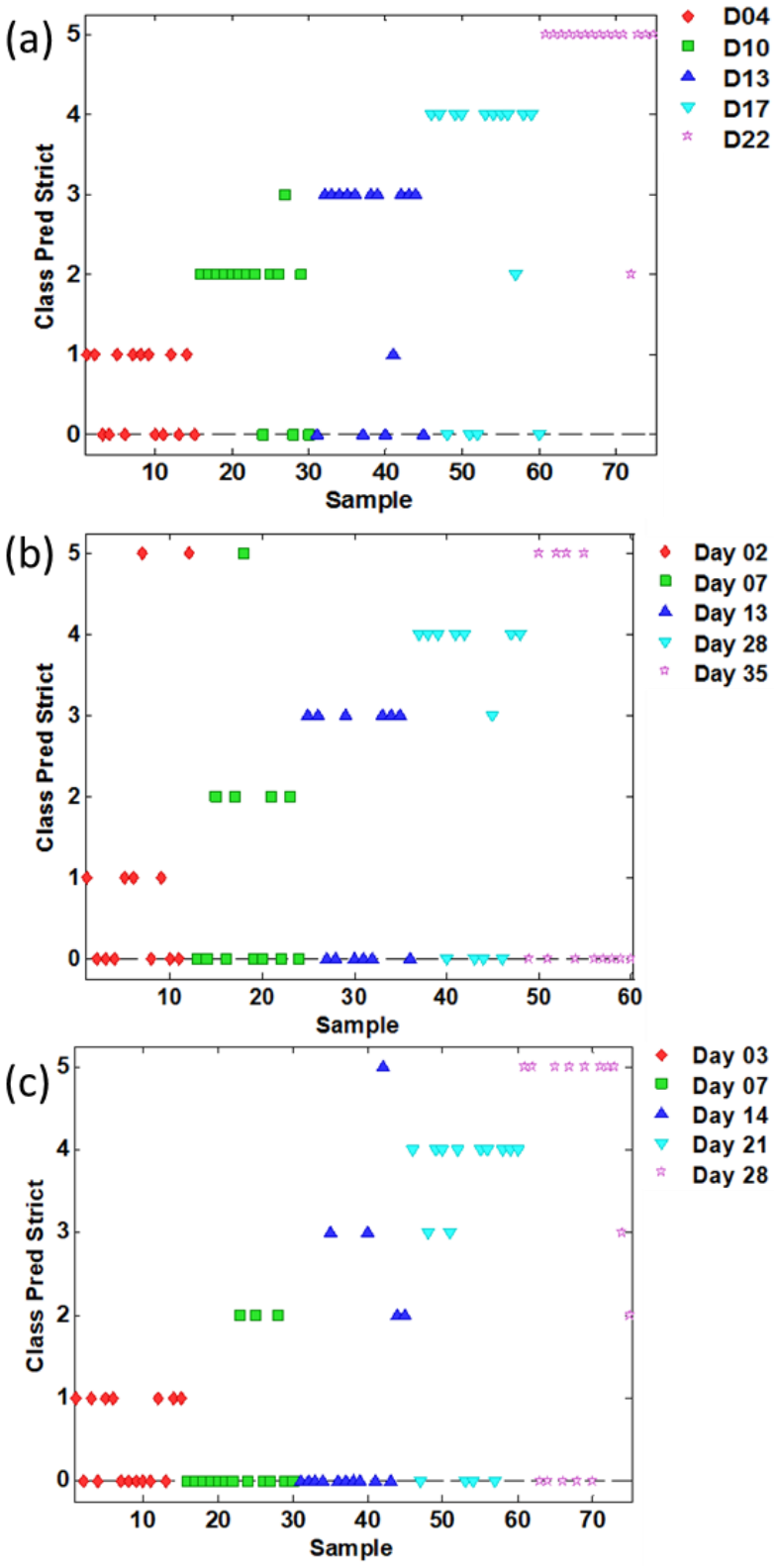

Figure 5.10 Class predict strict plot obtained with PLS-DA model displaying the predicted samples of (a) blesbok, (b) eland and (c) ostrich ageing days from spectra pre-treated with (i) SNV-Detrend and 2nd derivative (2nd order polynomial with 5 smoothing points), (ii) 2nd derivative (2nd order polynomial with 9 smoothing points) and (iii) SNV-Detrend pre-processing method, respectively. Samples located at 0 are unassigned.

Table 5.5 Confusion matrix for PLS-DA classification models for blesbok, eland and ostrich ageing days pre-treated with (i) SNV-Detrend and 2nd derivative, (ii) 2nd derivative and (iii) SNV-Detrend pre-processing method, respectively. The true positives, false positives, true negatives and false negatives of the models are presented.

Species	Class	True + (%)	False + (%)	True - (%)	False - (%)
Blesbok	Day 4	53.3	1.7	98.3	46.7
	Day 10	73.3	3.3	96.7	26.7
	Day 13	66.7	1.7	98.3	33.3
	Day 17	66.7	0.0	100	33.3
	Day 22	93.3	0.0	100	6.7
Eland	Day 2	33.3	0.0	100	66.7
	Day 7	33.3	0.0	100	66.7
	Day 13	50.0	2.1	97.9	50.0
	Day 28	58.3	0.0	100	41.7
	Day 35	33.3	6.2	93.8	66.7
Ostrich	Day 3	46.7	0.0	100	53.3
	Day 7	20.0	5.0	95.0	80.0
	Day 14	13.3	5.0	95.0	86.7
	Day 21	60.0	0.0	100	40.0
	Day 28	53.3	1.7	98.3	46.7

+ = positive, - = negative

Like the blesbok class models, the same misclassification explanation applies to the models of eland and ostrich. Thus, the number of correctly predicted samples in Figure 5.10 is the percentage of true positives outlined in the confusion matrix (Table 5.5); which was ultimately used to calculate the classification accuracy of the model.

In view of the confusion matrix presented in Table 5.5, it is obvious that the true negative values contributed to the high classification accuracies obtained in Table 5.4. Therefore, it will not be easy to predict blesbok, eland and ostrich ageing days in future using these models. That is why the cross-validated models obtained lower accuracies. In general, the prediction results attained in

this study ranged from 66-95, 56-71 and 52-68% classification accuracies of aged meat obtained from blesbok, eland and ostrich, respectively. This means that a handheld spectrophotometer could not be used as a prediction method to classify aged game meat.

On the other hand, Moran *et al.* (2018) investigated the prediction of the ageing time (3, 7, 14 and 21 days post mortem) of beef steaks to assess visible and near infrared spectroscopy (400–2400 nm) as an authentication tool. They applied PLS-DA to classify the ageing days. Their results achieved an overall correct classification ranging from 94.2 to 100%, which indicated the ability of the Vis-NIR instrument to discriminate the different ageing days of beef steaks. Moreover, Prieto *et al.* (2015) studied the rapid discrimination of enhanced quality pork with Vis-NIR spectroscopy in a wavelength range of 350-2500 nm and used PLS-DA to predict the ageing days; they correctly classified 94 and 97% of aged samples for the 2nd and 14th ageing days, respectively. In addition, Liu *et al.* (2003) managed to predict the colour and sensory attributes of steaks at 2, 4, 8, 14 and 21 ageing days in a wavelength range of 400–1080 nm using Vis-NIR spectroscopy. It is clear from the study of Moran *et al.* (2016) that the broad absorption bands responsible for the classification of aged meat are located at 412 and 1927 nm in the Vis and NIR regions, respectively. These bands are associated with myoglobin, and water content of the meat samples. As much as both Vis and NIR spectra gave good ageing day prediction results, it was observed from their PCA and coefficient of determination results that the Vis was more accurate than the NIR spectra. This could be the reason why the handheld MicroNIR™ OnSite spectrophotometer could not correctly classify the ageing days at the spectral range of 908-1700 nm. The darker muscles of game meat might have influenced game meat to age differently compared to beef. Again, the short NIR wavelength range might have also contributed to game meat ageing differently from beef.

It should also be noted that Moran *et al.* (2018) used the same breed of steers, which were of the same age. Bertram *et al.* (2007) discovered that the effect of slaughter age was found to affect the myo-water characteristics, which play a role during meat ageing. For the meat samples used in this study, it is important to note that the game species were free roaming, and it was not easy to determine their age. Moreover, it is reported that the animal history before slaughter, including pre-slaughter anxiety/stress contributes to the meat ageing (McGlone *et al.* 2005). Thus, there are many factors that need to be considered when meat is aged. It should be also considered that, in addition to the regular and external diffuse reflectance, some light energy is scattered within the meat sample. Moreover, the muscle structure, texture and chemical composition of meat samples change over time as the meat is being aged. Thus, the various changes occurring within muscles, combined with the scattered energy which might carry some important information contribute in the inability to achieve to correct results.

Conclusions

As the predicted samples were cross validated rather than from an independent test set, it is concluded that the model was not robust enough for acceptance. The overall prediction results suggest that the NIR spectra in the range of 908–1700 nm could not clearly distinguish the different ageing days of game meat within the three species. Moreover, the similarity of the spectral features characterizing different ageing days, which resulted in spectral overlapping indicates that absorption signatures could not distinguish the ageing days. This denotes that, in addition to the intramuscular fat and moisture contents that were identified by the loading's plots, some other parameter/s (e.g. enzyme protease, desmin degradation and sarcomere length) not characterized by the spectral data in the NIR range of 908–1700 nm could be responsible for meat ageing.

To our knowledge, this is the first study to assess NIR spectroscopy as an authentication tool for aged game meat, and there is an opportunity for improvement of the NIR models. It is recommended that a wider spectral range should be applied in future studies, as it has shown a potential of producing better results. Moreover, factors that could be evaluated in future studies are tenderness, sarcomere length and desmin degradation. It is also postulated that the smaller sample size/number of animals per species used might contribute to the poor prediction results. Thus, it is suggested that a larger sample size be used, where most of the factors known to influence meat tenderness (e.g., enzyme protease, desmin degradation and sarcomere length) are measured and included in analyses to develop a robust and accurate model.

References

Barbin, D., Elmasry, G., Sun, D.W. & Allen, P. (2012). Near-infrared hyperspectral imaging for grading and classification of pork. *Meat Science*, **90**, 259–268.

Barbin, D.F., Kaminishikawahara, C.M., Soares, A.L., Mizubuti, I.Y., Grespan, M., Shimokomaki, M. & Hirooka, E.Y. (2015). Prediction of chicken quality attributes by near infrared spectroscopy. *Food Chemistry*, **168**.

Barker, M. & Rayens, W. (2003). Partial least squares for discrimination. *Journal of Chemometrics*, **17**, 166–173.

Barnes, R. J., Dhanoa, M. S., & Lister, S. J. (1989). Standard normal variate transformation and de-trending of near-infrared diffuse reflectance spectra. *Applied Spectroscopy, **43**,* 772–777.

Bartoň, L., Bureš, D., Kotrba, R. & Sales, J. (2014). Comparison of meat quality between eland (Taurotragus oryx) and cattle (Bos taurus) raised under similar conditions. *Meat Science*, **96**, 346–352.

Bhat, Z.F., Morton, J.D., Mason, S.L. & Bekhit, A.E.A. (2018). Food Science and Human Wellness Role of calpain system in meat tenderness: A review. *Food Science and Human Wellness*, **7**, 196–204.

Bertram, H. C., & Andersen, H. J. (2007). NMR and the water-holding issue of pork. Journal of Animal Breeding and Genetics, **124**(s1), 35–42

Binning, J.M., Huff-Lonergan, E., Anderson, M.J., Fedler, C.A., Lonergan, S.M. & Prusa, K.J. (2012). Profile of biochemical traits influencing tenderness of muscles from the beef round. *Meat Science*, **91**, 247–254.

Cen, H. & He, Y. (2007). Theory and application of near infrared reflectance spectroscopy in determination of food quality. *Trends in Food Science and Technology*, **18**, 72–83.

Cheng, J.H., Nicolai, B. & Sun, D.W. (2017). Hyperspectral imaging with multivariate analysis for technological parameters prediction and classification of muscle foods: A review. *Meat Science*, **123**, 182–191.

Cowe, A., & McNicol, J. W. (1985). The use of principal components in the analysis of near infrared spectra. *Applied Spectroscopy, **39**,* 257-266.

Cozzolino, D. & Murray, I. (2004). Identification of animal meat muscles by visible and near infrared reflectance spectroscopy. *LWT - Food Science and Technology*, **37**, 447–452.

DAFF (Department of Agriculture, Forestry and Fisheries). 2004. Meat Safety Act (Act No. 40 of 2000), Red meat regulations (No. R. 1072 of 17 September 2004) (Regulation Gazette No. 8056). Government Printing Offices, South Africa.

Ding, H.B. & Xu, R.J. (1999). Differentiation of beef and kangaroo meat by visible/near-infrared reflectance spectroscopy. *Journal of Food Science*, **64**, 814–817.

Ding, H.B. & Xu, R.J. (2000). Near-infrared spectroscopic technique for detection of beef hamburger adulteration. *Journal of Agricultural and Food Chemistry*, **48**, 2193–2198.

Dixit, Y., Al-Sarayreh, M., Craigie, C.R. & Reis, M.M. (2021). A global calibration model for prediction of intramuscular fat and pH in red meat using hyperspectral imaging. *Meat Science*, 108405.

Djenane, D., Beltrán, J.A., Camo, J. & Roncalés, P. (2016). Influence of vacuum-ageing duration of whole beef on retail shelf life of steaks packaged with oregano (Origanum vulgare L.) active film under high O2. *Journal of Food Science and Technology*, **53**, 4244–4257.

Dransfield, E. (1994). Optimisation of tenderisation, ageing and tenderness, *Meat Science,* **36**, 105–121.

Elmasry, G., Iqbal, A., Sun, D.W., Allen, P. & Ward, P. (2011). Quality classification of cooked, sliced turkey hams using NIR hyperspectral imaging system. *Journal of Food Engineering*, **103**, 333–344.

ElMasry, G. & Sun, D. W. (2010). *{CHAPTER} 6 - Meat Quality Assessment Using a Hyperspectral Imaging System*. In: *Hyperspectral Imaging for Food Quality Analysis and Control*. pp 175-240. Elsevier Applied Sience Publishers, London.

Elmasry, G., Sun, D.W. & Allen, P. (2012). Near-infrared hyperspectral imaging for predicting colour, pH and tenderness of fresh beef. *Journal of Food Engineering*, **110**, 127–140.

Engel, J., Gerretzen, J., Szymańska, E., Jansen, J.J., Downey, G., Blanchet, L. & Buydens, L.M.C. (2013). Breaking with trends in pre-processing? *TrAC - Trends in Analytical Chemistry*, **50**, 96–106.

Harris, P. V., & Shorthose, W. R. (1988). Meat texture. In: R. A. Lawrie (Ed.) Developments in Meat

Science. pp 245-286. Elsevier Applied Sience Publishers, London.

Hildrum, K.I., Rødbotten, R., Høy, M., Berg, J., Narum, B. & Wold, J.P. (2009). Classification of different bovine muscles according to sensory characteristics and Warner Bratzler shear force. *Meat Science*, **83**, 302–307.

Hoffman, L.C. (2004). Post-mortem changes in the physical meat quality characteristics of refrigerated impala M . longissimus dorsi, **34**, 26–28.

Hoffman, L. C. (2007). The meat we eat: are you game? *Inaugural Addess.* Stellenbosch University, Western Cape, South Africa.

Honikel, K.O. (1998). Reference methods for the assessment of physical characteristics of meat. *Meat Science*, **49**, 447–457.

Jones, M., Hoffman, L.C. & Muller, M. (2015). Effect of rooibos extract (*Aspalathus linearis*) on lipid oxidation over time and the sensory analysis of blesbok (*Damaliscus pygargus phillipsi*) and springbok (*Antidorcas marsupialis*) droewors. *Meat Science*, **103**, 54–60.

Kamruzzaman, M., Elmasry, G., Sun, D.W. & Allen, P. (2011). Application of NIR hyperspectral imaging for discrimination of lamb muscles. *Journal of Food Engineering*, **104**, 332–340.

Konda Naganathan, G., Cluff, K., Samal, A., Calkins, C.R., Jones, D.D., Lorenzen, C.L. & Subbiah, J. (2015). Hyperspectral imaging of ribeye muscle on hanging beef carcasses for tenderness assessment. *Computers and Electronics in Agriculture*, **116**, 55–64.

Koohmaraie, M. & Geesink, G.H. (2006). Contribution of postmortem muscle biochemistry to the delivery of consistent meat quality with particular focus on the calpain system. *Meat Science*, **74**, 34–43.

Koohmaraie, M., Kent, M.P., Shackelford, S.D., Veiseth, E. & Wheeler, T.L. (2002). Meat tenderness and muscle growth : is there any relationship ? *Meat Science*, **62**, 345–352.

Leroy, B., Lambotte, S., Dotreppe, O., Lecocq, H., Istasse, L. & Clinquart, A. (2004). Prediction of technological and organoleptic properties of beef Longissimus thoracis from near-infrared reflectance and transmission spectra. *Meat Science*, **66**, 45–54.

Liu Y, Lyon BG, Windham WR, Realini CE, Pringle TDD, Duckett S (2003) Prediction of color, texture, and sensory characteristics of beef steaks by visible and near infrared reflectance spectroscopy. A feasibility study. *Meat Science,* **65**,1107–1115.

Majewska, D., Jakubowska, M., Ligocki, M., Tarasewicz, Z., Szczerbińska, D., Karamucki, T. & Sales, J. (2009). Physicochemical characteristics, proximate analysis and mineral composition of ostrich meat as influenced by muscle. *Food Chemistry*, **117**, 207–211.

Manley, M. (2014). Near-infrared spectroscopy and hyperspectral imaging: Non-destructive analysis of biological materials. *Chemical Society Reviews*, **43**, 8200–8214.

McGlone, A. V., Devine, C. E., & Wells, R. W. (2005). Detection of tenderness, post-rigor age and water status changes in sheep meat using near infrared spectroscopy. Journal of Near Infrared Spectroscopy, **13**(5), 277–285.

Moran, L., Andres, S., Allen, P. & Moloney, A.P. (2018). Visible and near infrared spectroscopy as

an authentication tool: Preliminary investigation of the prediction of the ageing time of beef steaks. *Meat Science*, **142**, 52–58.

Moran, L., Allen, P., & Moloney, A. P. (2016). Prediction of ageing time of beef steaks using visible and near infrared reflectance spectroscopy. *Paper presented at the 62nd International Congress of Meat Science and Technology* (ICOMST). August, 14–19, Bangkok, Thailand.

Moscetti, R., Radicetti, E., Monarca, D., Cecchini, M. & Massantini, R. (2015). Near infrared spectroscopy is suitable for the classification of hazelnuts according to Protected Designation of Origin. *Journal of the Science of Food and Agriculture*, **95**, 2619–2625.

Needham, T., Laubser, J.G., Kotrba, R., Bureš, D., Hoffman, L.C. (2020). Influence of ageing on the physical qualities of the *longissimus thoracis et lumborum* and *biceps femoris* muscles from male and female free-ranging common eland (*Taurotragus oryx*). Meat Science, 159, 107922.

Neethling, J., Hoffman, L.C. & Britz, T.J. (2014). Impact of season on the chemical composition of male and female blesbok (*Damaliscus pygargus phillipsi*) muscles. *Journal of the Science of Food and Agriculture*, **94**, 424–431.

Oliveri, P. & Downey, G. (2012). Multivariate class modeling for the verification of food-authenticity claims. *TrAC - Trends in Analytical Chemistry*, **35**, 74–86.

Osborne, B. G., Fearn, T., & Hindle, P. H. (1993). Practical NIR spectroscopy with applications in food and beverage analysis, 2nd edn.*Longman Scientific & Technical, Essex*.

Prieto, N., Andrés, S., Giráldez, F.J., Mantecón, A.R. & Lavín, P. (2008). Discrimination of adult steers (oxen) and young cattle ground meat samples by near infrared reflectance spectroscopy (NIRS). *Meat Science*, **79**, 198–201.

Prieto, N., Juárez, M., Larsen, I.L., López-Campos, Zijlstra, R.T. & Aalhus, J.L. (2015). Rapid discrimination of enhanced quality pork by visible and near infrared spectroscopy. *Meat Science*, **110**, 76–84.

Rhee, M.S., Wheeler, T.L., Shackelford, S.D. & Koohmaraie, M. (2004). Variation in palatability and biochemical traits within and among eleven beef muscles. *Meat Science,* **82**, 534–550.

Rinnan, Å., Berg, F. van den & Engelsen, S.B. (2009). Review of the most common pre-processing techniques for near-infrared spectra. *TrAC - Trends in Analytical Chemistry*, **28**, 1201–1222.

Rødbotten, R., Nilsen, B.N. & Hildrum, K.I. (2000). Prediction of beef quality attributes from early post mortem near infrared reflectance spectra. *Food Chemistry*, **69**, 427–436.

Savitzky, A. & Golay, M.J.E. (1964). Smoothing and Differentiation of Data by Simplified Least Squares Procedures. *Analytical Chemistry*, **36**, 1627–1639.

Shackelford, S.D., Wheeler, T.L. & Koohmaraie, M. (1995). Relationship between shear force and trained sensory panel tenderness ratings of 10 major muscles from Bos indicus and Bos taurus cattle. *Journal of animal science*, **73**, 3333–3340.

Shange, N., Makasi, T.N., Gouws, P. & Hoffman, L.C. (2017). The influence of normal and high ultimate muscle pH on the microbiology and colour stability of previously frozen black wildebeest meat, **135**, 14–19.

Smith, G.C., Culp, G.R. & Carpenter, Z.L. (1978). Postmortem Aging of Beef Carcasses. *Journal of Food Science*, **43**, 823–826.

Starkey, C.P., Geesink, G.H., Collins, D., Oddy, V.H. & Hopkins, D.L. (2016). Do sarcomere length, collagen content, pH, intramuscular fat and desmin degradation explain variation in the tenderness of three ovine muscles ? *Meat Science,* **113**, 51–58.

Starkey, C.P., Geesink, G.H., Oddy, V.H. & Hopkins, D.L. (2015). Explaining the variation in lamb longissimus shear force across and within ageing periods using protein degradation , sarcomere length and collagen characteristics. *MESC*, **105**, 32–37.

Strydom, P., Lühl, J., Kahl, C. & Hoffman, L.C. (2016). Comparison of shear force tenderness, drip and cooking loss, and ultimate muscle pH of the loin muscle among grass-fed steers of four major beef crosses slaughtered in Namibia. *South African Journal of Animal Sciences*, **46**, 348–359.

Van Schalkwyk, D.L. & Hoffman, L.C. (2010). *Guidelines for the Harvesting of Game for Meat Export*. Windhoek, Namibia: Printech cc 71pp.

Williams, P.J., Geladi, P., Britz, T.J. & Manley, M. (2012). Near-infrared (NIR) hyperspectral imaging and multivariate image analysis to study growth characteristics and differences between species and strains of members of the genus Fusarium. *Analytical and Bioanalytical Chemistry*, **404**, 1759–1769.

Wold, S., Esbensen, K., & Geladi, P. (1987). Principal component analysis. *Chemometrics and Intelligent Laboratory Systems*, **2**, 37–52.

Chapter 6

General discussion and conclusion

Deceitful labelling of meat products, including intentional substitution of high-value meat with low-cost muscle cuts provoke the importance of traceability and detection of meat species in the food chain. Thus, causing meat and meat products to be vulnerable to food fraud (a global problem). Because of this, meat products are in the list of top five categories of illegal import fraud examples in the European Union (EU) (Soon and Manning, 2018). Food fraud is as a collective term used to encompass the deliberate and intentional substitution, addition, tampering, or misrepresentation of food, food ingredients, or food packaging; or false or misleading statements made about a product, for economic gain (Spink and Moyer, 2011). Therefore, control measures have been put in place to prevent high numbers of food fraud incidents. Hence, proper labelling of food products is encouraged in South Africa by established regulatory bodies governing food legislation (DoH, 2010). For some time, standard analytical methods have been used to detect some authenticity issues related with meat products. However, to overcome their shortcomings, an alternative rapid, non-destructive, and less expensive approach is pivotal to support the authenticity of meat and meat products. A near infrared (NIR) spectrophotometer is proven to be a capable and innovative device for the evaluation of quality traits in food products, including meat (Cen and He, 2007). Coupled with multivariate data analysis techniques, the instrument can detect and quantify physical, chemical, and biological characteristics of food samples established from their spectral signature. In this study, the effect of muscle type and ageing on near infrared spectroscopy classification of South African game meat species was investigated by means of a portable NIR instrument.

In an attempt to distinguish between *Longissimus thoracis et lumborum* (LTL) muscle steaks of the selected game species (impala *(Aepyceros melampus),* blesbok *(Damaliscus pygargus phillipsi),* springbok *(Antidorcas marsupialis)*, eland *(Taurotragus oryx),* black wildebeest *(Connochaetes gnou)* and zebra *(Equus quagga))* in a spectral range of 908–1700 nm, satisfactory to good solutions were obtained. These results demonstrated that it was indeed possible to differentiate between muscle steaks of the different species with classification accuracies ranging from 67 up to 100%. It is important to highlight that the three discrimination methods (linear discriminant analysis (LDA), partial least squares discriminant analysis (PLS-DA), and soft independent modelling of class analogy (SIMCA)) applied could discriminate meat samples when they were grouped into medium-sized antelopes (impala, blesbok, and springbok) and large-sized species (eland, black wildebeest, and zebra) (Dumalisile *et al.*, 2020a). Two clear clusters, separating the medium-sized antelopes and large-sized species, were revealed in the PCA scores plot (PC1 vs. PC3) for all meat species when the spectral data was pre-treated with smoothing, standard normal variate, and de-trending (SNV-Detrend). The PCA scores plot (PC1 (92%) vs. PC3 (2%)) contributed 94% of the total explained variance while the loadings line plot indicated that the

waveband at 1372 nm, related to fat, was responsible for the separation of the two groups. For both discrimination as well as classification, models were developed within each of the medium- and large-sized clusters.

It is also important to note that throughout this section of the study, the spectra were pre-treated with two different pre-processing combinations: 1) smoothing, SNV-Detrend, and 2) SNV-Detrend and Savitzky-Golay 2nd derivative. Thus, the pre-processing method used had an influence on the classification accuracy results for the PLS-DA and the SIMCA models. In this study, SIMCA models performed better (from 67% (springbok) to 100% (impala and eland)) when treated with smoothing and SNV-Detrend; while PLS-DA models gave better accuracies (ranging from 70 to 96%) with SNV-Detrend and Savitzky-Golay 2nd (Dumalisile *et al.*, 2020a). This could be because a typical SIMCA methodology involves using disjointed PCA models (Brereton, 2011), and it was already evident from the PCA scores plot (PC1 vs. PC3) that clear clusters were noticeable when the spectra were treated with smoothing, SNV-Detrend. Therefore, the pre-processing method that gives best results (good separation) for PCA should certainly also work well for SIMCA. Generally, impala, black wildebeest and eland presented good classification results whereas blesbok and springbok did not perform well because of their spectral similarities. These spectral similarities might be due to the fact that the animals were harvested from the same farm, during the same season and feeding on the same pasture/fodder.

In the second section of this study, we applied the handheld NIR device to distinguish between different muscle types (*longissimus thoracis et lumborum* (LTL), *infraspinatus* (IS), *supraspinatus* (SS), *biceps femoris* (BF), *semitendinosus* (ST) and *semimembranosus* (SM)) within impala and eland species; muscle types (fan fillet (FF), big drum (BD), triangle steak (TS), moon steak (MS) and rump steak (RS)) within ostrich species; as well as to categorize species irrespective of the muscle. The results showed the potential of NIR spectroscopy to distinguish diverse muscle types with classification accuracies ranging from 85 to 100%. Nevertheless, the muscles were effectively differentiated when they were categorized according to their anatomical locations (forequarter, back and hindquarter regions) (Dumalisile *et al.*, 2020b). Initially, there was a similarity observed in the spectral features of impala and eland muscles. For both species the forequarter (IS and SS) muscles were overlapping throughout, and that contributed to 100% IS muscles misclassified as SS muscles. Similar misclassification was noticed in the hindquarter (SM, ST, and BF) muscles. A potential justification for this overlapping might be because of their close anatomical location and functions. For example, the Warner Bratzler shear force (WBSF) results confirmed that IS was the most tender muscle, followed by the SS muscle. Similarly, the toughest muscles were located in the hindquarter. For ostrich muscles, all the muscles were from the leg, and a large number of misclassifications were noticed between the triangle steak (TS) and rump steak (RS) muscles. It was then observed that TS and RS muscles were both in the same category of the silver side muscles of the ostrich thigh, which were then grouped together because of the high misclassification rate caused by their close anatomical location.

When the species were classified irrespective of the muscles, PLS-DA models pre-treated with SNV-Detrend and Savitzky-Golay 1st derivative produced accuracies of 97, 81 and 92% for eland, impala, and ostrich, respectively (Dumalisile *et al.*, 2020b). The wavelengths responsible for the variation were 963 nm (associated with water/moisture), 1143 and 1392 nm (associated with fat). From these observations it was easier to differentiate between species irrespective of the muscle, than to distinguish diverse muscles within each species. However, knowing that under general circumstances different species always differ in their DNA, the results were expected. These results revealed the establishment of classification methods for the authentication of impala, eland and ostrich muscles based on NIR analysis.

Finally, we aimed to differentiate between ageing periods of *Longissimus thoracis et lumborum* (LTL) muscles of blesbok and eland, and fan fillet muscles of ostrich species. The overall prediction results suggested that in the 908–1700 nm spectral region, we could not clearly distinguish the different ageing days within the three species. Prediction accuracies obtained with cross-validated PLS-DA models ranged from 66 to 95%, 56 to 71% and 52 to 68% for the different ageing periods of blesbok, eland and ostrich, respectively. Considering the blesbok muscles spectra pre-processed with SNV-Detrend and 2nd derivative, there was no prominent variation observed among the ageing days. This resulted in a high rate of misclassification across the ageing period. There are many reasons that could contribute to the misclassification of aged meat samples which include the breed, age, sex, muscle type, chilling conditions, and the ageing period (Strydom *et al.*, 2016).

Even though there were high prediction accuracies (66 to 95%), it is evident that the true negative rate contributed to the high classification accuracies obtained. As a result, true negatives contributed to the lower accuracies obtained for the cross-validated models. Thus, it will not be easy to predict blesbok, eland and ostrich ageing days in future using these models. That means a handheld spectrophotometer could not be used as a prediction method to classify aged game meat. It is recommended that a wider spectral range should be applied in future studies, as it has shown the potential of producing better results in a study by Moran *et al.* (2018). Moreover, future work should investigate factors related to tenderness, sarcomere length and desmin degradation. It is also postulated that the smaller sample size/number of animals per species used might have contributed to the poor prediction results. Thus, a larger sample size where most of the factors known to influence meat ageing (e.g., enzyme protease, desmin degradation and sarcomere length) will be measured and included in the analyses to develop a robust and accurate model. Therefore, the results from this section of the study did not support the use of a handheld NIR spectrophotometer as a reliable prediction tool for aged game meat.

In conclusion, a handheld MicroNIR™ OnSite spectrophotometer has demonstrated the potential of being able to discriminate different species of game meat, different muscle types within each species, and different species regardless of the muscle used. However, the instrument cannot be used as a reliable prediction tool for aged game meat. Although accurate models were obtained for species discrimination as well as muscle type classification, it is reckoned there is still room for

improvement by coupling spectroscopy with machine learning (ML) algorithms. The combination of spectroscopy and machine learning algorithms is becoming popular because of the high accuracies reported (Nolasco Perez *et al.*, 2018; Parastar *et al.*, 2020). It has been noted from the literature that some models that did not perform well were improved when ML was used. Therefore, it would be ideal to attempt the possibility of ML algorithms in differentiating the ageing days of game meat.

In addition to that, attempting an alternative classification method, for example, random subspace discriminant ensemble (RSDE) could give improved classification accuracies. Parastar *et al.* (2020) evaluated RSDE technique by comparing it with other common (PLS-DA, support vector machines (SVM), and artificial neural network (ANN)) techniques while classifying chicken fillets, and its performance outshone all other classification methods.

Now that the handheld MicroNIR™ OnSite spectrophotometer has demonstrated its capability in discriminating different species of game meat, this implies the instrument could potentially be used in the authentication of game meat, specifically impala, eland and ostrich in the abattoirs. Savoia *et al.* (2020) have previously used a handheld Micro-NIR Pro (905–1649 nm) in the abattoir for the analysis of the quality traits of young bulls, and good results were obtained. Again, when Savoia *et al.* (2020) were doing their abattoir studies, they used two different spectrophotometers, the portable Vis-NIR (350–1830 nm) and handheld Micro-NIR Pro (905–1649 nm), which both gave good results for meat quality attributes. This confirms that the handheld MicroNIR™ OnSite instrument could be good enough for abattoir purposes, as it is a better model than the handheld Micro-NIR Pro used to analyse the quality of traits of Piemontese young bulls. Therefore, we have identified a solution to screen game meat species under the fast-paced manufacture and handling environments. In conclusion, the findings of this study are promising in finding a less expensive, rapid, non-destructive screening method to promote the authenticity of game meat products in the fast-growing fraudulent population.

References

Brereton, R.G. (2011). One-class classifiers. *Journal of Chemometrics*, **25**, 225–246.

Cen, H. & He, Y. (2007). Theory and application of near infrared reflectance spectroscopy in determination of food quality. *Trends in Food Science and Technology*, **18**, 72–83.

DoH (Department of Health). 2010. Foodstuffs, Cosmetics and Disinfectants Act, 1972 (Act 54 of 1972): Regulations relating to the labelling and advertising of foods: R. 146 of 2010, As amended up to and including R.45 of 2012. Government Printing Offices, South Africa.

Dumalisile, P., Manley, M., Hoffman, L. & Williams, P.J. (2020a). Near-Infrared (NIR) Spectroscopy to Differentiate Longissimus thoracis et lumborum (LTL) Muscles of Game Species. *Food Analytical Methods,* **13**, 1220-1233.

Dumalisile, P., Manley, M., Hoffman, L. & Williams, P.J. (2020b). Discriminating muscle type of selected game species using near infrared (NIR) spectroscopy. *Food Control*, **110**, 106981.

Moran, L., Andres, S., Allen, P. & Moloney, A.P. (2018). Visible and near infrared spectroscopy as

an authentication tool: Preliminary investigation of the prediction of the ageing time of beef steaks. *Meat Science*, **142**, 52–58.

Nolasco Perez, I.M., Badaró, A.T., Barbon, S., Barbon, A.P.A.C., Pollonio, M.A.R. & Barbin, D.F. (2018). Classification of Chicken Parts Using a Portable Near-Infrared (NIR) Spectrophotometer and Machine Learning. *Applied Spectroscopy*, **72**, 1774–1780.

Parastar, H., Kollenburg, G. van, Weesepoel, Y., Doel, A. van den, Buydens, L. & Jansen, J. (2020). Integration of handheld NIR and machine learning to “Measure & Monitor” chicken meat authenticity. *Food Control*, **112**, 107149.

Savoia, S., Albera, A., Brugiapaglia, A., Stasio, L. Di, Ferragina, A., Cecchinato, A. & Bittante, G. (2020). Prediction of meat quality traits in the abattoir using portable and hand-held near-infrared spectrometers. *Meat Science*, **161**, 108017.

Soon, J.M. & Manning, L. (2018). Food smuggling and trafficking: The key factors of influence. *Trends in Food Science and Technology*, **81**, 132–138.

Spink, J. & Moyer, D.C. (2011). Defining the Public Health Threat of Food Fraud. *Journal of Food Science*, **76,** 157 - 163.

Strydom, P., Lühl, J., Kahl, C. & Hoffman, L.C. (2016). Comparison of shear force tenderness, drip and cooking loss, and ultimate muscle pH of the loin muscle among grass-fed steers of four major beef crosses slaughtered in Namibia. *South African Journal of Animal Sciences*, **46**, 348–359.

Appendix to Chapter 3

Figures A3.1–4 are given in this appendix. The large amount of data generated was placed in a separate Appendix to simplify the discussion section of this paper.

Figures

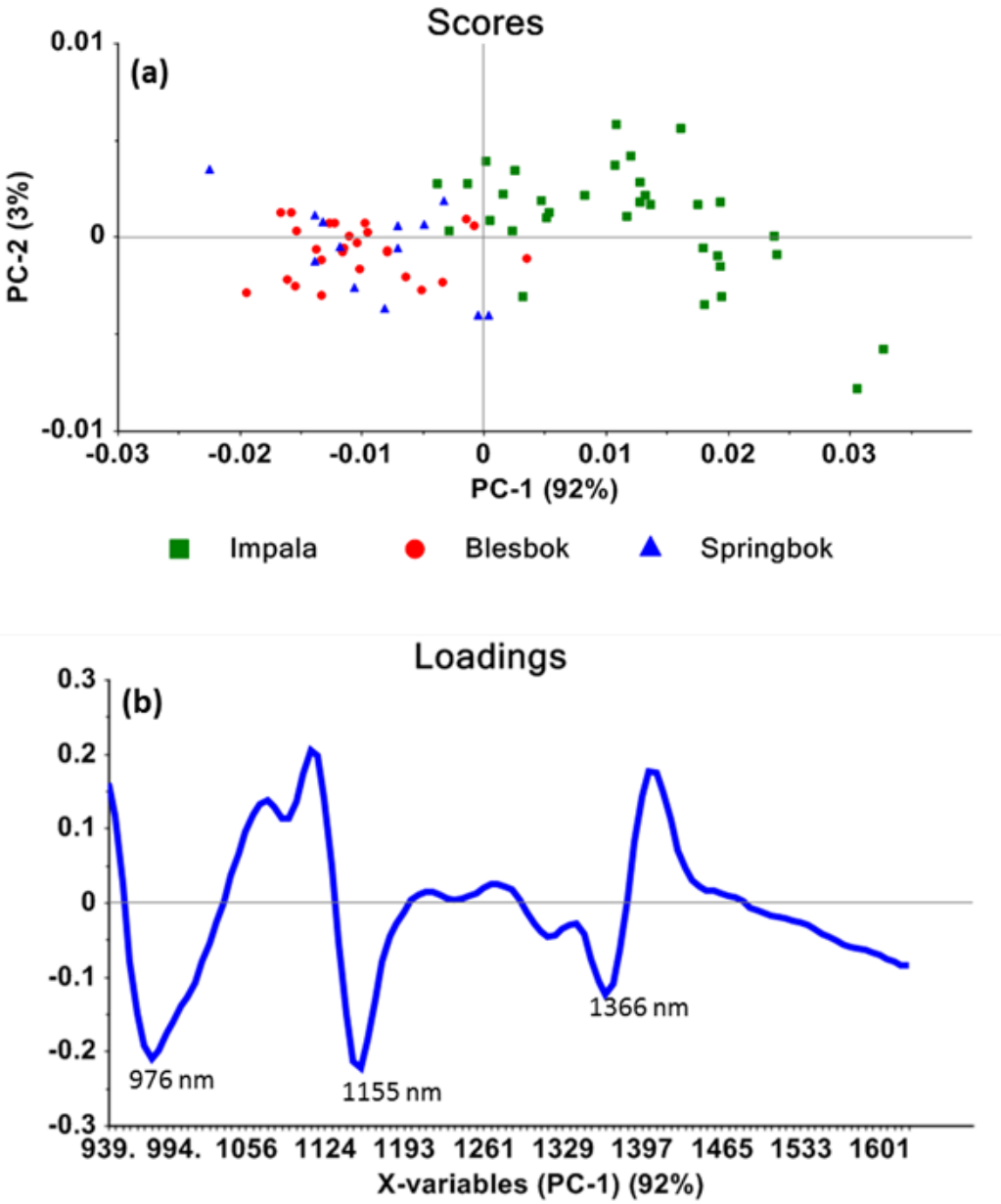

Figure A3. 1 (a) PCA scores plot (SNV-Detrend and 2nd derivative pre-processed spectra) of PC1 vs. PC2, (95% explained variance) illustrating the separation of the impala muscles from those of blesbok and springbok (b) PC1 loadings line plot, depicting wavebands associated with fat (1155 and 1366 nm) and moisture (976 nm) mainly contributing to the separation of impala from blesbok and springbok

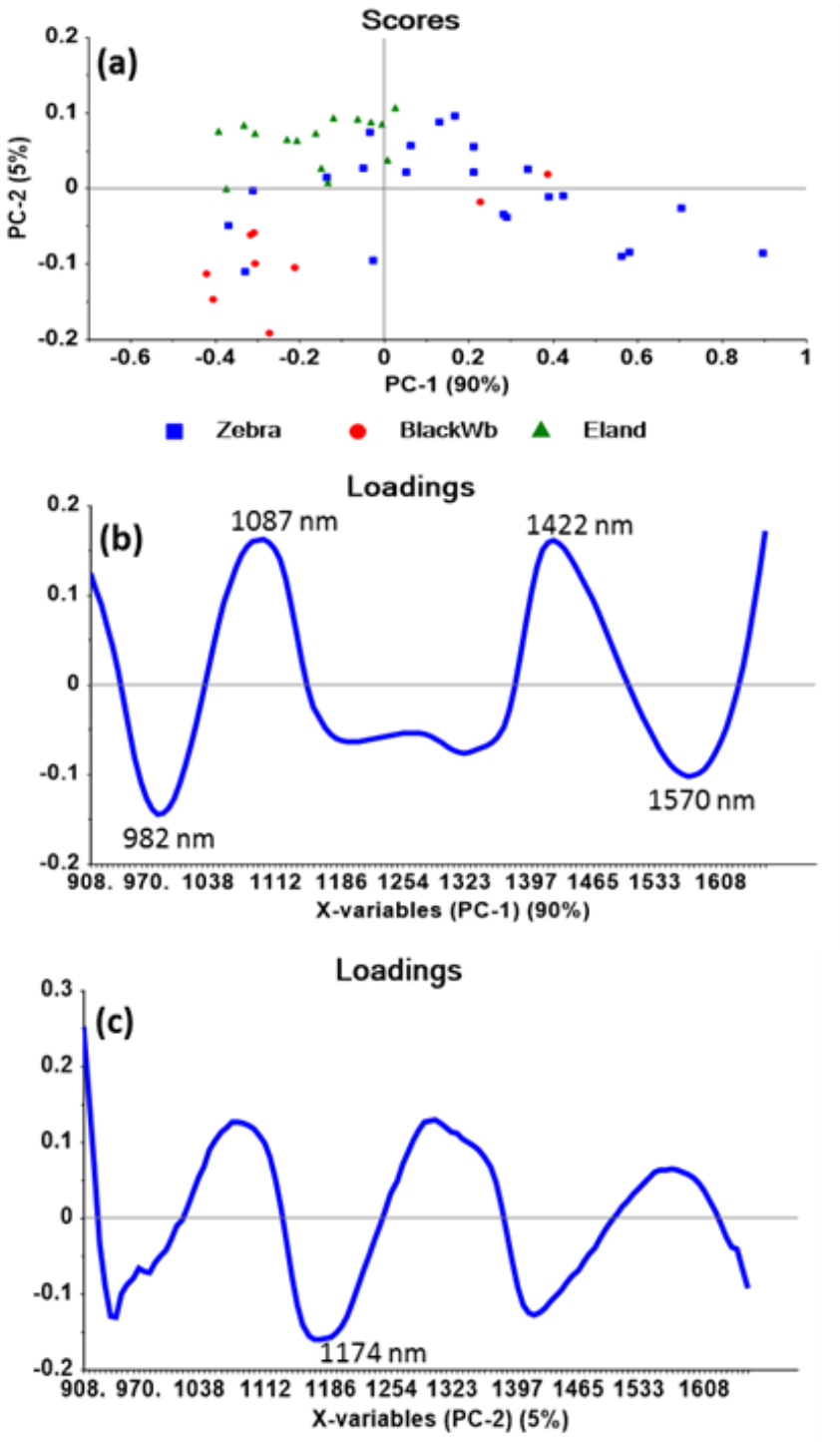

Figure A3. 2 (a) PCA scores plot (smoothing and SNV-Detrend pre-processed spectra) of PC1 vs. PC2 (95% explained variance) showing the grouping of eland, black wildebeest and zebra muscles (b) PC1 loadings line plot showing the bands associated with the separation of most of the zebra samples from those of eland and black wildebeest (982 and 1422 nm = moisture; 1087 and 1570 nm = protein); while (c) PC2 loadings line plot displays fat (1174 nm) being associated with eland and black wildebeest sample separation

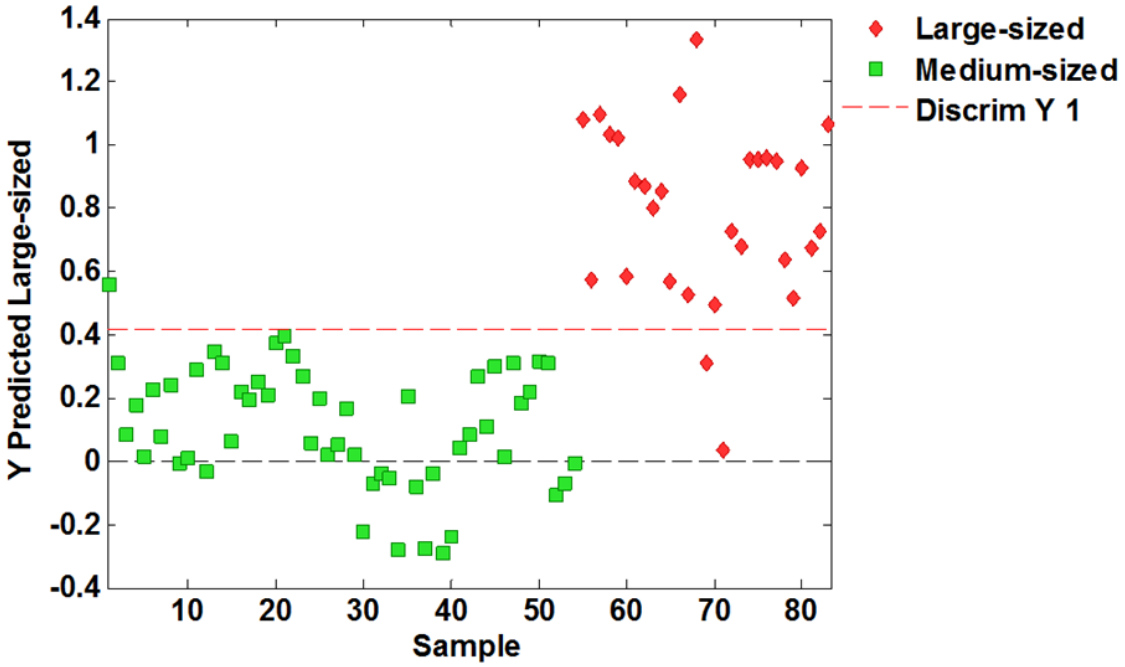

Figure A3. 3 PLS-DA model scores plot (spectra pre-processed with Combination 1 pre-processing) showing the differentiation of meat samples from medium-sized antelopes and large-sized game species. The red dotted line represents the discrimination line. Samples above the red dotted line are regarded as large-sized species and those below the red line as medium-sized antelopes

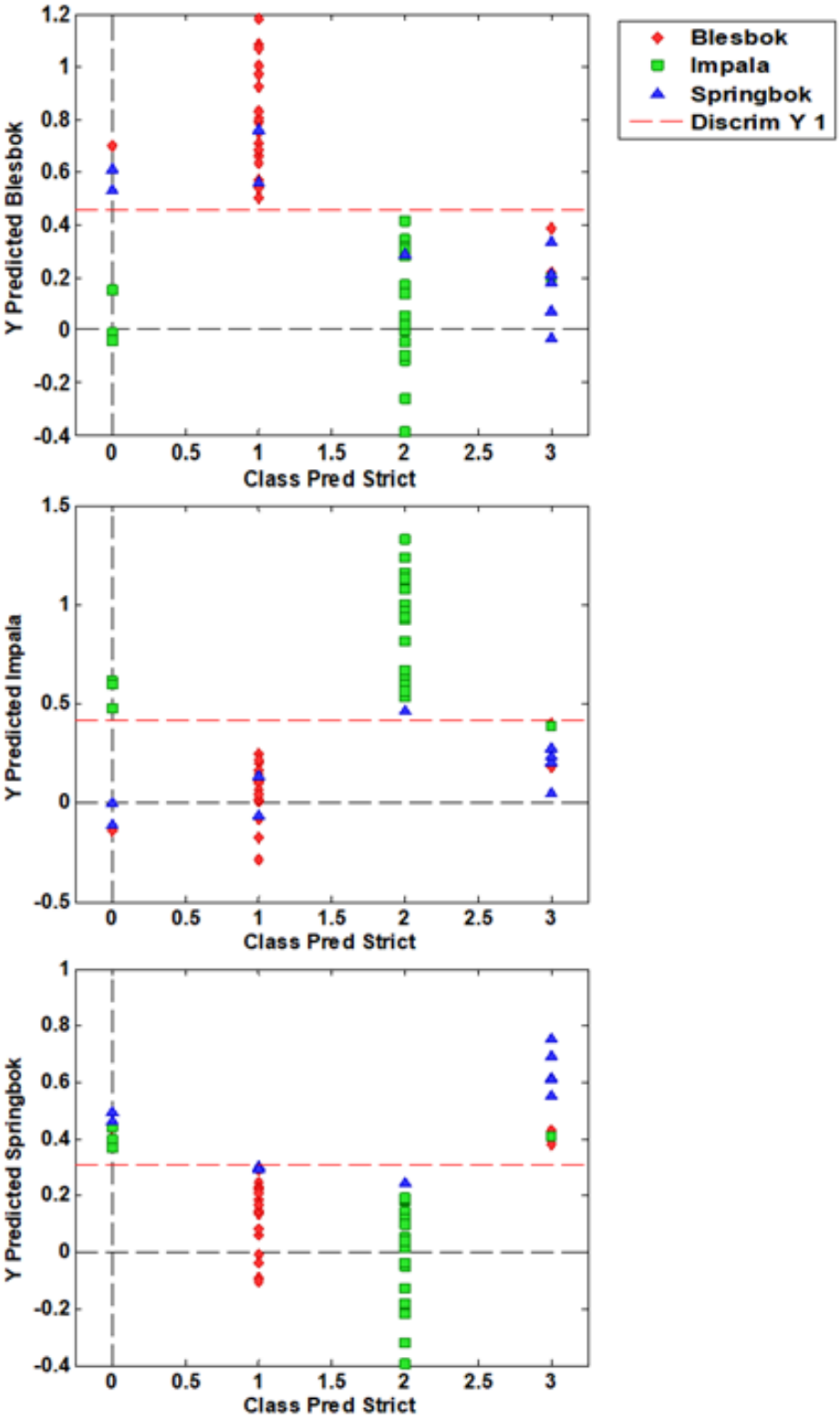

Figure A3. 4 PLS-DA model scores plot (Combination 2 pre-processed spectra) displaying the predicted samples from blesbok, impala and springbok species. The red dotted line represents the discrimination line (probability)

Appendix to Chapter 4

Tables A4.1–3 and Figures A4.1–6 are given in this appendix. The large amount of data generated was placed in a separate appendix to simplify the discussion section of this paper.

Abbreviations: LTL= *longissimus thoracis et lumborum*, BF= *biceps femoris*, SM= *semimembranosus*, ST= *semitendinosus,* IS= *infraspinatus*, SS= *supraspinatus*, FF= fan fillet, RS= rump steak, BD= big drum, MS= moon steak, TS= triangle steak, + = positive, - = negative

Tables

Table A4. 1 Percentage accuracies of PLS-DA models showing calibration (Cal) and validation (Val), for the classification of different muscles of impala and ostrich species pre-treated with SNV-Detrend and 2nd derivative pre-processing

Species	Muscle	Cal (%)	Val (%)
Impala	BF	66.7	66.7
	IS	50.0	50.0
	LTL	77.4	90.0
	SM	78.6	70.0
	SS	65.4	64.0
	ST	77.4	57.1
Ostrich	BD	90.9	62.5
	FF	82.2	58.4
	MS	85.0	70.0
	RS	73.8	100
	TS	56.7	50.0

Table A4. 2 Confusion matrix obtained with PLS-DA (pre-treated with SNV-Detrend and 2nd derivative) showing muscle types of ostrich. The true positives, false positives, true negatives, false negatives and the total number of muscle type used for the calibration model are presented.

Class	True + (%)	False + (%)	True - (%)	False - (%)	n
BD	81.8	0.0	100	18.2	11
FF	66.7	2.3	97.7	33.3	9
MS	70.0	0.0	100	30.0	10
RS	50.0	2.4	97.6	50.0	12
TS	18.2	4.8	95.2	81.8	11

Table A4. 3 Confusion matrix obtained with PLS-DA showing muscle types (when certain muscles are combined according to their anatomical locations) of eland (pre-treated with SNV-2nd derivative) and ostrich (pre-treated with SNV-Detrend and 2nd derivative). The true positives, false positives, true negatives, false negatives and the total number of muscle type used for the calibration model are presented.

Species	Class	True + (%)	False + (%)	True - (%)	False - (%)	N
Eland	BF,SM,ST	80.0	9.1	90.1	20.0	30
	IS,SS	87.0	2.5	97.5	13.0	23
	LTL	80.0	1.9	98.1	20.0	10
Ostrich	BD	90.9	0.0	100	9.1	11
	FF	77.8	0.0	100	22.2	9
	MS	70.0	0.0	100	30.0	10
	RS,TS	78.3	3.3	96.7	21.7	23

Figures

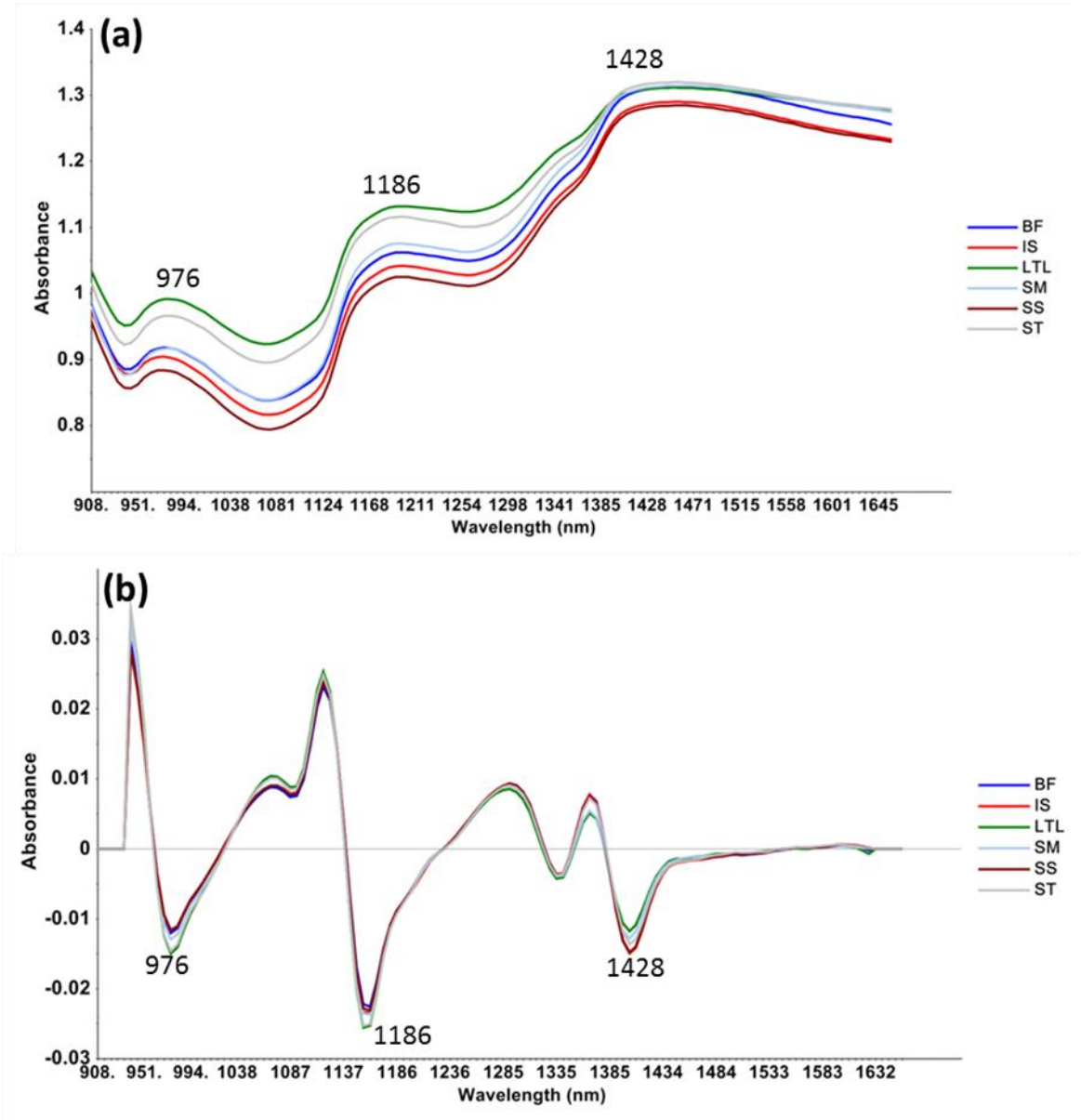

Figure A4. 1 Mean spectra of eland muscles (BF, IS, LTL, SM, SS and ST) showing the wavelength bands of (a) raw spectra, (b) SNV-2nd derivative pre-processed spectra.

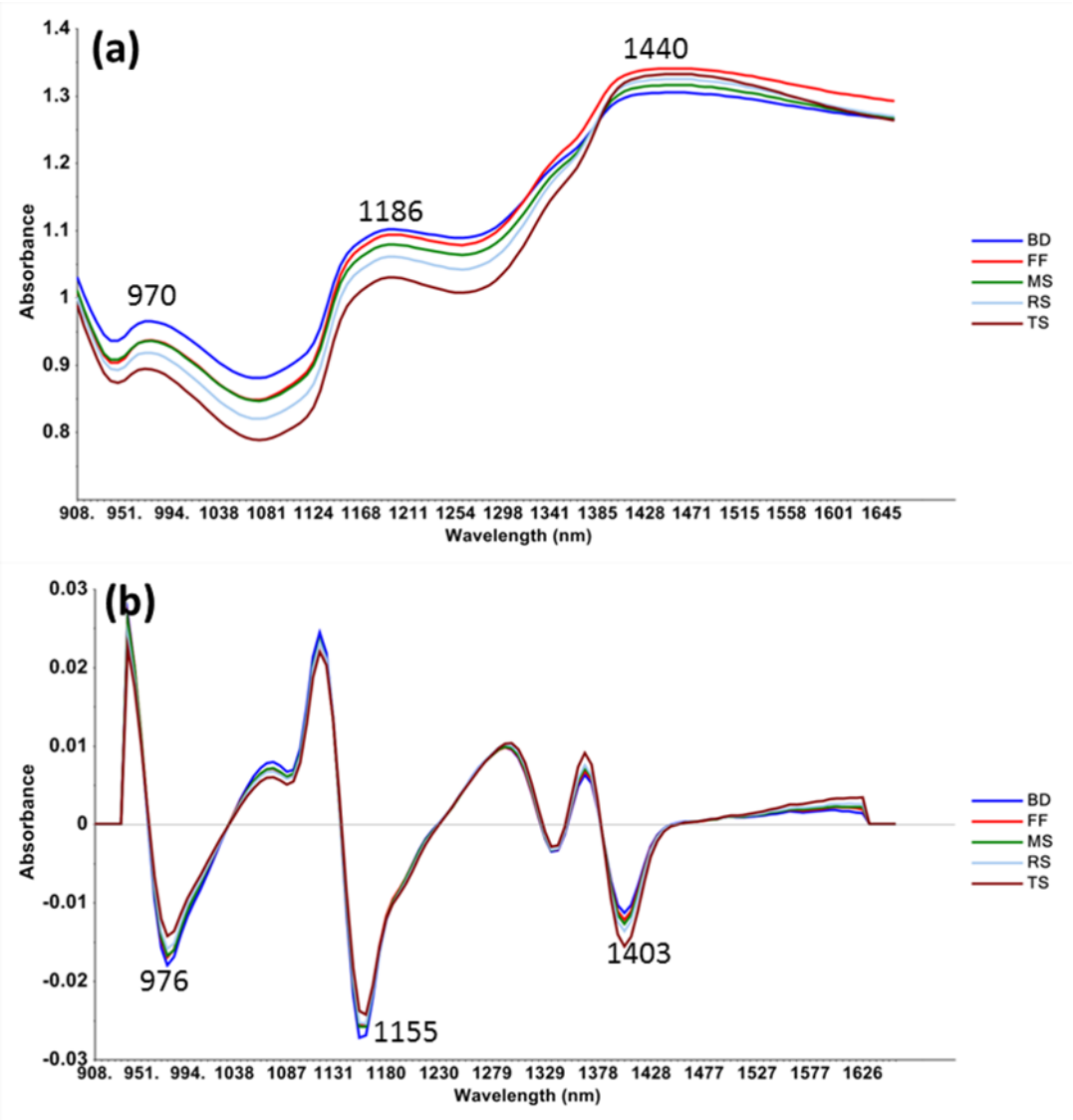

Figure A4. 2 Mean spectra of ostrich muscles (BD, MS, FF, RS and TS) showing the wavelength bands of (a) raw spectra, (b) SNV-Detrend and 2nd derivative pre-processed spectra.

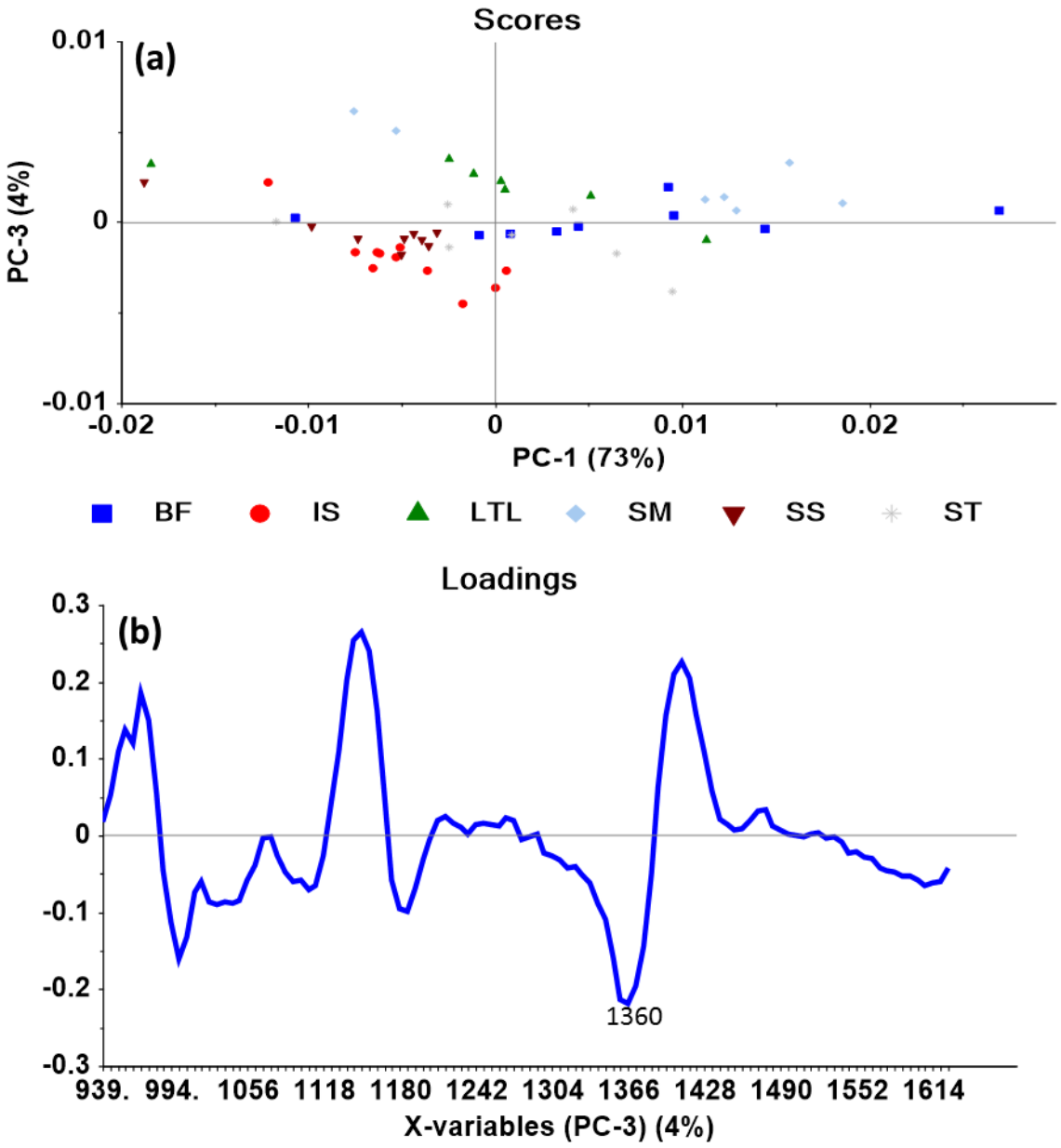

Figure A4. 3 (a) PCA scores plot of PC1 vs. PC3 accounting 77% explained variation of the model showing the clustering of the impala muscle types (SNV-Detrend and 2nd derivative pre-processed spectra). (b) PC3 loadings line plot showing the band responsible for the groupings of the muscle types.

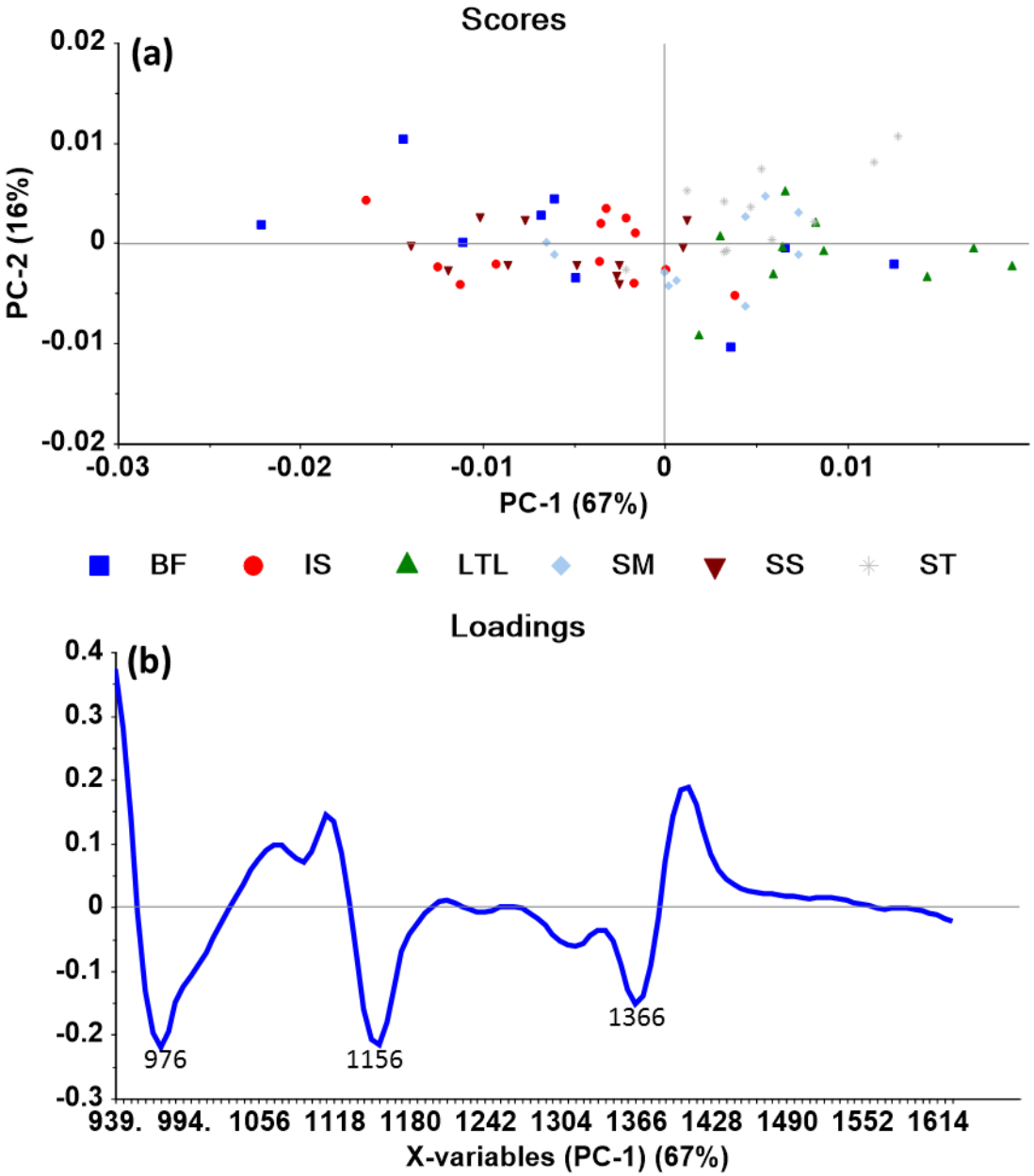

Figure A4. 4 (a) PCA scores plot of PC1 vs. PC2 contributing 83% explained variance of the model showing the clustering of the eland muscle types (SNV-2nd derivative pre-processed spectra). (b) PC1 loadings line plot showing the bands responsible for the clustering of muscle types.

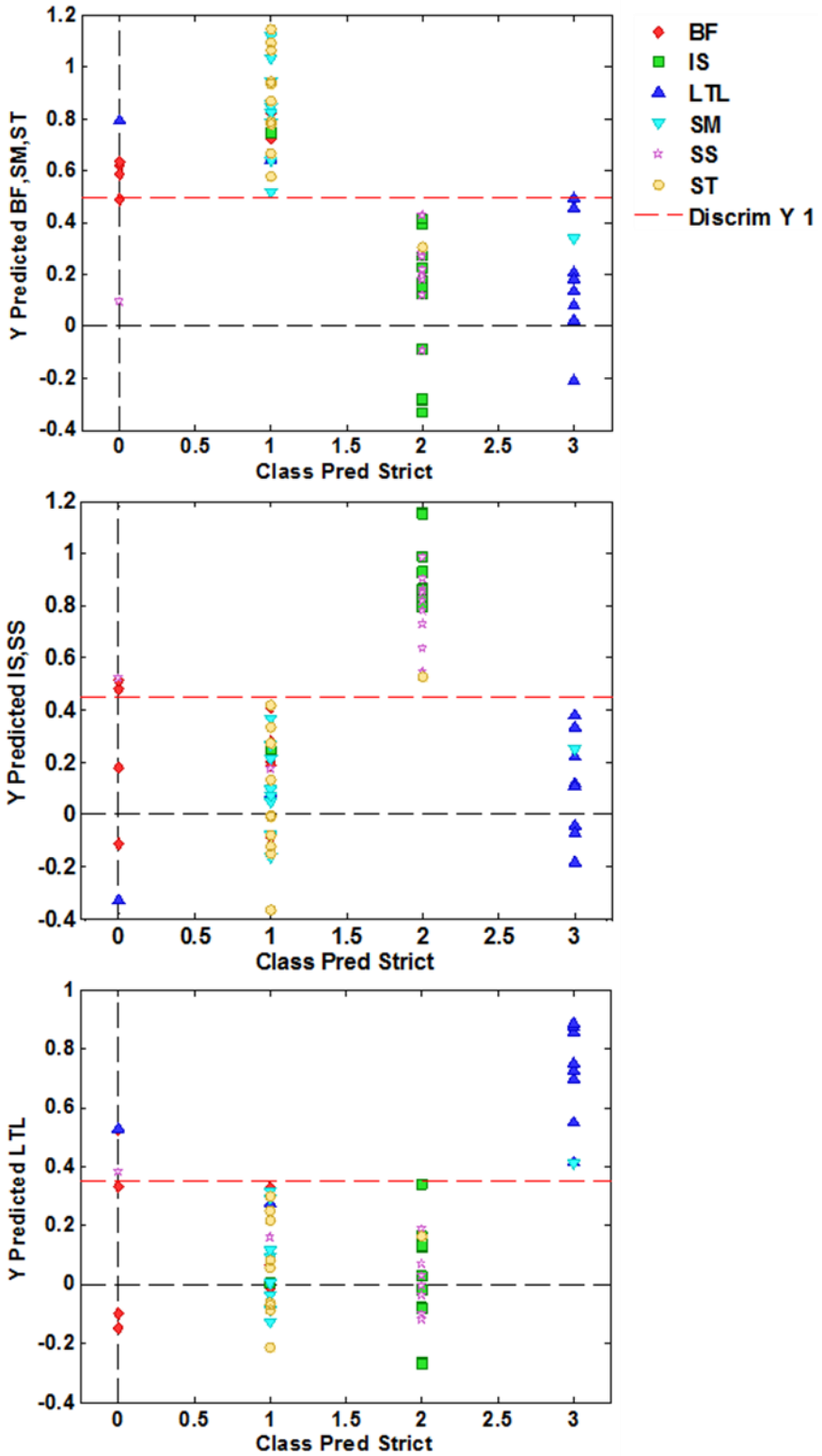

Figure A4. 5 Class predict strict plot obtained by PLS-DA pre-treated with SNV-2nd derivative pre-processing method showing the segregation of eland muscle types. The red dotted line represents the discrimination line. Any sample that is above the red dotted line is regarded as predicted in that class and those below the red line are regarded as the other classes not predicted in this class. Samples located at 0 are unassigned samples.

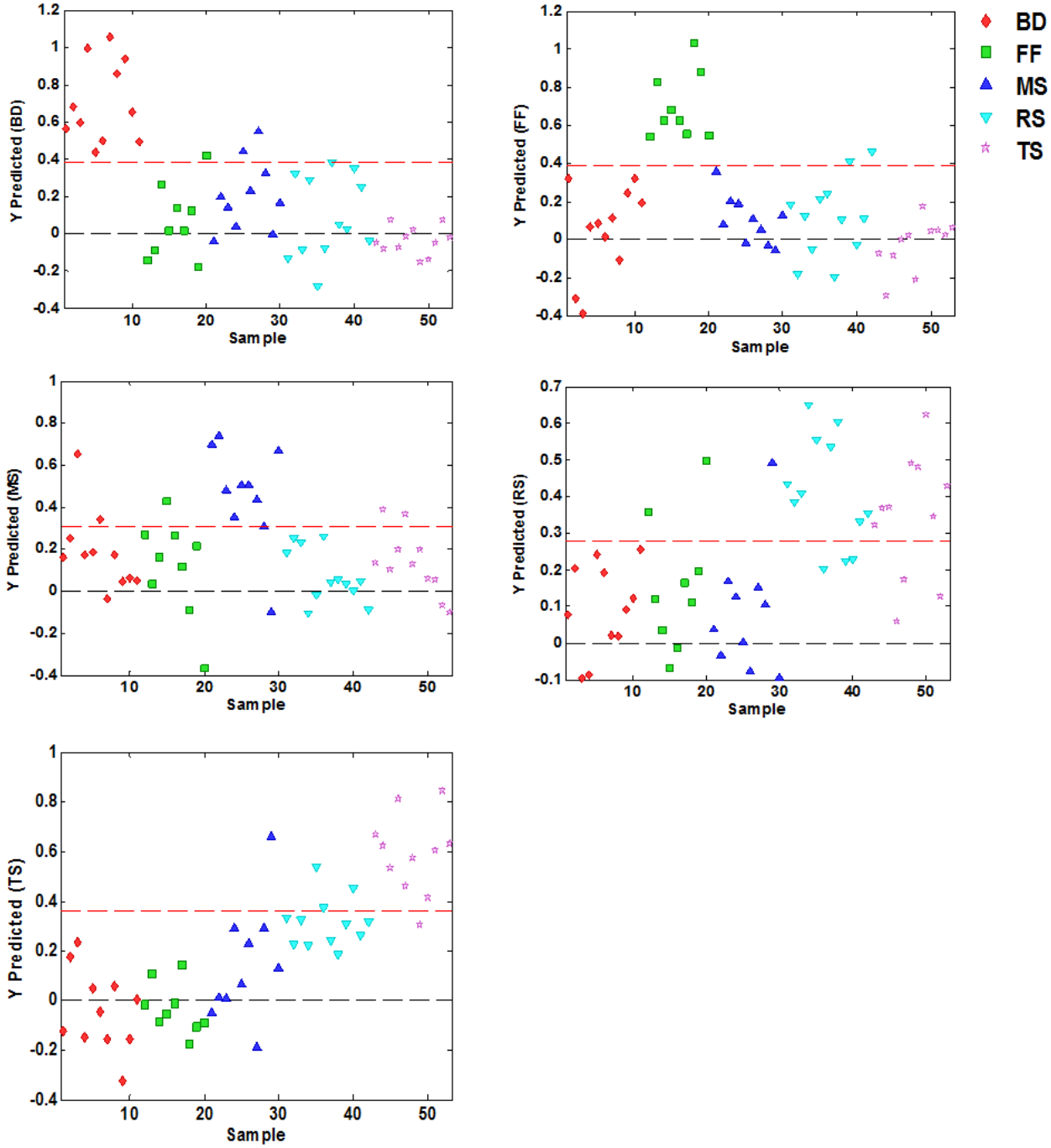

Figure A4. 6 Scores plot obtained by PLS-DA pre-treated with SNV-Detrend and 2nd derivative pre-processing method showing the segregation of ostrich muscle types. The red dotted line represents the discrimination line. Any sample that is above the red dotted line is regarded as predicted class and any sample that is below the red line is regarded as the other classes not predicted.